UNIVERSITA' DEGLI STUDI DI PARMA

Dottorato di ricerca in Biologia e Patologia Molecolare

XXV CICLO

CELLULAR AND MOLECULAR BASES FOR THE PRO-TUMORIGENIC ROLE OF NG2/CSPG4 PROTEOGLYCAN

Coordinatore:

Chiar.mo Prof. Valeria Dall'Asta

Tutori:

Chiar.mo Prof. Ovidio Bussolati

Chiar.mo Prof. Roberto Perris

Dottorando: Dr. Pier Andrea Nicolosi

A mamma e papà.

CONTENTS

ABSTRACT

CSPG4/NG2 is a unique, variably glycanated transmembrane proteoglycan that has been thoroughly documented to exhibit aberrant expression patterns in solid and haematological tumours. Hence, it has been strongly associated with the pathological traits and progression of several tumours, but the precise molecular mechanisms through which it controls tumour development are not fully unveiled. The aim of my thesis work was therefore to approach the cellular and molecular mechanisms underlying the capability of NG2 to confer to cancer cells a more malignant phenotype. This direct correlation, between ectopic/overexpression of surface NG2 and a higher degree of malignancy, was demonstrated by the diverse tumorigenic behaviour displayed *in vitro* and *in vivo* of*:* immunoselected NG2-expressing and NG2-deficient cell subsets; cells in which their endogenous NG2 was knocked down with siRNAs; or cells engineered to overexpress the full-length or truncated variants of the proteoglycan. *In vivo* tumorigenesis experiments were supported by comparative in situ analyses of the tumour masses formed by NG2-expressing and NG2 deficient cells, DNA microarray global gene profiling and wide spectrum antibody array-based phospho-proteomic screens. Accentuated malignant behaviour of NG2 expressing cells was corroborated *in vitro* by: the diverse capacity to grow anchorage independently; the increased survival capabilities; the higher migration rates; and a diverse capability to form cellular aggregates. A substantial part of my studies also addressed the role of the NG2-collagen type VI interaction in the control of malignant behaviour in sarcoma cells. Diversified cellular interactions and migratory abilities were observed between NG2-positive and NG2-negative sarcoma cells with purified Col VI, basement membrane matrices supplemented with Col VI, and cell-free matrices isolated from wild type and Col VI null fibroblasts. The NG2-mediated binding to Col VI triggered activation of convergent cell survival- and cell adhesion/migration-promoting signal transduction pathways, implicating PI-3K as a common denominator and supporting the idea that an NG2-Col VI interplay may govern cancer cell-host microenvironment interactions sustaining sarcoma progression.

Further, analysis of biopsies from soft-tissue sarcoma patients demonstrated that enhanced expression of NG2 in pre-surgical primary lesions predicts post-surgical metastasis formation. Thereby it could stratified patients into disease-free survivors and patients destined to succumb from the disease.

Cumulatively, the study provides insights into the complex and multivalent role of NG2 in the control of cancer cell behaviour and reinforces its putative effectiveness as a therapeutic target for ablation of malignant cancer cell subsets.

INTRODUCTION

Structural-functional characteristics of CSPG4/NG2

The Chondroitin Sulphate Proteoglycan 4 (CSPG4) , the human homologus of the rat Neural Glial Antigen 2 (NG2), is a high-molecular weight membrane proteoglycan (around 250 KDa), that could be found with or without a Choindroitin Sulphate chain, covalenty attached to its core protein. Although crystallographic data on the protein is not available, some structural information was obtained by the combination of data deriving from the computational analysis, based upon the amminoacid sequence, and different biochemical studies (Stallcup and Huang, 2008; Campoli et al., 2010; Price et al., 2011) The core protein can be divided into three domains (**Fig. 1**): the large extracellular domain (around 2195 amminoacids), a small hydrophobic transmembrane region of 21 amminoacid and a short cytoplasmic domain of 77 amminoacids ((Stallcup and Huang, 2008; Campoli et al., 2010; Price et al., 2011);http://www.uniprot.org/uniprot/Q6UVK1).

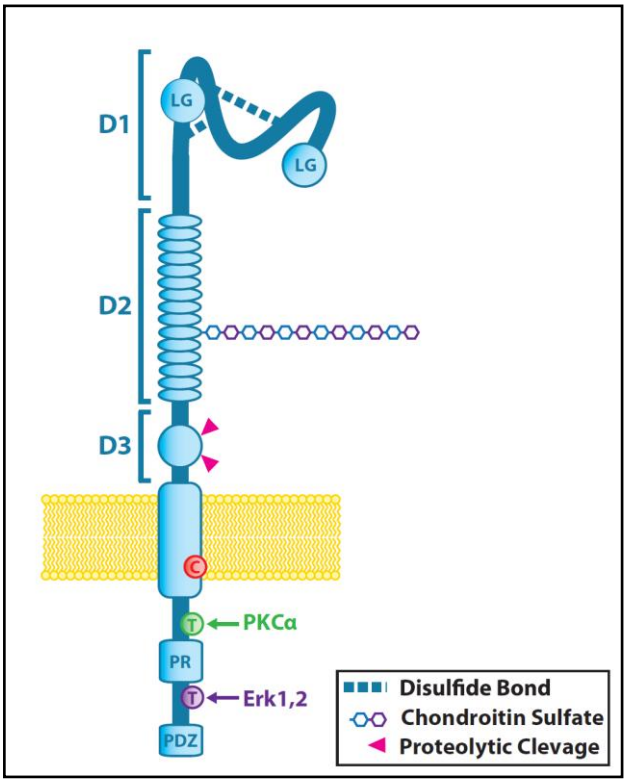

Figure 1. CSPG4 / NG2 is composed of three major structural components: the extracellular domain, the transmembrane region, and the cytoplasmic C-terminal domain (CTD). The extracellular domain contains an N-terminal globular subdomain (D1) consisting of laminin G-type regions (LG) and disulfide bonds. The D2 subdomain consists of 15 CSPG repeats and, in NG2, a single chondroitin sulfate glycosaminoglycan (CS-GAG) chain. This region of the core protein is known to bind certain soluble growth factor ligands, and the CS-GAG is responsible for CSPG4 binding to integrin and matrix metalloproteinases (MMPs). CS modification is also associated with distinct membrane distribution patterns of CSPG4 / NG2 on the cell surface. CSPG4 / NG2 can be expressed with or without CS modification. Proximal to the plasma membrane, the D3 globular subdomain contains sites for N-linked carbohydrate modification, binding sites for lectins (e.g., galectin 3), and proteolytic cleavage by MMPs or other proteases. The transmembrane region of CSPG4 contains a cysteine residue (C) at position 2230 that may play a role in CSPG4 membrane localization, although this

is yet to be evaluated. The CTD contains tyrosine residues (T) that serve as phosphoacceptor sites for PKCa and ERK 1,2 (CSPG4 residues 2252 and 2310, respectively). The proline-rich region (PR) may comprise a non-canonical SH3 protein interaction domain, and the C-terminus contains a 4 residue PDZ domain-binding motif (PDZ) that is responsible for interactions with various PDZ domain-containing binding partners (Price et al., 2011).

The predicted structure of extracellular region could be divided, in turn, into three sub-domains (D1,D2 and D3; **Fig. 1**). The N-terminus D1 globular sub-domain, stabilized by two disulfide bonds, is caracterizated by the presence of two laminin G-type motifs that usually are involved in the interaction with different molecules like integrins and extracellular ligands. The second sub-domain, D2, consists of an alpha helical region, which contains 9 potential N-linked GAG acceptor sites, an O-linked glycosilation site and potential type V and VI collagen-binding sites. The last sub-domain, D3, contains 6 potential N-linked GAG acceptor sites and it is characterized by the presence binding sites for alpha3-beta1 integrin. Moreover D3 is required to bind Galectin-3 or p-selectin (Stallcup and Huang, 2008; Campoli et al., 2010; Price et al., 2011), and involved in the shedding of CSPG4 for the presence of a number of cleavage site, targets of different proteases (Stallcup and Huang, 2008; Campoli et al., 2010; Price et al., 2011).

The cytoplasmic domain is caracterizated by the presence of a PDZ domain, that seems to be involved in the modulation of CSPG4/NG2 interaction with different scaffold protein like MUPP1 , GRIP1 and syntenin-1 (Stallcup and Huang, 2008; Campoli et al., 2010; Price et al., 2011), and the presence of threonine residues, Thr-2256 and Thr-2314, target respectively of the PKC-alpha and ERK1/2 phosphorillation activity (**Fig. 1**). Moreover, although a classical SH3 binding domain is not present, the C-terminus tail is very rich in prolines, even though until now, its function is not completely known.

Expression patter of CSPG4/NG2

Distribution of CSPG4 in healthy tissues

In the last years online databases are a useful instrument to compare and collect information about the distribution and/or the expression of a particular molecule. However in this analysis two important aspects have to be considered: 1) the data could be obtained from samples deriving by different protocols, conditions and reagents' settings; 2) the number of samples could change

depending on tumor type, often with a low number of lesions analyzed, making difficult to draw definitive conclusions regarding the level of a protein/mRNA expression.

The Swedish Human Protein Atlas project, for example, has been set up to allow for a systematic exploration of the human proteome using Antibody-Based Proteomics. This is accomplished by combining high-throughput generation of affinity-purified antibodies with protein profiling in a multitude of tissues and cells assembled in tissue microarrays. Confocal microscopy analysis using human cell lines is performed for more detailed protein localization (http://www.proteinatlas.org/about/project). For the CSPG4 expression profile three different antibodies were used and in many cases two (or more) antibodies yielding partly similar staining patterns, which are partly consistent with gene/protein characterization data or consistent with limited gene/protein characterization data. For each tissue sample the cell type positive for the staining and the cell compartment localization are reported. From their analysis on healthy tissue the proteoglycan resulted moderate or high express in 60% of CNS samples, in 88% of hematopoietic samples, in 80% of pancreas and liver, in 93% of digestive tract (GI-tract), in 75% of lung samples, in the single sample of cardiovascular tissue, in 61 % of female tissues analyzed, in 67% of the urinary tract, in 33% of the skin and soft tissues, in all male tissues, endocrine and placenta samples (http://www.proteinatlas.org/ENSG00000173546; **Fig. 2**).

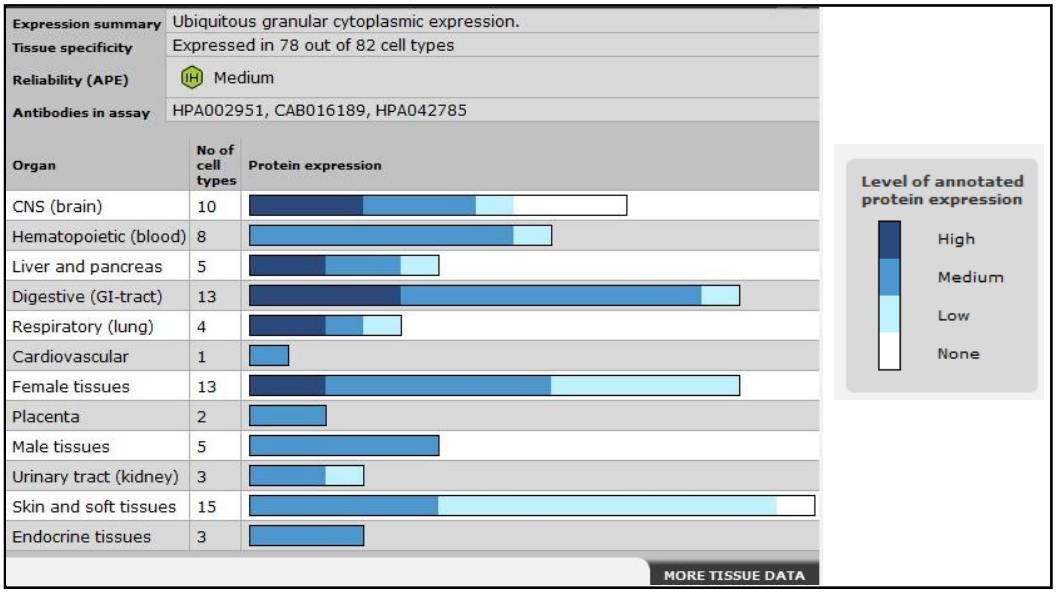

Figure 2. The analysed normal tissues are grouped into organs, and the number of annotated cell types for each organ type is given, followed by the annotated protein expression (blue color scale). The intensity of the color represents the relative level of expression/staining, as described by the scale in the box to the *right*. In the bars, the fraction of the protein expression/antibody staining with certain intensity represents the percentage of the analysed cell types with that relative expression/staining (www.proteinatlas.org)

More information on protein expression could be obtained also from the literature. At the beginning, the IHC analysis performed on normal tissues confirmed the expression of CSPG4 in melanocytes, endothelial cells and perycites (Campoli et al., 2010; Schlingemann et al., 1990; Schlingemann et al., 1991). In particular, the expression in perycites seems to correlate with the activated form of these cells, since it is preferentially expressed on perycites associated with neovascularization in vivo (Schlingemann et al., 1991). More recently, in restrict area of the interfollicular epidermis as well as in the basal layer of normal oral mucosa and follicular papilla of hair follicle (Ghali et al., 2004). Moreover CSPG4 was found on chondrocytes in adult articular cartilage (Midwood and Salter, 1998), smooth muscle cells (Tordsson et al., 2000),differentiated myofibers of the sarcolemma and neuromuscular junction of human postnatal skeletal muscle (Petrini et al., 2003), and microglial and mesangial cells of the renal glomerulus(Pouly et al., 1999). CSPG4 is also expressed on oligodendrocyte progenitor cells(Chang et al., 2000) and in human bone marrow mesenchymal stromal cells (Campoli et al., 2010; Kozanoglu et al., 2009).

Furthermore, to clarify the mRNA expression profiles of CSPG4 in different healthy and pathological tissue, instead, a good tool could be another online database: GENT (Gene Expression database of Normal and Tumor tissues). It is a web-accessible database that provides gene expression patterns across different human cancer and normal tissues. More than 40000 samples, profiled by Affymetrix U133A or U133plus2 platforms in many different laboratories across the world, were collected from public resources and combined into two large data sets, helping the identification of cancer outliers that are over-expressed in only a subset of these patients (http://medicalgenome.kribb.re.kr/GENT/overview.php;(Shin et al., 2011)). They pre-processed the collected data using the MAS5 algorithm (Affymetrix package; (Gautier et al., 2004)) a single-array algorithm in which expression values are independent of other data, than normalizing each sample to a target density of 500. The new data sets released on the Gene Expression Omnibus (http://www.ncbi.nlm.nih.gov/geo/) and ArrayExpress (http://www.ebi.ac.uk/microarray-as/ae/) are monitored and updated every month (Barrett et al., 2009; Parkinson et al., 2011).

From this database, considering the U133plus2 platform data set, CSPG4 results higher expressed in cancer (C) than in co-respective healthy tissue (N) in many tissues as: brain, colon, head-neck, liver, ovary, pancreas, skin and vulva (http://medicalgenome.kribb.re.kr/GENT/overview.php; **Fig. 3**).

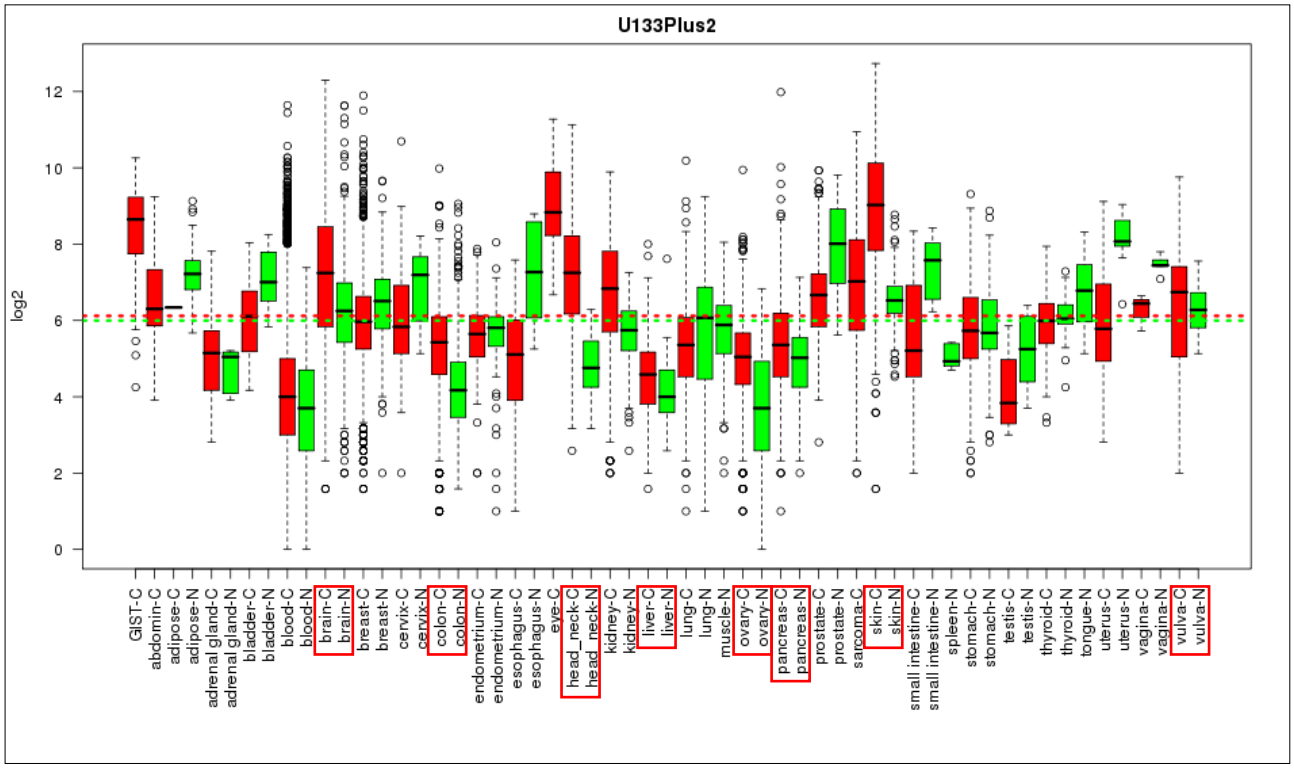

Figure 3. Log-base-2 values of CSPG4/NG2 expression, obtained after analysis of collected Affymetrix arrays (U133plus2 platforms), in different healthy (-N; green bars) or cancer tissues (-C; red bars).The red boxes highlight the cases in which the CSPG4 expression was higher in cancer than in the co-respective healthy tissue (http://medicalgenome.kribb.re.kr/GENT/search/view_result.php).

For mRNA expression in normal tissues, few information could be obtained from literature. For example, Erfurt and collaborators (Erfurt et al., 2007), with qPCR, detected CSPG4 transcripts in a variety of normal tissues as in normal tissues such as lung, heart, kidney, and thymus.

Pattern of CSPG4 expression in cancer tissues

Online databases are useful to obtain many information, also for the expression profiles in tumors. Referring yet to Protein Atlas, it is possible to find that their antibodies stained in a moderate or strong way in 86% of breast cancer, 82% of carcinoid, 66% of cervical cancer, 97% of colorectal cancer, 83% of endometrial cancer, 47% of glioma, 92% of head and neck cancer, 75% of liver cancer, 85% of lung cancer, 39% of lymphoma, 89% of melanoma and of ovarian cancer, 91% of pancreatic cancer, 88% of prostate cancer, 51% of renal cancer, 72% skin cancer, 97% of stomach cancer,92 % of testis cancer, 83% of thyroid cancer and 85 % of urothelial cancer (**Fig. 4**).

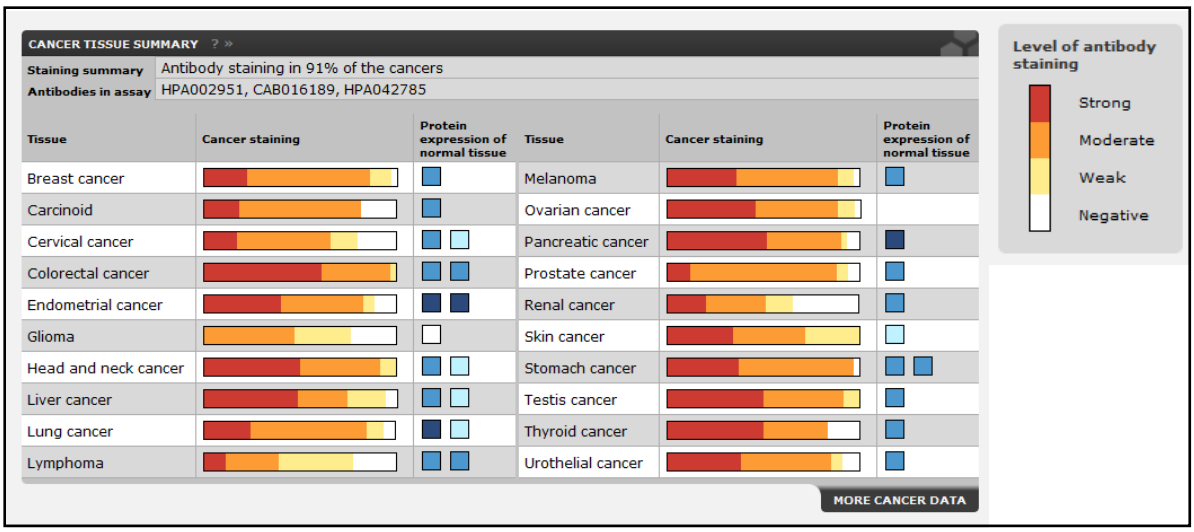

Figure 4. The cancer tissue summary section shows a summary of antibody staining in numerous different cancer tissues. The staining summary reports the percent of analysed samples where antibody staining could be detected. For each cancer tissue, the relative level of antibody staining for the analysed samples using the available antibodies is reported in the antibody staining bar (as described by the scale in the box to the right). To the right of the bar is the antibody staining (if yellow color scale)/annotated protein expression (if blue color scale) for the corresponding normal cell types. For ovary cancer there is no corresponding normal cell types (www.proteinatlas.org).

Elsewhere in the literature other information could be obtained on CSPG4 expression in tumors, but it is very difficult to defined his expression profile in a univocal pattern in these samples. Indeed, in many cases, could be found a variability due to the low number of patients analyzed in each paper and the different reagent used for the analysis (for instance the antibody in the immunohistochemistry (IHC) analysis). Moreover, considering that CSPG4 is also expressed in correspondence of the vasculature in both healthy or pathological tissue, sometimes the authors didn't distinguish the CSPG4-positivity of tumor cells from that observed on the tumor vessels, evaluating the staining of the tumor as a whole.

CSPG4, also called high molecular weight- melanoma associated antigen (HMW-MAA) , was first identified on human melanoma cells by Wilson and collaborators in 1981 (Wilson et al., 1981). This proteoglycan has been found to be expressed on more than 90% of the nevi and melanoma lesions analyzed, with a limited degree of intra-and interlesional heterogeneity (Campoli et al., 2010; Price et al., 2011; Natali et al., 1981; Natali et al., 1983). Furthermore, if CSPG4 is expressed in over 85% of primary and metastatic melanoma lesions, with similar levels of expression among lentigo maligna, nodular, and superficial spreading melanomas (Wilson et al., 1981; Kageshita et al., 1993; De Giorgi et al., 2011), a more variable and generally lower CSPG4- expression has been reported in acral lentiginous melanomas, ranging from 30% (Kageshita et al., 1993) to 53.6%

(Campoli et al., 2010; De Giorgi et al., 2011; Nishi et al., 2010). In this tumor type the expression of the proteoglycan is significantly higher in metastatic than in primary tumors (Campoli et al., 2010; Kageshita et al., 1993; Nishi et al., 2010; Kageshita et al., 1991), and, since it is correlated with the clinical course of the disease (Kageshita et al., 1993), his expression in primary tumors is associated with poor prognosis (Campoli et al., 2010; Kageshita et al., 1993). In mucosal melanoma the expression of CSPG4 was found to be lower than in nodular melanoma lesions , although, as the authors pointed out, the low number of cases cannot allow to reach definite conclusions (Campoli et al., 2010; Kageshita et al., 1994).

The proteoglycan was found expressed also in desmoplastic melanoma (DM) (Goto et al., 2010). In this study, CSPG4 resulted more sensitive than HMB-45 and MART-1,two melanocyte biomarkers, for IHC diagnosis of primary DM. Moreover, the CSPG4 mAb cocktail is valuable for detecting occult DM metastases, especially in regional tumor-draining lymph nodes. The study indicates that HMW–MAA is more sensitive than MART-1 as mRNA biomarker for primary DM. Because HMW–MAA mRNA was detected in metastatic DM that did not express MART-1 mRNA, combining these biomarkers for qRT-PCR assay might increase the sensitivity of mRNA assessment for high-risk DM that may metastasize to LNs. Thus HMW–MAA has potential value as a component of a multimarker probe for qRT-PCR assessment of DM metastases (Goto et al., 2010).

In uveal melanoma, the expression of the proteoglycan showed contradictory results (Campoli et al., 2010). Indeed if the expression of CSPG4 in these tumors in some studies seems to be lower than in primary cutaneus melanoma lesions (Natali et al., 1983; van der Pol et al., 1987), it resulted high expressed ,similar to the primary lesions, in other (Bomanji et al., 1987; Li et al., 2003).

In conjunctival melanoma (CoM), lymph node metastases of cutaneous melanoma (CM) and conjunctival nevi (CoN) , was found that CSPG4 was expressed at significantly higher levels in CoM and in the lymph node metastases of CM than in CoN (Westekemper et al., 2010). However, surprisingly, CoM tumours with lower CSPG4 expression had a higher risk for local recurrence and developed their first recurrence earlier than tumors with high MCSP expression. (Westekemper et al., 2010).

The expression of proteoglycan was observed in different tumor type correlating with the aggressive phenotype. In malignant mesothelioma (MM) 24 of 41 biopsies were positive to CSPG4 staining in IHC(Rivera et al., 2012), and, in particular, in 5 of 5 sarcomatoid MM biopsies , in 5 of 5 biphasic MM and in 15 of 31 epithelioid MM.

In sarcoma primary lesions showed de novo expression or amplification of NG2 when compared to adjacent healthy tissue . NG2 transcription was further found to be significantly increased in metastases when compared to primary lesions of the same patient (Benassi et al., 2009). In particular this difference was most striking for malignant fibrohistocytoma-like (MFH-like) and leiomyosarcoma (LMS).

In hematologic tumors , CSPG4 resulted expressed in childhood and adult acute lymphoblastic leukemias (ALL) with mixed lineage leukemia (MLL) gene rearrangements (Behm et al., 1996; Smith et al., 1996; Mauvieux et al., 1999; Drake et al., 2009). His expression was restricted to monoblastic cases in acute myeloid leukemias (AML) (Mauvieux et al., 1999). The expression of the proteoglycan is present in ALL poor-prognosis patients with abnormalities of chromosome band 11q23 (Smith et al., 1996), and seem to be a good marker in childhood ALL to identify the patients with t(4;11) MLL rearrangement (Behm et al., 1996), the most important criteria for high-risk stratification in protocols for childhood ALL. However, despite the fact that an antibody specific against CSPG4 reduced AML cell growth and enhanced the anti-proliferative effect of cytarabine *in vitro,* it had no detectable effect on survival or growth of leukemia cells *in vivo* (Drake et al., 2009).

Other evidences highlight the role of proteoglycan also in squamos cell carcinoma (SCC) to hijack the homeostatic controls that operate in normal stem cells, eliminating those that maintain stem cell quiescence (Jensen et al., 2008). Moreover the expression of CSPG4 was confirmed also in ALDH positive cells, marker of normal and malignant human mammary stem cells, in squamous cell carcinoma of head and neck (SCCHN) and in basal breast carcinoma (Wang et al., 2010b). The specific treatment in mouse model of CSPG4 positive tumors in xenograft experiments indicate that CSPG4 can mediate the destruction of cancer stem cells (CSC). If the results in mice will be duplicated in humans, CSPG4-targeted immunotherapy has the potential to target and eradicate CSC, which are responsible for recurrence of lesions and for metastasis, according to the cancer stem cell theory (Wang et al., 2010b). The capability of an anti-CSPG4 therapy to reduce the recurrence was analyzed also in triple negative breast cancer (TNBC) (Wang et al., 2010a). The hypothesis was suggested by the evidence that the expression of CSPG4 protein was noted in 32 of the 44 (72.7%) primary TNBC lesions ,considering also 10 weak positive tumors, but it was detected in only eight of the 28 (28.6%) ER^+ and in three of the 18 (16.7%) $HER2^+$ breast cancer primary lesions. However the authors performed the experiment to inhibit the tumor recurrency

targeting CSPG4, performed using only MDA-MB-435 cells line, a tumor cell line that was confirmed to have a melanoma and not breast origin (Ross et al., 2000; Rae et al., 2007).

The IHC staining for CSPG4 on patients biopsies in many types of malignant brain tumors, resulted negative in meningioma (Chekenya et al., 2002), week positive or absent in astrocytoma (Chekenya et al., 2002; Shoshan et al., 1999), moderate or high expression in medulloblastoma end oligodendroglioma, (Chekenya et al., 2002; Shoshan et al., 1999). On the contrary, the expression of the proteoglycan in glioblastoma multiforme tumors (GBM) seems to be controversial. Indeed if Shoshan Y. and collaborators (Shoshan et al., 1999) observed that only 1 of 5 GBM biopsies from patients were CSPG4 positive, Schrappe M. and colleagues (Schrappe et al., 1991) observed positivity on 5 of 5 GBM biopsies using the same antibody for the IHC analysis (the clone 9.2.27). Moreover, if Wang performed experiments with CSPG4-positive tumor cells obtained from 3 different patients cells (Wang et al., 2011a), Svedensen analyzed 76 biopsies by IHC analysis (Svendsen et al., 2011) and observed that the staining was strong in both tumor and vasculature cells in 27 cases, only in cell tumors in 11 cases, while in 15 cases it was strong only in the tumor vasculature . They, considering the high expression of the proteoglycan in the tumor, suggested that CSPG4 could identified the 50% of GBM patients who respond poorly despite optimal treatment.

NG2/CSPG4 influences tumor cell-microenvironment interactions

CSPG4 does not exhibit any known catalytic activity and seems to have modest signal transducing capabilities of its own, but serves as a mediator of membrane-ECM interactions, modulating the crosstalk between the tumor cell and their microenviroment . Indeed, there are evidences that this proteoglycan could directly interact with different ECM molecules and growth factors present in the microenviroment, but also with growth-factor receptors, integrins and metalloproteinases present on the surface of tumor cells. CSPG4 modulates the adhesion and motility of cells binding Collagen types II, V, and VI, Laminin 2, tenascin and fibronectin, activating indirectly such cytoplasmic kinases as FAK and ERK 1/2. Moreover this proteoglycan seems involved directly in the binding of FGF or PDGFaa, presenting these growth factors to their receptors and modulating the cell proliferation (Stallcup and Huang, 2008; Cattaruzza et al., 2012). Cell adhesion and migration, could be regulated also by CSPG4 interacting with integrins ,as alpha 4-beta1 and alpha 3-beta1 (Iida et al., 1995; Eisenmann et al., 1999), and regulating the activity of some MMP (such

as MT1-MMP, MT3-MMP, MMP2 and MMP7) conferring to the cell an higher invasion capability, being then of key importance in tumor progression (Airola et al., 1999; Iida et al., 2001).

Role of CSPG4/NG2 in the control of tumor cell motility and invasion

The first demonstration that NG2 can be important for cell motility came as a result of the finding that NG2 is a cell surface ligand for type VI collagen (Stallcup et al., 1990; Nishiyama and Stallcup, 1993). Rat B28 and human U251 glioma cells were trasfected with recombinant deletion mutants of NG2 to verify the adhesion and motility in presence of a collagen type VI coating. The expression of deleted mutant NG2 without the D2 domain improve the ability of cells to adhere and migrate if compared with the NG2 full-length trasfected cells. Moreover under basal conditions, the motilities of U251 and U251/ NG2 cells were similar. Upon stimulation with PMA or PDGF, however, U251/NG2 motility increased significantly compared to that of U251 cells. Further investigation showed that PMA or PDGF triggered PKCalpha-dependent phosphorylation of NG2 at Thr-2256 (Makagiansar et al., 2004) and that this phosphorylation event was required for the increase in motility. NG2 phosphorylated at Thr-2256 was found to be co-localized with alpha3-beta integrin in broad lamellipodia at the leading edges of motile cells (Makagiansar et al., 2004).
Moreover the involvement of CSPG4 was verified in melanoma cells too. Indeed using an antibody isolated from Rabbits specific for the protoglycan, were affected the sprading, the migration on Collagen I and Matrigel invasion of MV3 melanoma cells (Luo et al., 2006). The data regarding the M14 trasfected cells to induce the expression of CSPG4, presented in the same paper, are less clear and contradictory. Indeed, despite the authors confirm the constitutive absence of the proteoglycan in the M14 cell line, used as control in the migration experiments, different biotechnology company commercialize specific antibody against CSPG4, obtained immunizing mice or rabbit with human M14 melanoma cell extract depleted of fibronectin, considering the results obtained by other research groups ((Bumol et al., 1984); Santa Cruz, Millipore).
The importance of CSPG4 in the modulation of melanoma cells invasion capability was analized in different cell lines : WM164, 1205Lu, WM1341D expressing CSPG4 constitutively, and WM1552C, indicated as negative, transfected in order to induce the over expression of the proteoglycan. In this case CSPG4 seems to stimulate EMT-related changes in radial growth phase (RGP) cells and enhance the expression of c-Met and hepatocyte growth factor (Yang et al., 2009). Moreover this

proteoglycan is required to cause a robust and sustained activation of Erk1,2 in several melanoma cell lines that express mutant active BRAF (Yang et al., 2009; Smalley, 2003; Yang et al., 2004; Satyamoorthy et al., 2003). The consequences of Erk1,2 pathway activation include entry into the cell cycle, increased expression of key melanoma transcription factors, and other key factors important for invasion such as matrix metalloproteinases (Smalley, 2003). Erk1,2 activation can also lead to increased adhesion by increasing the expression of specific (e.g., beta 3) integrin subunits and elevated resistance to apoptosis (Smalley, 2003).

In melanoma cells CSPG4 is also known to stimulate the integrin-alpha4 beta1-mediated adhesion and spreading. The proteoglycan, in these case, recruits tyrosine-phosphorylated p130cas, an adaptor protein important in tumour cell motility and invasion. CSPG4 stimulation also results in a pronounced activation and recruitment of the Rho-family GTPase Cdc42. CSPG4-induced spreading of melanoma cells is dependent upon active Cdc42, a Cdc42-associated tyrosine kinase (Ack-1) and tyrosine phosphorylation of p130cas (Eisenmann et al., 1999; Majumdar et al., 2003).

Moreover in the highly metastatic melanoma amoeboid cell line A375M2, siRNA-mediated down-regulation of CSPG4 induced an amoeboid-mesenchymal transition associated with decreased invasiveness in 3D collagen and inactivation of the GTPase Rho. Conversely, the expression of NG2 in mesenchymal sarcoma K2 cells as well as in A375M2 cells resulted in an enhanced amoeboid phenotype associated with increased invasiveness and elevated Rho-GTP levels. Remarkably, the amoeboid-mesenchymal transition in A375M2 cells triggered by CSPG4 down-regulation was associated with increased extracellular matrix-degrading ability, although this was not sufficient to compensate for the decreased invasive capability caused by down-regulated Rho/ROCK signaling. Conversely, in K2 cells with overexpression of the proteoglycan, the ability to degrade the extracellular matrix was greatly reduced (Pankova et al., 2012).

A great importance of CSG4 in the modulation of motility and invasion capability of tumor cells was confirmed also in malignant mesothelioma (MM) (Rivera et al., 2012). The use of a specific antibody against CSPG4 resulted in decreased phosphorylation of focal adhesion kinase (FAK) and AKT, reduced expression of cyclin D1 and apoptosis. Moreover, the same antibody, significantly reduced MM cell motility, migration, and invasiveness (Rivera et al., 2012).

Less clear is the role of CSPG4 in the modulation of motility in Triple Negative Breast Cancer (TNBC). Indeed, the CSPG4 protein expression was assessed in 32 of 44 primary TNBC lesions, referred 10 of 32 weak positive, and in TNBC cell lines as HS578T, MDA-MB-231, MDA-MB-435, and SUM149,(Wang et al., 2010a). However the researchers excluded from the analysis different

TNBC cell lines negative for CSPG4, analyzed in our laboratories (for example MDA-MB-468 or HCC1937), assuming that their cell lines were representative of all TNBC. Moreover the migration and adhesion analysis in vitro was performed only with MDA-MB-231 and MDA-MB-435 cell lines ,but the last one, positive for CSPG4, since from 2000 is reported to have a melanoma origin, (Ross et al., 2000), resulting essentially identical to M14 cell lines as far as to cytogenetic characteristics as well as gene expression patterns (Rae et al., 2007). Furthermore for tumor-recurrence experiments the authors used only the MDA-MB-435 cell tumors (Wang et al., 2010a).

CSPG4/NG2 promotes tumor cell proliferation and survival

CSPG4/NG2 is widely accepted as a marker for oligodendrocyte progenitor cells (OPCs) throughout development. However, NG2 positive cells residing in the adult Central Nervous System (CNS) do not resemble embryonic or neonatal NG2-cells in terms of their morphology or proliferation characteristics, but instead represent a unique type of glial cell that has the ability to react rapidly to CNS damage (Polito and Reynolds, 2005). Based on the fact that cell proliferation makes an obvious contribution to tumor growth and progression, a key finding with regard to the role of NG2 in cell proliferation, in particular in glioma, in which it is highly expressed, was that the proteoglycan is capable of binding with high affinity to growth factors FGF2 and PDGF-AA (Stallcup and Huang, 2008; Cattaruzza et al., 2012; Goretzki et al., 1999). In fact it seems that depending from the interaction with these growth factors, it is possible to find a phosphorylation at Thr-2314 of NG2 catalyzes by ERK 1/2 , stimulating cell proliferation (Stallcup and Huang, 2008).
Interestingly, alpha3beta1 integrin activation is also required for this NG2-dependent increase in proliferation, but in a different way, as compared to the activation of motility pathway. This seems dependent to the localization of the NG2/ integrin complex to two distinct microdomains, depending on the NG2 phosphorylation status. NG2 phosphorylated at Thr-2314 is co-localized with alpha3beta1integrin on microprojections on the apical cell surface. NG2 phosphorylated at Thr-2256 is co-localized with alpha3beta1 integrin in leading edge lamellipodia. For this reason if in apical microprojections the integrin must interact with a different set of signaling molecules required for proliferation, in lamellipodia it interacts preferentially with cytoplasmic machinery required for motility (Stallcup and Huang, 2008). Moreover the NG2-dependent activation of alpha3beta1 integrin also has effects on cell survival due to increased signaling through the PI3K/AKT pathway (Chekenya et al., 2008).

Further studies in multiple melanoma cell lines expressing the mutant BRAF ^{V600E}, the most common present in tumors with BRAF mutation (Namba et al., 2003), have shown that these cells requires expression of a full-length CSPG4 expression sustained and maximal ERK 1,2 activation (Price et al., 2011; Wang et al., 2010b; Yang et al., 2009; Satyamoorthy et al., 2003). The treatment with CSPG4 antibodies also enhance the effects of BRAF^{V600E}-specific inhibitors in glioblastoma multiforme and melanoma cells, preventing or deleing the development of resistance to the inhibitors in these tumors, and implying that CSPG4-mediated activation of ERK 1,2 may also occur through a BRAF-independent mechanism, enhancing the tumor growth (Price et al., 2011).

In the last years the importance of CSPG4 in the modulation of the growth and aggressiveness was emphasized in many tumor types. Indeed, its high expression has also been found in basal cell carcinoma, astrocytomas, neuroblastomas, sarcomas, breast carcinoma lesions. Treatment of these tumors with specific antibody against CSPG4 in a xenograft model seems to impaired the tumor growth and induced a reduction of metastasis formation (Rivera et al., 2012; Wang et al., 2011a; Ghose et al., 1991; Hafner et al., 2005; Wagner et al., 2008; Wang et al., 2011b; Burns et al., 2010). Same results were obtained in similar experimental conditions using some glioblastoma multiforme (GBM) tumors cell lines (Wang et al., 2011a).

Other studies have shown that the expression of NG2/CSPG4 in GBM cells correlate with resistance to ionizing radiation (IR), rapidly recognised DNA damage and effectuated cell cycle checkpoint signaling (Svendsen et al., 2011). Moreover, in these experiments, the proteoglycan seems to mediate the resistance to radiotherapy through induction of ROS scavenging enzymes and modulating the DNA damage signalling.

CSPG4/NG2 contributes to tumor angiogenesis

An important step in the increase of tumor aggressiveness is the new vessels formation within the tumor microenviroment. The role of CSPG4 in this process could be suggested, first of all, by the fact that the proteoglycan is usually expressed in pericytes in healty tissues and also in pericytes tumor associated. An explanation of his role in vasculature modulation could be highlighted by the modulation CSPG4-dependent of FGF pathway in perivascular cells. Indeed CSPG4 may serve as a dual modulator of the availability/accessibility of FGF2 at the cell membrane of perivascular cells, as well as the result of FGFR transducing activity, interacting with FGFR1 and FGFR3 (Cattaruzza et al., 2012). The high expression of proteoglycan was confirmed in vasculature associated to glioma

tumors (Stallcup and Huang, 2008; Schlingemann et al., 1990; Chekenya et al., 2002; Schrappe et al., 1991; Wesseling et al., 1995), in correlation with different aspect of vasculature, first of all the augmentation of proliferating capillary endothelial cells in high malignant phenotype tumors (Stallcup and Huang, 2008; Schlingemann et al., 1990; Chekenya et al., 2002; Schrappe et al., 1991; Wesseling et al., 1995). An explanation could be suggested by the finding that NG2 seems able to bind angiostatin blocking its ability to inhibit endothelial cell proliferation (Stallcup and Huang, 2008; Chekenya et al., 2002; Goretzki et al., 2000). At the same time the increase of vasculature in these tumors might be due to the ability of pericyte-derived NG2 to mediate recruitment of endothelial cells via engagement of galectin-3 and alpha3beta1 integrin (Stallcup and Huang, 2008; Fukushi et al., 2004). Moreover xenograft implantation of spheroids obtained from U251N-CSPG4, glioblastoma cells trasfected to overexpress the proteoglycan, induced the formation of tumors characterized by highly angiogenicity, indicated by the presence of large, leaky and haemorrhagic vessels, with morphological features of “vascular lakes” (Wang et al., 2011a). The treatment of these glioblastoma multiforme (GBM) tumors with NG2 shRNAs reduced NG2 expression and resulted in morphologically smaller and less hemorrhagic vessels. The same result was obtained with xenograft implantation of cells obtained from biopsies, however none clinical information could be inferred about the two patients from which the tumors were explanted, and no other GBM cell line was used for this kind of experiments (Wang et al., 2011a).

Clinical significance of CSPG4/NG2

The capability of this proteoglycan to modulate different pathways associated with oncogenic transformation, as cell proliferation, migration and invasion highlights CSPG4 as a good candidate for being a prognostic factor or a therapeutic target in different tumor types.

CSPG4 as a putative prognostic factor

As described previously the link between CSPG4 and melanoma progression was first appreciated as a result of its widespread expression in the majority (80% or greater) of superficial spreading and nodular human melanomas (Campoli et al., 2010). In superficial spreading and ⁄ or nodular melanoma, the core CSPG4 protein is expressed at multiple stages of melanoma progression and is even detected prior to tumor initiation in melanocytes within nevi. In these subtypes of

melanoma, CSPG4 is not considered a prognostic factor, because it is expressed prior to the initiation of tumor formation and, indeed, it has been detected on melanocytes in vitro (Price et al., 2011). Although not considered as prognostic factor in superficial spreading or nodular melanoma, some studies have suggested that it may be negatively prognostic in acral lentiginous melanomas (Kageshita et al., 1993).

Also circulating melanoma cells (CMCs) are thought to be valuable in improving measures of prognosis in melanoma patients and may be also a useful marker of residual disease to identify non-metastatic patients requiring adjuvant therapy. The presence of circulating tumour cells is associated with poor prognosis in early stage uveal melanoma (Ulmer et al., 2008) and other metastatic cancers (Cohen et al., 2008; de Bono et al., 2008; Cristofanilli, 2006; Lucci et al., 2012). Anti-CSPG4 antibodies have been commonly used to isolate CMCs through positive immunomagnetic enrichment (Ulmer et al., 2008; Kitago et al., 2009; Sakaizawa et al., 2012) as well as for identification of CMCs by flow cytometry (Fusi et al., 2012). Moreover, considering that the expression of another molecule, the melanoma cell adhesion molecule (MCAM), is associated with an aggressive, invasive phenotype and upregulation is linked with disease progression (Mangahas et al., 2004; Shih et al., 1994; Medic and Ziman, 2010), recent results seem to support and suggest the use of CSPG4 in combination with MCAM to enrich the general CMC population (Freeman et al., 2012).

Moreover Smith and collaborators (Smith et al., 1996) observed that Acute Myeloid Leukemia (AML) patients expressing CSPG4 had a poorer outcome as far as survival and event-free survival, with an actuarial survival rate at 4 years of 16.7%.

In another tumor type, glioblastoma, the expression of CSPG4 seems to predict not only poor survival outcome of the patients (Svendsen et al., 2011), but also the resistance of the tumor to ionizing radiation.

CSPG4 overexpression could rather function as a metastasis predictive factor also in sarcoma tumors (Benassi et al., 2009). Indeed, the expression levels of NG2 proteoglycan in presurgical original lesions of soft-tissue sarcoma (STS) patients defines with 55% probability the risk to develop postsurgical secondary lesions, independently of any other clinical trait. Moreover in the cohort of high-grade STS cases, transcription of CSPG4 also showed a 81-fold amplification in metastatic lesions, when compared to primitive ones. In a similar manner as seen in primitive lesions, patients with higher levels of metastatic NG2 encountered a significantly more dismal clinical course (Benassi et al., 2009).

CSPG4 as a putative therapeutic target

Being highly expressed in human melanoma cells, CSPG4 has been selected for development of various vaccine- and antibody-based therapeutic approaches. These include antagonistic monoclonal antibodies (Hafner et al., 2005), T cell engaging trifunctional antibodies(Ruf et al., 2004), immunotoxins (Spitler et al., 1987), and bispecific antibodies (Pfosser et al., 1999). Furthermore, a humoral and/or a cellular immune response to the nominal antigen has been elicited in a variable percentage of patients with melanoma immunized with anti-idiotypic antibodies, which mimic the HMW-MAA (Murray et al., 2004; Mittelman et al., 1990; Mittelman et al., 1992; Mittelman et al., 1994; Mittelman et al., 1995; Quan et al., 1997; Pride et al., 1998). This immune response has been found to be associated with regression of metastases in a few patients (Mittelman et al., 1994) and with disease-free interval and/or survival prolongation (Mittelman et al., 1990; Mittelman et al., 1995; Quan et al., 1997). However ,so far, none of these candidates has advanced to later stages of clinical development (Bluemel et al., 2010), open to a new possibility like 'bispecific T cell engager' (BiTE) (Baeuerle et al., 2009),antibodies which can transiently connect T cells and target cells via binding to CD3 and a selected surface target antigen (Bluemel et al., 2010). On the other hand, although still in a preclinical model, Schmidt P. and collaborators (Schmidt et al., 2011) addressed the scenario by adoptive transfer of cytotoxic T cells (CTLs) with redirected specificities toward the bulk of melanoma cells and toward specific melanoma cell subsets, respectively, of an established tumor lesion. T cells were engineered with a chimeric antigen receptor (CAR, immunoreceptor) whose extracellular antibody domain binds to a predefined antigen in a MHC-independent manner and triggers T-cell activation upon antigen engagement via the intracellular CD3ζ signaling domain. By adoptive transfer of CAR-redirected CTLs, they revealed that established tumor lesions can be efficiently eradicated by targeted elimination of the less than 2% subset of melanoma cells with the CD20 and CSPG4 positive phenotype, without targeting the tumor cell mass, whereas targeted elimination of any other minor subset is less effective (Schmidt et al., 2011). In this way they induce a differential effect of targeting tumor cell subsets with different proliferative and tumor-sustaining capacities, caracterizated by the expression of the proteoglycan.

Moreover, recent studies emphasized the induction of HMW-MAA-specific humoral immunity by using mimotopes as immunogens in melanoma (Wagner et al., 2008; Latzka et al., 2011). Mimotopes are small peptides that mimic conformational B cell defined-epitopes of antigens and

can be selected by screening random peptide phage libraries with a mAb of interest. However, despite confirmed affinity selections as well as analog immunization protocols , not every mimotope truly mimics the relevant epitope of the original antigen. On one hand, limitations might originate during affinity selection, as phage displaying peptides may bind to residues of the mAb that are not part of the paratope (Latzka et al., 2011). Although such peptides might inhibit the binding of their defined mAb to the original epitope, these will fail to induce a specific immune response to the original antigen (Latzka et al., 2011). In addition, B cell epitopes are known to be conformational in nature (Yang and Yu, 2009). Hence, it is possible that mAbs recognize certain conformations of epitopes which are not displayed in the same structural context by the natural antigen (Latzka et al., 2011).

The evidences that CSPG4/NG2 plays a functional role in angiogenesis and tumor development, induced to consider as therapeutic target not only the proteoglycan expressed by tumor cells, but also, although still in preclinical models, the blood vessels CSPG4-expression in glioblastoma and melanoma tumors (Wang et al., 2011a). More recently this aspect was emphasized also in another tumor model. Indeed, Krissa Gibby and collaborators (Gibby et al., 2012) defined the importance of NG2 in mediating the respective effects of pericytes, myeloid cells, and adipocytes on mammary tumor progression. These evidences suggest that targeting the proteoglycan may be an even more powerful approach due to inhibitory effects on both tumor and stromal compartments (Gibby et al., 2012).

Furthemore, there are other aspects that seems to highlight the importance of CSPG4 in the aggressiveness of cancer. Indeed, some evidence suggests that CSPG4 may also influence drug resistance. Chemoresistance is a major factor in the successful treatment of melanoma and other cancers. Although tumors in many patients initially respond to therapy, resistance to treatment develops over time leading to cancer progression. The development of drug resistance in melanoma appears to be particularly linked to the use of single-target inhibitors, such as those that target $BRAF^{V600E}$ (Price et al., 2011). CSPG4 expression is associated with multidrug resistance in glioblastoma and melanoma tumor experimental models, and this is mediated by its association with integrin- induced activation of PI3K pathways (Chekenya et al., 2008). The ability of anti-CSPG4 mAb to prolong the growth inhibitory effects of PLX4032, a $BRAF^{V600E}$ inhibitor, on melanoma cell lines in culture provides direct evidence for a role of this proteoglycan in promoting chemoresistance (Price et al., 2011; Yu et al., 2011).

MATERIALS AND METHODS

Cell lines and RNAi

Human sarcoma and melanoma cell lines MeWo, SW872, SW982, HT1080, MES-SA, 143B, MG63, A375, RD/KD, SK-UT-1,Wi38,VA-13 (fibroblastSV40 transformed) and SK-LMS-1 were obtained from ATCC and grown in DMEM (Lonza Walkersville, Maryland, USA) with 10% FBS (Sigma-Aldrich). The sarcoma cell line GCT was provided by Istituto Zooprofilattico Sperimentale della Lombardia e dell'Emilia Romagna (Brescia, Italy) and maintained in McCoy's 5A medium (GibcoTM, Invitrogen) with 10% FBS. Wild type and Col VI knock-out embryonic fibroblasts was provided by Prof. Paolo Bonaldo(University of Padova) and mantained in DMEM (4.5 g/L glucose) containing 15% of FBS. Uterine Smooth muscle cells (UtSMC) and Mesenchymal Stem Cells (MSC) were obtained by Lonza and grown in SmGM2 medium (Lonza),the Human Umbilical Vein Endothelial cell (HUVEC- Lonza) were grown in M199 medium with 20% and supplemented with bovine brain extract (100μg/ml; Sigma) siRNA probes against NG2 ,integrin β1 and scrambled versions of these probes were obtained through Ambion (Austin, TX). Transfections were performed by using siLentFect Lipid Reagent (Bio-RAD) according to manufacturer's protocol. The optimal siRNA concentration was observed at 20nM and 3μl/ml of siLentFect Reagent. For each well to be trasfected (12 well plate) was prepared 50μl of serum free-medium containing 3μl of siLentFect Reagent , and ,separately, 50μl of serum free-medium containing the siRNA. The two solution were mixed and incubated for 20 minutes at room temperature. Then the mix was added directly to cells in complete medium.

Transfection constructs and gene transduction

Sarcoma cell lines were transiently or stably transfected (using Lipofectamine Plus as a delivery vehicle; Life Technologies Inc.) with a plasmid containing either the cytoplasmic tail and membrane-spanning domain of the PG, or the membrane spanning domain plus the entire ectodomain. All these plasmids were provided by Prof. Stallcup (La Jolla Cancer Research Center).
Human NG2 cDNA clones B, C and D (Pluschke et al., 1996) were cut with XhoI and SacI, SacI and HindIII, HindIII and BamHI, respectively. These fragments were ligated and inserted into the pEGFP-N1 vector (Clontech Laboratories Inc.), and the sequence of the entire insert comprising bases 4030-7216 of the CSPG4 sequence reported with the NCBI accession number X96753 was verified by automated DNA sequencing. Dominant-negative-like mutant cells named $NG2^{cyto}$ were generated by treatment of cells stably transduced with a deletion construct encompassing the

transmembrane domain and cytoplasmic tail of NG2 with the 3'-end-directed siRNA probe NG21279 to specifically abrogate the constitutively produced NG2 and spare the transduced deletion construct. Dominant-negative mutant cells (with respect to the putative signal transducing activity of NG2 upon extracellular ligand binding) named $NG2^{extra}$ were analogously generated by stable transfection of the same cell lines with a GFP-plasmid containing the entire extracellular portion and the transmembrane domain of human NG2 (Cattaruzza et al., 2012). For this purpose, NG2 cDNA clones H, G and F 29 were cut with XhoI and ApaI, ApaI and BamHI, BamHI and HindIII, respectively, and inserted between the XhoI and HindIII sites in pEGFP-N1 vector (BD Biosciences Inc.). Total cDNA from A375 melanoma cells was used as the template to amplify the sequence corresponding to nucleotides 2230-5025, the fragment was inserted into a pGEM-T vector (Promega), and its sequence verified by automated DNA sequencing. The construct was then subcloned into the pEGFP-N1 expression vector containing fragments H, G and F as described above (BD Biosciences Inc.). Cells stably transfected with this plasmid were treated with a 5'-end-directed NG2 siRNA probe ($NG2^{C\text{-}terminus}$) to differentially eliminate the endogenous NG2 without affecting the transduced deletion construct. In both types of dominant-negative mutants, relative levels of expression of the full-length endogenous NG2, following siRNA knock-down, versus transduced truncated NG2 were determined at the mRNA level by quantitative real-time PCR as described above and by FACS and immunoblotting (Cattaruzza et al., 2012). Deletion constructs lacking different segments of the putative extracellular region of the PG involved in Col VI binding were obtained as previously described (Tillet et al., 1997; Burg et al., 1997) and provided by Prof. Stallcup (La Jolla Cancer Research Center). D1Δ1,D1Δ2 and D1Δ3 are three different deletion of Domain 1 of extracellular portion of NG2; D2Δ4 is the deletion of Domain 2; D1D2Δ5 is a deletion of NG2 extracellular domain comprised between Domain 1 and Domain 2.

ECM substrates

The various forms of Col VI as the monomeric forms of the collagen (*Monomers*), pepsin-digested tetramers (*P-tetramers*; i.e. tetrameric forms of the collagen lacking the *N*- and *C*-terminal globular domains of each of the constituent chains), a tetrameric fragment embodying only the collagenous portion of the molecule (*Collagenous fragment*) , the separated *N*- and *C*-terminal globular domains (*Globular domains*) and his intact tetramers, were purified as previously described by Perris and collaborators (Perris et al., 1993) and provided by Dr. Luigi de Marco (Centro di

Riferimento Oncologico - Aviano). The native Col VI microfilaments and disorganized oligomeric aggregates of tetramers formed in the presence of Ca2+ and at 37°C were shadowed in a Balzers MRD 010 evaporator and photographed in a Philips 410LS transmission electron microscope as described earlier (Morris et al., 1986). For purification of human Col VI microfilaments, human amnion was solubilized by digestion with bacterial collagenase from *Clostridium histolyticum* (Washington Biochemicals Corp., containing minor trypsin and clostripain activities), 2 x 5,000 U/200 g washed tissue, at room temperature for 48 hours (Rousselle et al., 1991) to liberate the (Wu et al., 1987)microfibrillar matrix components (Perris et al., 1993; Wu et al., 1987)). After removal of the Kalinin-Klaminin complex (which is a primary contaminant of Col VI placental preparations) from the digest using antibody affinity columns (Rousselle et al., 1991), material in the unbound fraction was concentrated by a 50% saturated ammonium sulfate precipitation. The precipitate was dissolved in 10 times (v/w) 0.2 M bicarbonate buffer, then fractioned on a molecular sieve column (Sephacryl S-400, superfine, Pharmacia) equilibrated with the same solution. Col VI microfilaments were excluded from the column and collected in the void volume fraction. Intact human Col VI tetramers were extracted from amniotic membranes with 0.05 M Tris-HC1, pH 7.0, containing 6 M guanidine hydrochloride and protease inhibitors (Kuo et al., 1997). To obtain the dissociation of α-chain, isolated tetramers were dialyzed against 50 mM Tris-HC1 buffer, pH 8.0, containing 0.4 M NaCl, 0.1 M KCl, and 5 mM EDTA and 8 M urea. The collagen then was incubated for 24 hr at 12°C in the presence of 25 mM dithiothreitol (DTT; Sigma), followed by alkylation with 0.1 M iodoacetamide or N-ethylmaleimide for 1 hr at room temperature. Denatured and reduced/ alkylated samples were dialyzed exhaustively against the original EDTA-containing Tris-HC1 buffer or against 0.1 M glacial acetic acid prior to being used in cell adhesion and migration assays. Other purified ECM molecules were obtained as follows: human fibronectin, collagen type III, tetrameric collagen type IV and vitronectin from Sigma-Aldrich; rat tail Col I and Matrigel from BD Biosciences; dimeric mouse collagen type IV from Merck Laboratories-Collaborative Research.

Isolation of cell-free native ECMs

Native Col VI-containing and Col VI-negative matrices were isolated from 3 to 7 passage embryonic fibroblasts derived from wild type, Col $VI^{+/+}$, and Col VI knockout, Col $VI^{-/-}$, mice. Other matrices were isolated from UtSMC,MSC,HUVEC,Wi38,VA-13. The cells were grown on glass coverslip for 4-

5 days in the presence of 0.25 M ascorbic acid until they reach confluence. Cells were extensively rinsed with Dulbecco's PBS at room temperature and then treated on ice for three periods of 10 minutes according to a procedure modified from Hedman ((Hedman et al., 1979); Nicolosi et al., *in preparation*), using 0.2% sodium deoxycholate (DOC) in 10 mM Tris-Cl buffered saline, pH 8.0, supplemented with a cocktail of proteinases inhibitors including, 4-(2-Aminoethyl) Benzene Sulfonyl Fluoride hydrochloride (AEBSF) 1mM; 6-aminohexanoic acid 5mg/ml; antipain 100 nM; aprotinin 800 nM; chymostatin 100 μM; E-64 10 μM; N-ethylamide 1μM; leupeptin 100 μM; pepstatin 1μg/ml (Sigma-Aldrich). Cell dishes were then gently washed 3 times for 10 minutes each on ice with a low ionic strength buffer, 2mM Tris-HCl, pH 8.0, containing the above proteinases inhibitors. Extreme care was taken during pipeting of the solution to avoid detachment of their matrix and to preserve the coverslips on ice. Isolated matrices were visualized by phase-contrast microscopy. For immunolabelling, samples were fixed in cold methanol (-20°C) for 7 min, washed in PBS and incubated for 15 min at 4°C with blocking solution (PBS 0.1% BSA). Samples were then incubated overnight at 4°C with anti-murine fibronectin (BD), with an anti-murine Col VI (ABCAM), or anti-human Col I polyclonal antiserum (Millipore Corp.) followed by FITC-conjugated antibody reaction (1 hr at 4°C). Samples were washed three times in PBS and mounted as previously described.

RNA extraction and qPCR

Total RNA was extracted from tumor cell lines (≈3.000.000), healthy and tumor specimens (≈150mg) and from peripheral blood lymphocytes obtained after informed consent using TRIzol Reagent (Invitrogen, Carlsbad CA) and stored at -80°C in RNA secure reagent (Ambion, Inc, Austin TX). RT of mRNA was carried out in 100μl final volume from 400ng total RNA using High Capacity cDNA Archive kit (Applied Biosystems, Foster City, CA) according to manufacturer's instructions. Quantitative PCR reaction was performed on cDNA, by ABI PRISM 7900 Sequence Detector (PE Applied Biosystems), with TaqMan technology. Expression of target genes, NG2 (CSPG4) and α3(VI) chain (COL6A3) was quantified using TaqMan Gene Expression Assays (Applied Biosystems) according to manufacturer's protocol and using Assay-on-demand primers with codes Hs99999905_m1 for GAPDH, Hs00426981_m1 for NG2 and Hs00365098_m1 for COL6A3. PCR mixture contained 1.25 μl Target or Endogenous Reference Assay Mix 20X, 22.2ng DNA diluted in 11.25 μl of distillate water, 12.5 μl TaqMan Universal Master Mix 2X (Applied Biosystems) in a 25

ml final reaction volume. Following activation of UNG (Uracil-N-Glycosylase) for 2 min at 50°C and of AmpliTaq Gold DNA polymerase for 10 min at 95°C all genes were amplified by 45 cycles for 15 seconds at 95°C and for 1 min at 60°C. For calculation of gene expression we used 2-ΔΔCT comparative method. The amount of target was normalized to an endogenous reference (GAPDH) and relative to a calibrator (cDNA from healthy lymphocytes). Each gene was considered up-regulated when the value was >1 (SD and under-expressed when the value was <1 ± SD. Value 1 corresponds to fluorescence emission in each amplification reaction for target and reference in pool of lymphocytes. Standard deviation of each 2-ΔΔct value were less than 0.2, according to protocol required for data reliability.

Immunohistochemistry and TUNEL assay

Immunohistochemical staining of human sarcoma samples was performed on formalin-fixed, paraffin-embedded specimens with a rabbit polyclonal antiserum to NG2 (antiserum D2; (Virgintino et al., 2007; Virgintino et al., 2008), an anti-α3(VI) chain monoclonal antibody (Novocastra), a mAb against Ki-67 (ABCAM) and a mouse mAb that we have produced in the past against human fibromodulin (clone 636B12). This latter antibody was used in conjunction with Masson's staining to highlight the intralesional stromal content. Antibody binding was revealed with the avidin-biotin-peroxidase complex method (BIOMEDA, Foster City CA). Surgical specimens of melanoma were used as reference. Tumor masses derived from human $NG2^+$ sarcoma cells grown in nude mice were fixed, embedded in OCT, and sectioned. The sections (7-μm thick) were incubated overnight at 4°C with a monoclonal anti-NG2 antibody (1:200; Millipore), with anti-α3(VI) chain monoclonal antibody (1:200), with a rat anti-CD31 (1:200) or with a rabbit polyclonal anti-SmActin (1:200), then washed with phosphate-buffered saline (PBS) and incubated with an Alexa fluor 488-conjugated or Alexa fluor 546- conjugates secondary antibody (1:400, Alexa Fluor, Life Technologies, Inc.). Cell nuclei were counterstained with either TO-PRO-3 (Life Technologies, Inc) or DAPI . The sections were washed three times with PBS, mounted under coverslips in mounting medium and examined with the use of a fluorescence microscope. The TUNEL assay was performed by "In Situ Apoptosis Detection Kit- Fluorescein TUNEL-based Apoptosis Detection Assay" (R&D System) according to manufacturer's protocol.

Immunocytochemistry and FACS

Cells to be stained were washed twice in PBS with 0.1% BSA and fixed with 4% PFA for 10 min. Fixed cells were further washed in PBS and sequentially incubated with: 2% v/v non-immune goat serum (Life Technologies Inc.) in PBS-BSA, primary antibodies (mouse anti-NG2 and rabbit anti-Actin) , secondary antibodies (anti-mouse or anti-rabbit Alexa Fluor-conjugated; Life Technologies Inc.), each diluted 1:100 in PBS-BSA and incubated for 1 hour at room temperature. Cell nuclei were counterstained with either TO-PRO-3 (Life Technologies, Inc) or DAPI and immunostained specimens mounted with Mowiol 4-88 (BD Biosciences) supplemented with 2.5 mg/ml DABCO (Sigma-Aldrich) anti-fading reagent. FACS analyses were carried out primarily with the anti-NG2 PE-conjugated antibody 7.1 (Beckman-Coulter) and the corresponding isotype matched control antibody. Immunosorting of $NG2^+$ and $NG2^-$ sarcoma cells was accomplished MACS-based magnetic bead separation using either the anti-NG2 antibody 9.2.27 (Millipore Corp.). Relative efficiency of the immunosorting procedure and approximate yield of $NG2^+$ cells was on average 23.4% for MG63 cells, 13.6% for HT1080 cells, and 18.7% for SKUT-1 cells.

Cell adhesion

Adhesion of siRNA-treated and untreated cells to various purified ECM components was examined using a previously detailed cell adhesion assay denoted CAFCA (*Centrifugal Assay for Fluorescence-based Cell Adhesion*; (Spessotto et al., 2009)), which allows for both qualitative and quantitative parameters of cell-substratum adhesion to be established (briefly described below). The CAFCA system briefly: 6-well strips of flexible polyvinyl chloride–denoted centrifugal assay for fluorescence-based cell adhesion (CAFCA) miniplates covered with double-sided tape (bottom units) were coated with 20 µg/ml of interested protein. Cells were labeled with the vital fluorochrome calcein acetoxymethyl (Invitrogen) for 15 min at 37°C and were then aliquoted into the bottom CAFCA miniplates, which were centrifuged to synchronize the contact of the cells with the substrate. The miniplates were then incubated for 20 min at 37°C and were subsequently mounted together with a similar CAFCA miniplate to create communicating chambers for subsequent reverse centrifugation. The relative number of cells bound to the substrate (i.e., remaining in the wells of the bottom miniplates) and cells that failed to bind to the substrate (i.e., remaining in the wells of the top miniplates) was estimated by top/bottom fluorescence detection

in a computer-interfaced GENios Plus microplate reader (Tecan Group Ltd.).

In assays involving signalling antagonists, immunosorted $NG2^+$ and $NG2^-$ cells and siRNA-treated cells were confronted with Col I and Col VI substrates in the presence of the following inhibitors: calphostin-C (PKCα; at 50 nM), UO126 (MEK1/MEK; up to 10 μM), UO124 (control drug for MEK1/MEK2 inhibitors; up to 10 μM), SB203580 and PD169316 (p38MAPK; up to 10 μM), suramin (CAMK; at 1 μM), PP2 (Src,; up to 1 nM), okadaic acid (PP1 and PP2A; up to 10 μM), SB216763 (GSK3α up to 10 μM), SB202474 (control drug for MAPK inhibitors; up to 10 μM), Y27632 (ROCK-1; up to), LY294002 (PI-3K; up to 10 μM), Wortmannin (PI-3K; up to 5 μM), GDC-0941 (p110α; up to 1 μM), TGX-221 (p110β; up to 1 μM) and AS252424 (p110γ; up to 5 μM); obtained from Sigma-Aldrich; Merck Laboratories-Calbiochem Research; Santa Cruz Biotechnology Inc, Santa Cruz, CA, USA; Enzo Lifesceinces AG, Lausen, Switzerland; and Axon Medchem, Groningen, Netherlands). Drugs doses were initially calibrated through cytotoxity tests on the specific sarcoma cells to be treated. Optimal doses were next established through proliferation assays with pre-starved cells plated on Col VI or fibronectin. We then performed pilot migration tests that revealed that many of the agents indiscriminately affected the process of locomotion on both the NG2-dependent Col VI substrate and NG2-independent substrates such as Col I and fibronectin. We therefore applied our CAFCA system to evaluate the role of the phoshorylations induced by the NG2-Col VI interaction in the context of short-term cell-substrate adhesion. This was done using immunosorted $NG2^+$ and $NG2^-$ cell subsets and siRNA-treatred cells.

Cell-cell aggregates and colony forming assay

To verify cell-cell aggregation capability, 5X 10^5 tumor cells were plated on 24 well plate, previously coated with a 0.5% solution of PolyHEMA (SIGMA), dissolved in 95% ethanol. Col VI or Col I was added in solution to a final concentration of 20μg/ml. The aggregated was analyzed after four hours from cells' plating; for each condition 20 random fields was captured with the microscopic Leica system. The experiments were performed in triplicate, in three independent experiments.

Anchorage-independent growth and colony formation were assessed by cell cultivation in soft agar. For this purpose, cells were suspended in 1 ml of serum-contening medium supplemented with 0.5% agarose (type VII Low Gelling temperature, Sigma Aldrich) and seed at a density of 7.5 X 10^4 and 3.75 X 10^4 cells/well, in presence of soluble Col I or Col VI (20 μg/ml), on top of a solid

underlay of 2 ml 0.7% agarose alone. Cells were embedded in agarose and grown in this conditions for up to 15 days. Colony formation was determined by direct counting of representative fields under phase-contrast microscopy, following cells staining with 0.1% p-iodonitrotetrazolium violet (Sigma-Aldrich) for 24h. Colonies were classified according to the number of cells composing them, i.e. doublets (2 cells),small aggregates (3-5 cells), large aggregates (5-30 cells), and full colonies (>30 colonies).

Cell migration

Cell migration and invasion assays were carried out using a modified version of FATIMA (*Fluorescence-Assisted Transmigration, Invasion and Motility Assay*; (Spessotto et al., 2009)). For this purpose, FluoBlock inserts (BD Biosciences) with fluorescence shielding membranes carrying 8μm pores were coated with either purified ECM components, Matrigel or polymerized on their lower or upper side. In the case of Matrigel and Col I solutions, these were diluted in cold serum-free DMEM medium at a concentration of 0.5-1 mg/ml and 50 μl of the solution was dispensed onto the porous membrane. FluoBlock inserts were then incubated for 1hr at 37°C to form a semisolid thin gel across the membrane. siRNA-treated and untreated cells were fluorescently tagged FAST Dil (Life Technologies Inc) as previously described (Spessotto et al., 2009) and plated at a density of 5×10^5 cells in 500 μl of DMEM containing 0.1% BSA onto the coated membranes and grown on this substrate for up to 24 hours. The lower compartment of the inserts was filled with 1.5 ml of DMEM with 0.1% BSA. The percentage of transmigrated and "stationary" cells was assessed using the SPECTRA Fluor microplate fluorometer (TECAN Group, Maennedorf, Switzerland). Haptotactic migration of siRNA-treated and untreated cells in response to purified EMC molecules was examined by coating overnight at 4°C the lower side of the porous membranes with 20 μg/ml of rat tail Col I and Col VI, both diluted in 0.05M bicarbonate buffer, pH 9.6. For invasion assays , Matrigel at a stock protein concentration of about 8 mg/ml was used as is or diluted to 1 mg/ml and supplemented with 1-20 μg/ml purified Col VI. In other cases, Col I gels were produced at a concentration of 1 mg/ml and similarly supplemented with 1-20 μg/ml Col VI.
For scratch-assay the tumor cells were seeded at 80% confluency and grown to total confluency. The monolayer was starved over-night in reduced level of serum (1%), wounded with a P200 pipet tip. After screaping the cells were rinsed twice with PBS to removed cell-aggregates and debris. After soluble addiction of Col VI (20μg/ml) in DMEM with 0.5% of serum, real-time video

microscopy was done with an inverted phase-contrast microscope (Leica) equipped with an on-stage mini-chamber providing routine incubation conditions (37°C, 5% CO_2). Phase-contrast images were taken in 5 min intervals, contrasted digitally and exported into conventional image analyses software for elaboration and presentation. For video display image stacks were compressed and processed as Quick Time movies. Quantification of migratory parameters such as speed of movement, vectorial directional persistency and distance migrated by individual cells was accomplished using the dedicated software provided with the microscopic Leica system.

For 3D movement in Matrigel, spheroids, obtained plating for 16 hours the tumor cells on polyHEMA, were embedded into a solution of DMEM and Matrigel with a ratio of 1:1. After solidification (1 hour at 37°C) was added DMEM without serum. The migration was followed by real-time video microscopy (Leica) as previously described. For evaluation of cell attachment dynamics to native matrices deposited in vitro by embryonic fibroblasts isolated from wild and Col VI null mice, sarcoma cells within representative areas of the matrix substrate were inspected at 15 and 30 min after plating for their morphology prior to (by phase-contrast microscopy) and after staining for actin microfilaments. In these experiments the number of cells plated was of $1x10^5$/well in 24-well plate. At the indicated times, the matrix was rinsed two times with DPBS to wash out the unattached cells and then we fixed all with 4% PFA for 20 min at room temperature and washed two times with DPBS. Assessments of cell binding to native matrices were carried out in triplicate independent experiments by cell counting under phase contrast microscopy adopting 15-20 different representative fields of the substrate with discernible matrix deposits. Parallel substrates of purified Col VI were used as reference.

Cell adhesion under shear forces

For isolation of cell-free ECMs under flow cells were seeded at high density (from 3 to $5x10^5$ cells depending on cells type) onto sterile coverslips (25x50 mm), such as to obtain a confluent monolayer the following day. Cells were then further cultivated for up to 5 days. To avoid delays in the washing step at time of ECM isolation, 1 ml of “washing buffer” was flushed into the liquid-bearing tube before its insertion into the perfusion chamber and this latter was then assembled (Munn et al., 1994). The cell “lysis solution” was next gently injected into the perfusion chamber and allowed to come in contact with the cells for 90 sec. The tubing containing the “washing buffer” was connected to a syringe pump (Harvard Scientifics Inc) which was set at a share rate of

$25s^{-1}$. The isolation procedure was monitored by phase-contrast microscopy and topology and integrity of the isolated matrices contained within the perfusion chamber was verified by immunostaining for FN. Analysis of cell-matrix interactions under defined shear-rates was performed according to previously described procedures (Mazzucato et al., 2009). After the isolation of cell-free matrices under perfusion, HT1080 cells were re-suspended at final concentration of $1x10^6$ cells/ml in M199 medium supplemented with 0.5% FCS. A volume of 1.5 ml of the cell suspension was used for each perfusion. The shear rate was set at 25 s^{-1} and the perfused cells were recorded by capturing 20 random fields on each coverslip at 5 and 10 min after the beginning of the perfusion.

Protein extraction from tumor samples and Western blotting

To perform the protein extraction from tumor semples was used a lysis buffer , the same of Phospho-proteomic profiling described later, composed by:

- 20 mM MOPS, pH 7.0 ;
- 2 mM EGTA (to bind calcium);
- 5 mM EDTA (to bind magnesium and manganese);
- 30 mM sodium fluoride (to inhibit protein-serine phosphatases);
- 60 mM β-glycerophosphate, pH 7.2 (to inhibit protein-serine phosphatases);
- 20 mM sodium pyrophosphate (to inhibit protein-serine phosphatases);
- 1 mM sodium orthovanadate (to inhibit protein-tyrosine phosphatases);
- 1% Triton X-100
- 1 mM phenylmethylsulfonylfluoride (to inhibit proteases);
- 3 mM benzamidine (to inhibit proteases);
- 5 µM pepstatin A (to inhibit proteases);
- 10 µM leupeptin (to inhibit proteases);
- 1 mM dithiothreitol (to reduce disulphide linkages)

The final pH of the buffer was adjusted to 7.2.

For the tissue lyses procedure, briefly: we used 1 ml of lysis buffer per 250 mg wet weight of the chopped tissue. Rinsed the tissue pieces in ice-cold PBS three times to remove blood contaminants, we homogenized the tissue on ice 3 times for 15 seconds each time with a Brinkman Polytron Homogenizer. We sonicated the homogenate 4 times for 10 seconds on ice

each time to shear nuclear DNA and centrifuged the sample at 90,000 x g for 30 min at 4°C in a Beckman Table Top TL-100 ultracentrifuge. Then, we transferred the resulting supernatant fraction to a new tube for protein quantification, using Bradford (Bio-Rad) system by spectrophotometer . Bovine serumalbumin (BSA) was used as the protein standard **.**

For Western blot analysis, the samples were resolved by SDS-PAGE on 4-12% gradient gels (Bio-Rad Laboratories, Inc) under reducing conditions and transferred to nitrocellulose membranes. The saturated with 5%BSA in TBST for 1 hour at room temperature and incubated with primary antibodies, 9.2.27 (anti-NG2) and an anti-β-actin antiserum (ABCAM) at 4°C overnight. Membranes were then washed and incubated with peroxidase-labeled goat anti–rabbit or anti-mouse antibodies (Life Technologies) followed by chemiluminescent detection using the ECL Plus kit (Amersham Biosciences).

Phospho-proteomic profiling

The relative expression levels and phosphorylation patterns of signal transduction components elicited by NG2-presence on tumor cell surface was defined by relying upon the Kinetworks^{TM} KAM-1.2PN 300 Phospho-Ab microarrays (Kinexus Bioinformatic Corporation, Vancouver, Canada). The arrays were performed in duplicate using a pool of the same amount of protein-extract deriving from three different tumor masses of same type. Then, the comparison was performed between the two subtypes, $NG2^+$ and $NG2^-$, for each tumor type : HT1080 or MeWo. The results obtained were further compared to exclude the patterns strictly correlated to the melanoma or sarcoma tumor type.

Relative expression levels and phosphorylation patterns of signal transduction components elicited by engagement of NG2 in Col VI interactions were defined by relying upon the Kinetworks^{TM} Immunoblot KPSS 1.3 Phospho-Site Screen, entailing detection of >70 phospho-sites in 64 molecules, and Kinex™ (KAM 1.1) antibody microarray services (Kinexus Bioinformatic Corporation, Vancouver, Canada). Through the antibody array approach, platforms of 1,278 antibody spots were adopted to comparatively examine 627 signal transduction components in duplicate. The platform comprises 273 antibodies directed against specific phosphorylation sites and 378 antibodies recognizing the cognate antigens in any phosphorylation state. Since cell binding to Col VI substrates was strongly compromised in cells with abrogated NG2 it was not technically possible to use an experimental paradigm involving direct plating of the cells onto Col

VI substrates. Furthermore, because of the confounding intracellular signals that could be elicited by unrelated substrate molecules introduced into the system, it was not either possible to use cells bound to a different "NG2-independent" substrate than Col VI (or to a mixture of Col VI and another ECM component), and then add Col VI to the system. This forced us to use an alternative paradigm for efficiently accomplishing our four-way comparative analysis. Thus, in a first series of experiments SK-UT-1 $NG2^+$ and $NG2^-$ cell subsets were treated with a β1 integrin-directed siRNA probe (Tebu-bio Lab), whose efficiency was independently validated by flow cytometry and cell adhesion on fibronectin. Cells were starved for 24 hrs in culture medium containing 0.5% FCS, plated on poly-L-lysine (0.1% coating), treated with a function-blocking antibody against the α2 integrin subunit (kindly provided by Luigi De Marco, The National Cancer Institute Aviano) and alternatively incubated for 30 min with molar equivalents of Col I (160 μg/ml) or tetrameric Col VI (20 μg/ml). Cells were lysed in the presence of protease inhibitors and the lysates processed by semi-quantitative immunoblotting with the KPSS 1.3 phosphosite screen. For this purpose an amount of 600 μg per sample of whole cell lysate from collagen-exposed $NG2^+$ and $NG2^-$ cells was prepared according to the instructions provided by the service company. Briefly, after removal of the medium, cells were rinsed in dish with ice-cold PBS once; detached with trypsin, followed by the addition of equal volume of medium. Cells were collected in a 15-ml conical tube and centrifuge at 500xg for 2 min at 4°C. The pellets were washed twice with ice-cold PBS and add ice-cold lysis buffer. After cell scraping, the liquid was collected, sonicated four times and assayed protein concentration. Sample (2mg/ml) was then frozen. In a subsequent series of experiments, we used B16 murine melanoma cells stably transfected with rodent NG2 and compared these cells to mock-transfected ones using the same collagen-induction paradigm and Western blotting-based phosphosite screening described above. Prior to exposure to Col I and Col VI cells were incubated with anti-murine β1 integrin-directed siRNA probe (Santa Cruz Biotechnology, Inc, Santa Cruz, CA), which was similarly validated in our system by flow cytometry and cell adhesion to fibronectin. For global phosphosite/proteomic analyses we used the experimental set up described above involving SK-UT-1 $NG2^+$ and $NG2^-$ cells and the antibody microarray platform. The 18 phosphorylation sites found to be most divergent according to hierarchical clustering were next confirmed by semi-quantitative immunoblotting (Kinetworks™ Hit Validation Service, Kinexus Bioinformatic Corp.).

In vivo tumorigenesis

All experiments in mice were approved by the Review Board on animal experimentation of the National Cancer Institute of Aviano and were performed in accordance with the international guidelines for tumorigenesis by xenografting in nude mice. Experiments aimed at assaying tumor formation in relation to NG2 surface expression involved the evaluation of 170 nude mice, out of 208 animals that were totally manipulated. In pilot tests we performed a dose-escalation analysis of the number of implanted cells needed to obtain detectable subcutaneous tumor lesions and assayed implantations ranging from 10^6 to $5x10^6$ cells/animal co-injected with Matrigel at a protein concentration of >5 mg/ml. Mice receiving unilateral subcutaneous tumor cell implantations were 7 weeks of age at the time of the implant and were monitored by visual inspection at 2 days intervals for up to 65 consecutive days. For end-point evaluations of tumor formation, we adopted an arbitrary scoring based upon assessment of three primary parameters, i.e. transplanted cell dose, final size of the tumor lesion and latency of tumor formation (i.e. number of days needed to generate a tumor mass of the allowed size; see below). Scoring values were defined accordingly using the formula: fraction number of inoculated cells (expressed as number of millions of cells, ranging from 1 to 1/5) x final tumor volume (cm^3) at time of euthanizing divided by number of days of tumor growth: score 0 = no engraftment/growth (values = 0-0.00045); score 1 = minimal tumor mass (values = 0.00046-0.00409); score 2 = small tumor mass (values = 0.00410-0.00773); score 3 = medium-sized tumor mass (values = 0.00774-0.01138); and score 4 = large tumor mass (0.01139-0.01502). In another series of experiments a total of 93 nude mice (85 successfully evaluated) were subcutaneously inoculated with 10^6, 3×10^6 or $5x10^6$ immunosorted $NG2^+$ or $NG2^-$ STS cells (unsorted cells were used as reference for each of the experiments) suspended in Matrigel and implanted unilaterally into the flank of the animals as described above. In some cases, comparable bilateral subcutaneous implantations were done using $NG2^+$ and $NG2^-$ cells for each of the flanks. In comparative analyses of tumor formation/growth of $NG2^+$ versus $NG2^-$ cells, all animals were euthanized at the time that any of subjects manifested signs of morbidity or tumor masses had reached overt sizes of 1.5-2.0 cm^2 in diameter. Euthanized animals were subjected to macroscopical evaluation and photographic documentation of the tumor lesions, and eventually processed by autopsy to verify tumor cell infiltrations in primary organs. During the period of the experiments, care was further taken that the tumor burden did not obviously impair the primary needs of the animals, that is, ambulation,

eating, drinking, defecating, and urinating. Tumor masses that formed in manipulated animals were regularly excised and in most cases subjected to histological and immunohistochemical analyses.

Tumor specimens

Informed consent for collection of sarcoma specimens was given to Rizzoli Orthopaedic Research Institutes and the study was carried out with the full approval of the institutional Ethical Committee. Ages of patients from whom tissue samples were collected ranged from 34-79 years with a median age of 59 years. Clinical follow-up of these individuals was evaluated considering time to metastasis, metastasis-free survival and overall survival, which was calculated from the date of diagnosis to event, or the last day of follow-up, and ranged from 3-138 months with a mean of 27.8 months. The minimal time of follow-up for defining a metastasis-free condition was 5 years. 47 patients were disease-free, 61 developed metastases during the post-surgical follow-up period. 33 patients died from the disease and 7 from other causes. Tumor samples, including both primary and metastatic lesions, and 20 paired normal tissue were available as both frozen tissue and paraffin-embedded material and in all specimens the percentage of tumor cells estimated after hematoxylin-eosin staining of serial tissue sections was equal or more than 90%. Paired primary and metastatic (lung derived) tissues were available from a total of 46 of the patients. Enrolled patients were diagnosed to suffer of primary spindle cell or polymorphic STS of the following histologic subtypes: malignant fibrous histocytoma-like pleomorphic sarcoma (MHF; n=16); leiomyosarcoma (LMS; n=28) poorly differentiated, pleomorphic, myxoid or round-cell liposarcoma (LS; n=47); fibrosarcoma (FS; n=6) and monophasic synovial sarcoma(SS; n=11). Diagnoses were according to the WHO guidelines with complementary immunohistochemical analysis of standard markers for differential diagnosis. Conventionally MFH is a diagnosis of exclusion and hence this subgroup included various types of poorly differentiated pleomorphic sarcomas. Primary tumors were all deeply localized, had a size exceeding 5 cm in diameter and were classified according to the three-wired variant of the sixth edition of the American Joint Committee for Cancer (AJCC) STS staging. The 46 metastatic specimens were consistently derived from surgically removed lung lesions.

Statistical analyses

Data on human tumor specimens are shown as median (m) and 25-75th percentile for their strong non-Gaussian distribution. Non-parametric Mann-Whitney U test and Kruskal-Wallis one-way analysis of variance were performed to compare gene expression in unpaired and paired samples, respectively; p values <0.05 were consistently considered to be statistically significant. Metastasis-free survival was calculated by Kaplan-Meier analysis and comparison of curves was performed through Breslow's test. Multivariate meta-analyses were according to Cox proportional hazard regression and significance levels in cell adhesion and migration assays in vitro were established by Student's two-tailed *t* test and one- and two-way ANOVA of variance.

RESULTS

NG2 surface expression correlates with malignancy

To verify whether NG2 could be directly responsible for the aggressiveness of the PG overexpressing cells, we assayed, by xenograft experiments, the tumorigenic capacity of sarcoma cells with different NG2 surface levels (**Table 1**).

Table 1. NG2 expression pattern of sarcoma tumor cells.

Designation	Patient code	Histological subtype	NG2 expression levels (%)[a]
SK-LMS-1	NA	Leiomyosarcoma	88.5
SK-UT-1	NA	Leiomyosarcoma	63.6
MES-SA	NA	Leiomyosarcoma	58.3
MG63	NA	Osteosarcoma	83.5
SW982	NA	Synovial sarcoma	26.3
GCT	NA	Fibrous histiocytoma	47.8
HT1080	NA	Fibrosarcoma	37.5
143B	NA	Osteosarcoma	61.8
SW872	NA	Liposarcoma	99.4
RD/KD	NA	Rhabdomyosarcoma	43.2
A375	NA	Melanoma	91.2
NT-LS-1[c]	91818	Liposarcoma	34.1
NT-LS-2	108876	Liposarcoma	0.9
NT-LS-3	110543	Liposarcoma	1.7
NTI-MFH-1	97441	Fibrous histiocytoma	1.0
NTI-MFH-3	98337	Fibrous histocytoma	51.6
NTI-OS-2	128246	Osteosarcoma	81.2
NTI-LMS-1	94278	Leiomyosarcoma	76.8
NTI-LMS-2	95058	Leiomyosarcoma	37.5
NTI-LMS-4	98035	Leiomyosarcoma	2.3
NTI-LMS-7	109541	Leiomyosarcoma	11.8
NTI-FS-1	91266	Fibrosarcoma	32.4

Independently of their histological derivation, growth rates and overall capability of sarcoma cells to engraft and form subcutaneous tumour masses was found to closely correlate with their NG2 surface levels (**Fig. 5**).

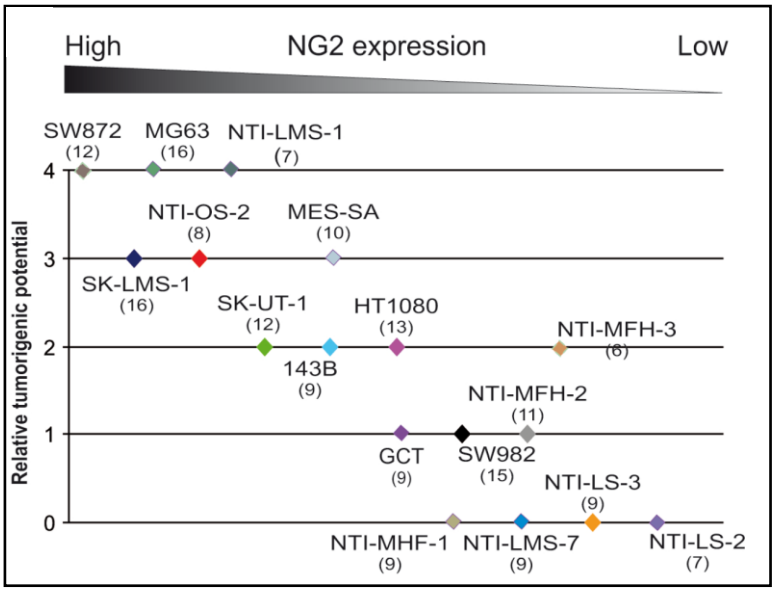

Figure 5. Graphic representation of the relative degree of tumor engraftment and local growth as a function of the constitutive surface levels of NG2 (**Table 1**). Relative tumorigenic potential of the implanted sarcoma cell lines was arbitrary scored 0-4 by adopting the algorithm reported in *Materials and Methods*.

These findings suggest that NG2-positive and -negative cells of STS lesions could correspond to subsets with different tumorigenic potential (e.g. NG2-expressing cells being a putative tumour initiating cell subset).

Since a similar diversity of NG2 expression was noted in several of our sarcoma cell lines, we separated by immunosorting the $NG2^+$ and $NG2^-$ subpopulations (*see Material and Methods*) and compared the tumorigenic potential of these subsets in vitro and by transplantation into nude mice. Antibody-assisted enrichment of $NG2^+$ cell subsets was only performed on cell lines in which the NG2-expressing subpopulation represented >20% of the entire cell population and when the two subsets (i.e. $NG2^+$ and $NG2^-$) could be confirmed to maintain their phenotype for up to 40 population doublings.

Both unilateral and paired bilateral flank transplantations (i.e. each of the cell subsets was implanted on either flank of the same animal) were performed, yielding two distinct xenograft scenarios: (I) the $NG2^+$ cell subset developed conspicuous tumours, whereas the $NG2^-$ subset largely failed to engraft (NTI-LMS-1 $NG2^+/NG2^-$); and (II) the $NG2^-$ cell subset was delayed in its engraftment and subsequent growth, but eventually formed masses analogous to those seen with the $NG2^+$ subset (HT1080 $NG2^+/NG2^-$ and NTI-LS-1 $NG2^+/NG2^-$) (**Fig. 6**).

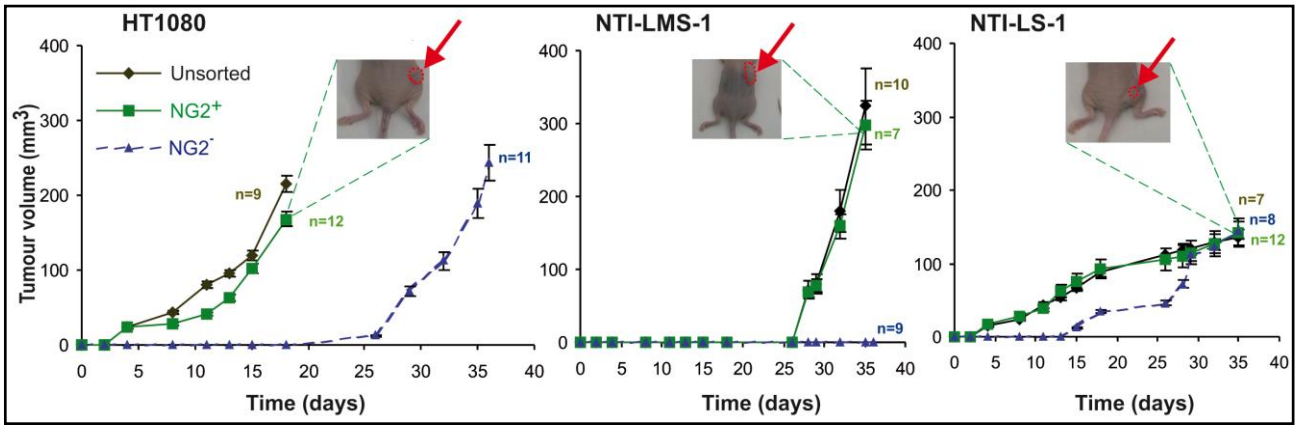

Figure 6. Representative growth kinetics of locally growing tumors induced by subcutaneous implantation into nude mice of the indicated $NG2^-$ and $NG2^+$ cell subsets. Behaviour of the "unsorted" cell population is indicated for reference

Histological and immunohistochemical analyses of explanted tumour lesions formed by $NG2^+$ and $NG2^-$cells show that they had indistinguishable morphologies but differed in their neovascularisation degree. This aspect was observed not only in sarcoma but also in melanoma tumors (obtained from immunosorted MeWo $NG2^+$ or MeWo $NG2^-$ cells lines, **Fig. 7**). If CD31, a marker of vasculature cells, did not show any difference between the $NG2^+$ and $NG2^-$ tumors (**Fig. 8**),different results were obtained looking for intra-tumor pericytes. Indeed Desmin, a marker for all pericytes, resulted equally expressed in $NG2^+$ and $NG2^-$ tumors. On the contrary Smooth-muscle Actin (SmActin), a marker of mature pericytes, seems to be more expressed in $NG2^-$ tumors (**Fig. 9A,B**), suggesting a different maturation degree of vessels.

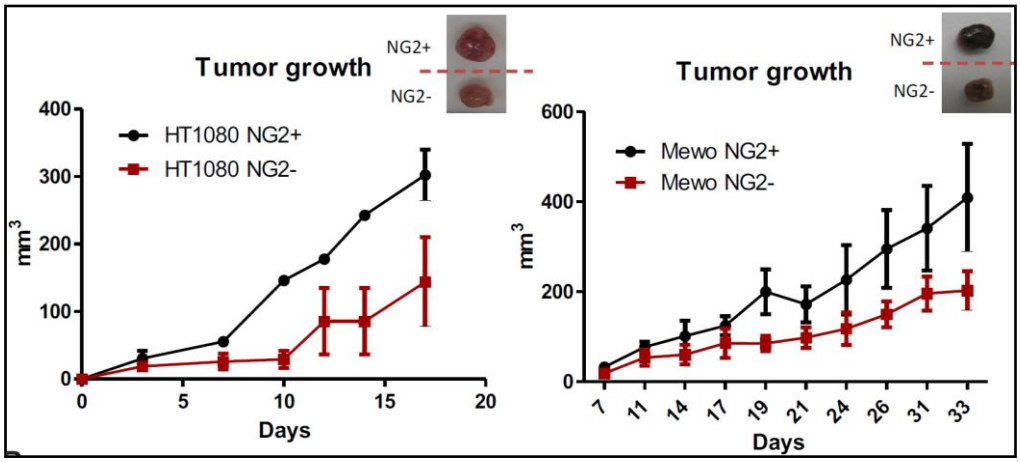

Figure 7. Representative growth kinetics of locally growing tumors induced by subcutaneous implantation into nude mice of HT1080 $NG2^+$ and $NG2^-$ or MeWo $NG2^+$ and $NG2^-$ cell subsets.

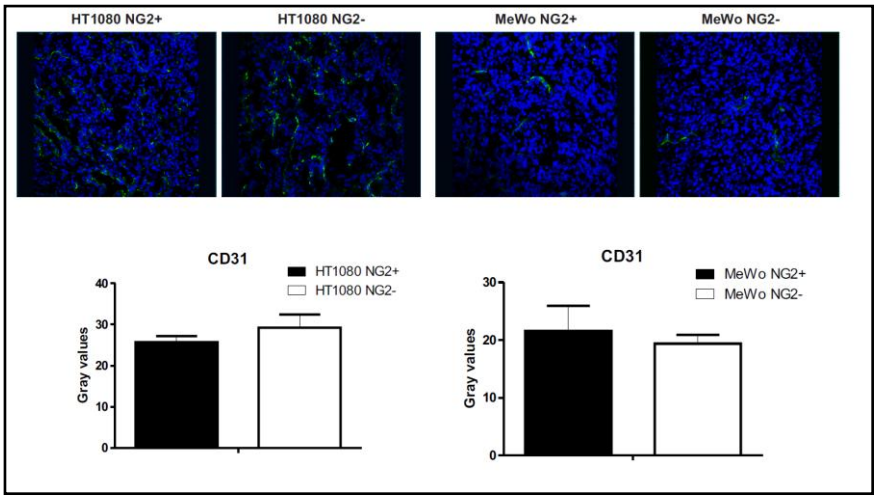

Figure 8. Immunofluorescence analysis of CD31 (green) on $NG2^+$ and $NG2^-$ tumors. To-PRO3 (blu) was used for nuclei counterstaining. The graphs reported the quantification of CD31 signal in the different tumor subset.

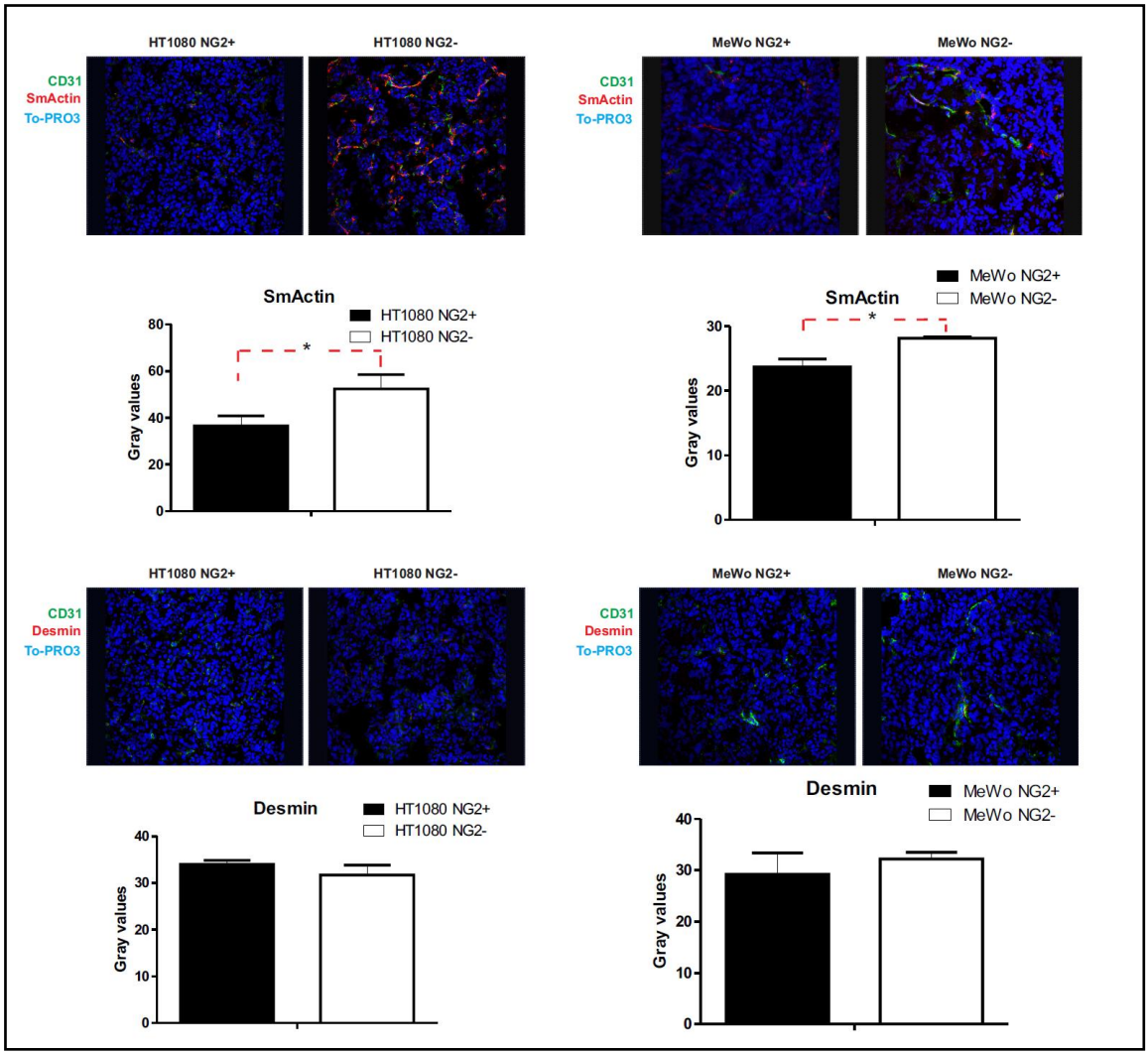

Figure 9. (A) Immunofluorescence analysis of CD31 (green) and SmActin (red) on tumor masses. To-PRO3 (blu) was used for nuclei counterstining. The graphs report the quantification ("*"= $p<0.05$ by Student T-test). **(B)** The same analysis was performed for Desmin .

Importantly , to verify that both NG2 cell subset preserved their phenotype, we performed immunochitochimical analysis noting that lesions formed by the $NG2^+$ subset contained roughly 80% of the cells exhibiting a detectable NG2 expression, whereas the small lesions formed by $NG2^-$ cells were composed nearly exclusively of NG2-negative cells (i.e. only 7% of cells of the entire lesion including microvascular pericytes and stromal cells were positive for NG2; **Fig. 10A**). This was confirmed also by western blot, after the protein extraction from tumor masses (**Fig. 10B**).

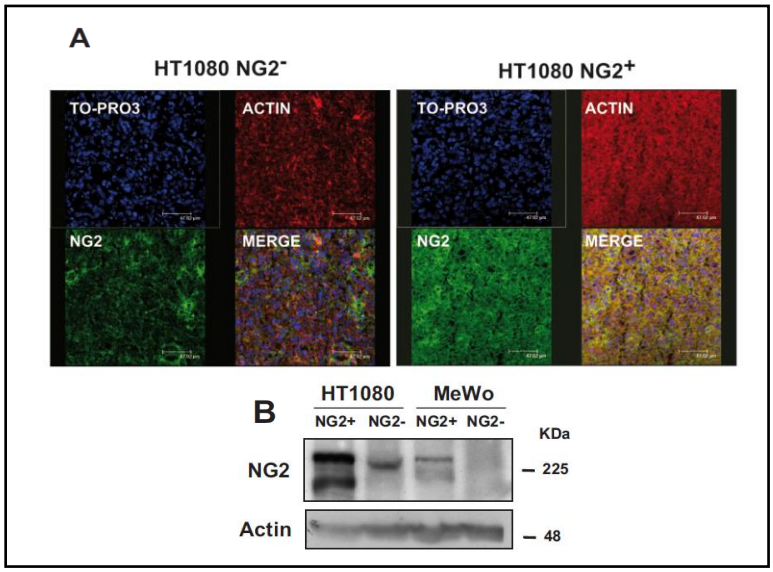

Figure 10. **(A)** Representative confocal laser microscopy images of sections from tumour masses formed by HT1080 $NG2^-$ and $NG2^+$ cells, double stained with antibodies against NG2 (mAb 9.2.27) and F-actin. The patchy staining in masses formed by $NG2^-$ cells corresponds to intra-lesional neovascular pericytes. **(B)** Western blot analysis performed on pretein extracted from $NG2^+$ and $NG2^-$ tumor masses.

Moreover Ki-67 staining of lesions explanted at experimental end-points showed equally high cycling frequencies in the two types of tumour masses (**Fig. 11A**) **.** Conversely in situ cell death assay seems to show an higher apoptotic rates in the NG2- sub-type than in NG2+ tumours (**Fig. 11B**)

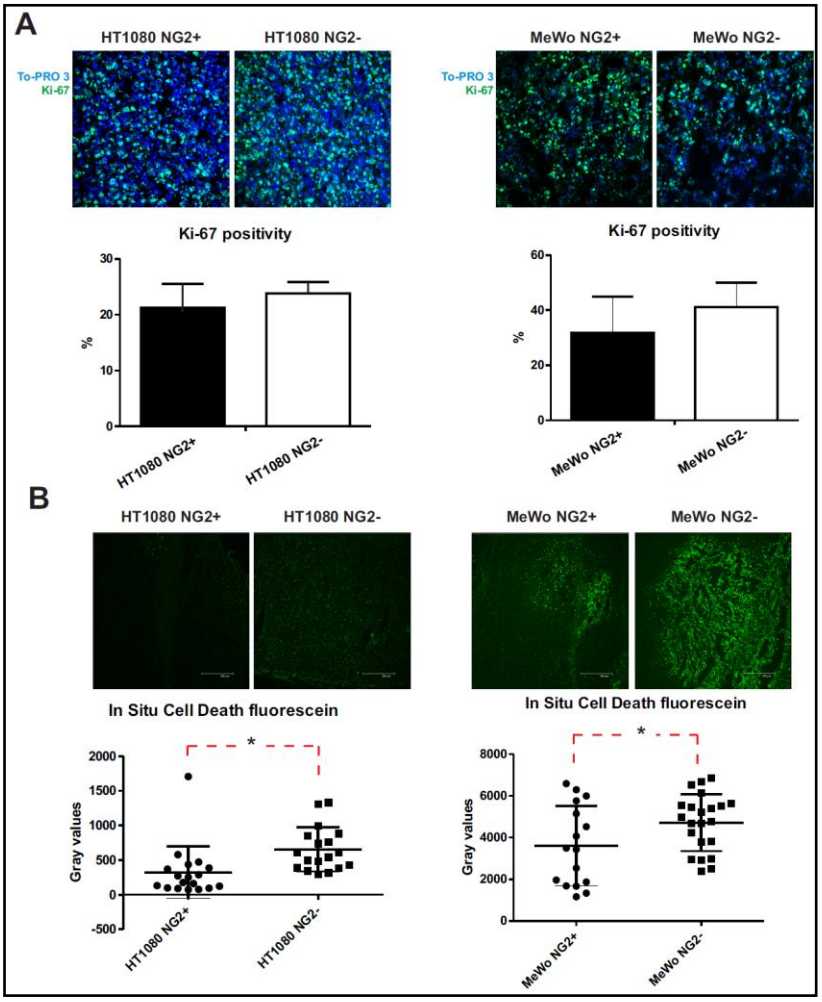

Figure 11. (A) Distributions and quantification (*lower graph*) of Ki-67-positive cells in the two types of HT1080 and MeWo tumour masses. Nuclear counterstaining was performed with TO-PRO-3. **(B)** In situ cell death assay performed on NG2+ and NG2- tumor masses and his quantification (*lower graph*). ("*"=p<0.05 by Student T-Test)

These observations suggested that size differences of the $NG2^+$ and $NG2^-$ tumour masses were presumably accounted by differences in the engraftment capacities and stress-resistance capability of the two cell phenotypes.

To verify the changes of the protein expression profiles in the two tumor subtypes, we performed a phospho-proteomic screening by antibody-array that, although needing o further validation, in $NG2^+$ subsets seems to confirm an increase of proliferation (contrary to our data by Ki67 staining shown before) and survival pathway (**Table 2**).

Table 2. Common up-grade in the phosphorylation patterns in HT1080 or MeWO tumor masses. In the table are reported the ratio between the NG2+ and NG2- subtype. Phospho-proteomic screening was performed in duplicate, on a pool of three different masses for each kind of tumors.

Target Protein Name	Phospho Site (Human)	RATIO HT^+/HT^-	RATIO $MeWo^+/MeWo^-$
Kit	Y730	1,53	2,45
PKBa (Akt1)	S473	1,61	1,51
MAPKAPK2	T222	2,02	1,59
FAK	Y576/Y577	2,04	2,90
PKCq	S695	2,14	10,06
Jun	Y170	2,22	2,90
Syk	Y323	2,55	26,65
Msk1	S376	2,61	1,50
PKA Cb	S339	2,82	2,14
Jun	S243	2,99	84,98
IRS1	S639	3,10	3,14
Histone H3	T12	3,20	1,51
PKA R2a	S99	3,88	2,58
Cbl	Y700	3,96	2,72
PKCe	S729	4,08	3,65
IGF1R	Y1165/Y1166	4,87	6,35
CDK6	Y13	6,21	2,46
Rb	T356	7,65	3,65

NG2 mediates cell adhesion and spreading

As reported in the literature (Campoli et al., 2010; Price et al., 2011) NG2/CSPG4 could modulate different aspects of adhesion in different tumor cell lines. Our idea was to analyzed *in vitro* the modulation of adhesion in two different setting: (I) In static condition, to verify the modulation of tumor cells' interaction with the ECM of microenvironment that could be found around the primary tumors; (II) in perfusion condition, to analyze the interaction between tumor cell and ECM in distant sites , typical of first metastatic steps .

The protocol that we had set (*see Material and Methods*) gave us the possibility to isolate native, cell-free, matrices from different cell culture (**Fig. 12A**), and dissect the capability of tumor cells to interact with them (**Fig. 12B**)

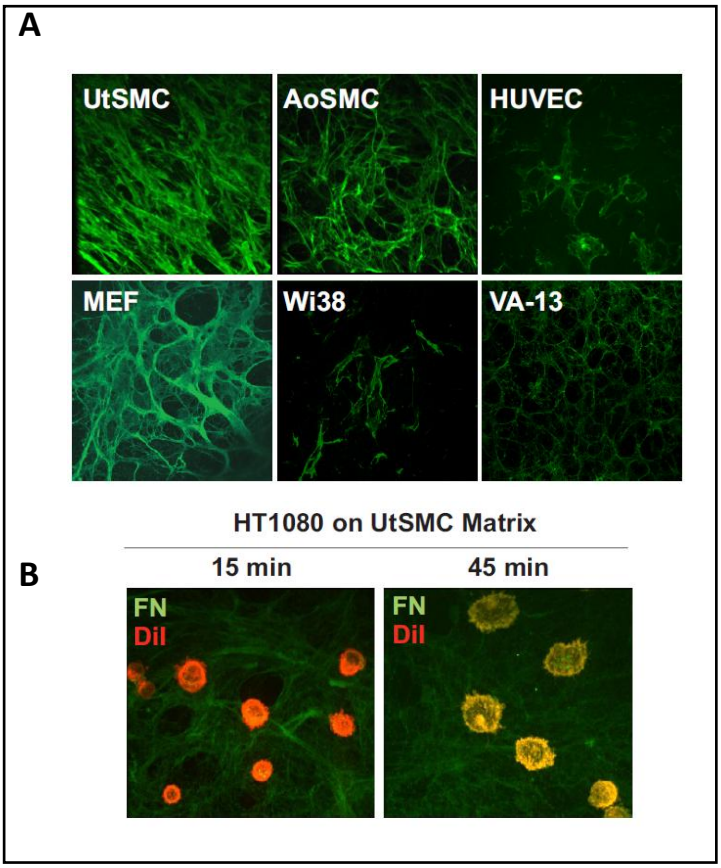

Figure 12. (A) Immunolabellings of FN contained in ECMs isolated from different cell types. **(B)** Adhesion and spreading of DiI-labelled HT1080 cells plated onto the same UtSMC ECM , after 15 and 45 minutes.(Magnification 40X)

First of all we decided to analyzed the adhesion capability of a tumor type, on different matrices. We performed an adhesion assay on Uterine Smooth Muscle Cells (UtSMC) and Mesenchymal stem cells (MSC) with immunosorted HT1080 cells, observing that the presence of the proteoglycan on the cells' surface ($NG2^{+}$), could increase the adhesion of tumor cell on MSC matrix (after 30 min) but not on UtSMC (**Fig. 13**).

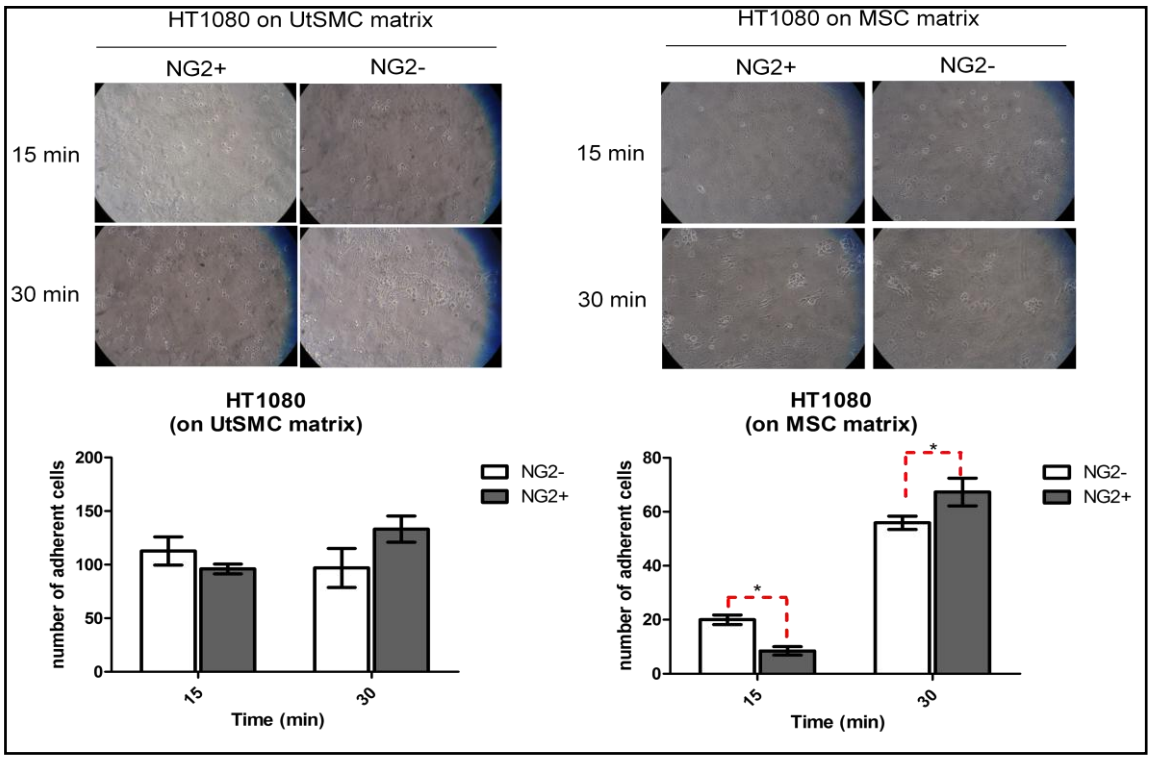

Figure 13. Adhesion of NG2+ and NG2- HT1080 cells on UtSMC (left) or MSC (right) matrices. The quantification is reported in the lower graphs ("*"=p<0.05 by Student T-test)

To verify the adhesion mediated by NG2 in perfusion condition, we readapted the isolation protocol of native matrices (*see Material and Methods)*. With this procedure it was possible to maintain the integrity of matrices, working with shear rate that mimic the rheological condition typical of small capillary veins (**Fig. 14A,B**)

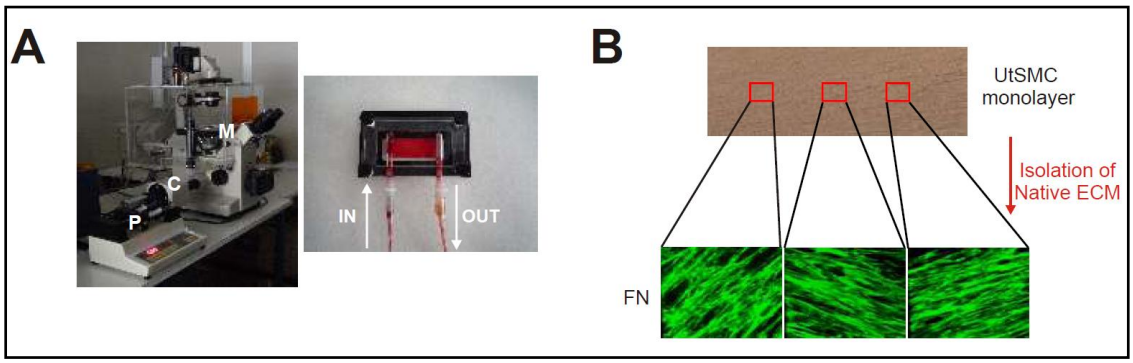

Figure 14. (A) Experimental set up: *left panel* shows the pump *(P)* and video-camera *(C)* connected to an inverted microscope *(M)*, whereas *right panel* shows the perfusion parallel-flow chamber assembly with the collection tubings. The inner tube on the left (*IN*) permits the access to the HT1080 cell suspension into the chamber; the tube connected to the pump (*OUT*) on the right is intended for the aspiration of the perfused liquid. *Arrows* indicate the direction of the applied flow. (**B**) FN immunostaining of ECM isolated from UtSMC

Perfunding immunosorted HT1080 cells, after UtSMC matrix isolation, we observe a high capability

of NG2^{+} cells to adhere on the matrix, after 5 and 10 minutes (**Fig. 15A**) . Moreover these tumor cells show the formation of bigger cell-cluster on the matrix than the NG2^{-} counterpart (**Fig. 15B**).

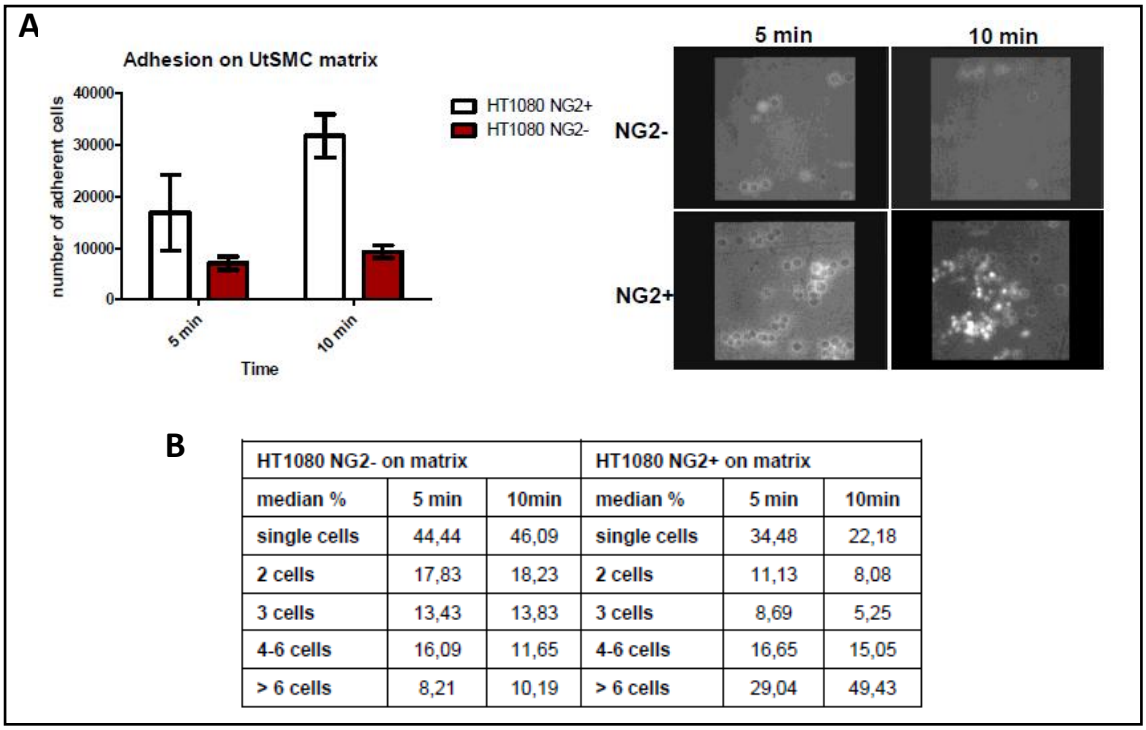

B

HT1080 NG2- on matrix			HT1080 NG2+ on matrix		
median %	5 min	10min	median %	5 min	10min
single cells	44,44	46,09	single cells	34,48	22,18
2 cells	17,83	18,23	2 cells	11,13	8,08
3 cells	13,43	13,83	3 cells	8,69	5,25
4-6 cells	16,09	11,65	4-6 cells	16,65	15,05
> 6 cells	8,21	10,19	> 6 cells	29,04	49,43

Figure 15. **(A)** Quantification of number of tumor cells that have adhered to UtSMC matrix at indicated time points. On the *right* indicative images captured for the quantification. **(B)** The table report the size of HT1080 cluster on the matrix

Interaction NG2-Col VI by cooperating with integrin $\alpha 2\beta 1$

Our results suggest an important role of NG2/CSPG4 for modulating the interaction between tumor cell and ECM. Moreover NG2 has been shown to bind Col VI (Stallcup et al., 1990; Nishiyama and Stallcup, 1993; Tillet et al., 1997; Tillet et al., 2002; Burg et al., 1997; Midwood and Salter, 2001), which, in turn, has been implicated in the progression of multiple tumour types (Daniels et al., 1996; Sherman-Baust et al., 2003; Iyengar et al., 2005; You et al., 2012). We therefore hypothesized that the interaction between sarcoma NG2 and stromal Col VI could be a determining factor in controlling growth and dissemination of these tumors. Our panel of sarcoma cells attached and spread on Col VI substrates with an efficacy that was largely commensurate to their constitutive NG2 surface levels (**Fig. 16**).

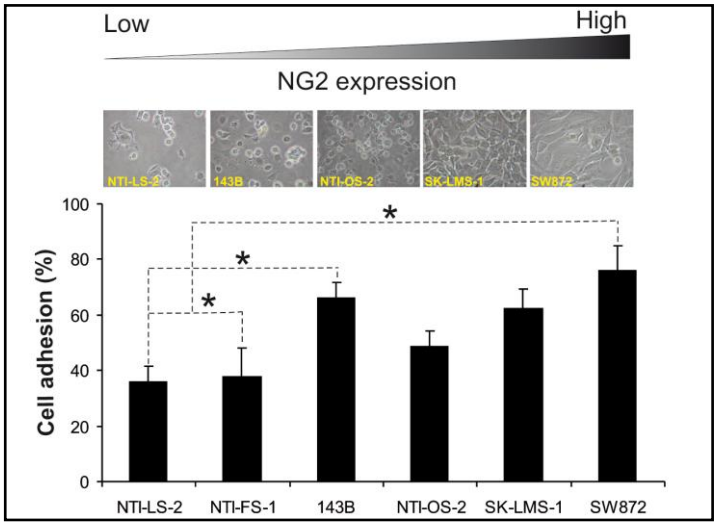

Figure 16. Extents of cell adhesion to intact Col VI tetramers in relation to the surface levels of NG2 displayed by the cells ("*"=p<0.05 by Student T-Test)

Accordingly, siRNA-mediated NG2 abrogation significantly reduced both adhesion and spreading of the cells onto these substrates, but did not affect binding to other ubiquitous ECM components, as Collagene I (Col I) (**Fig. 17A-C**).

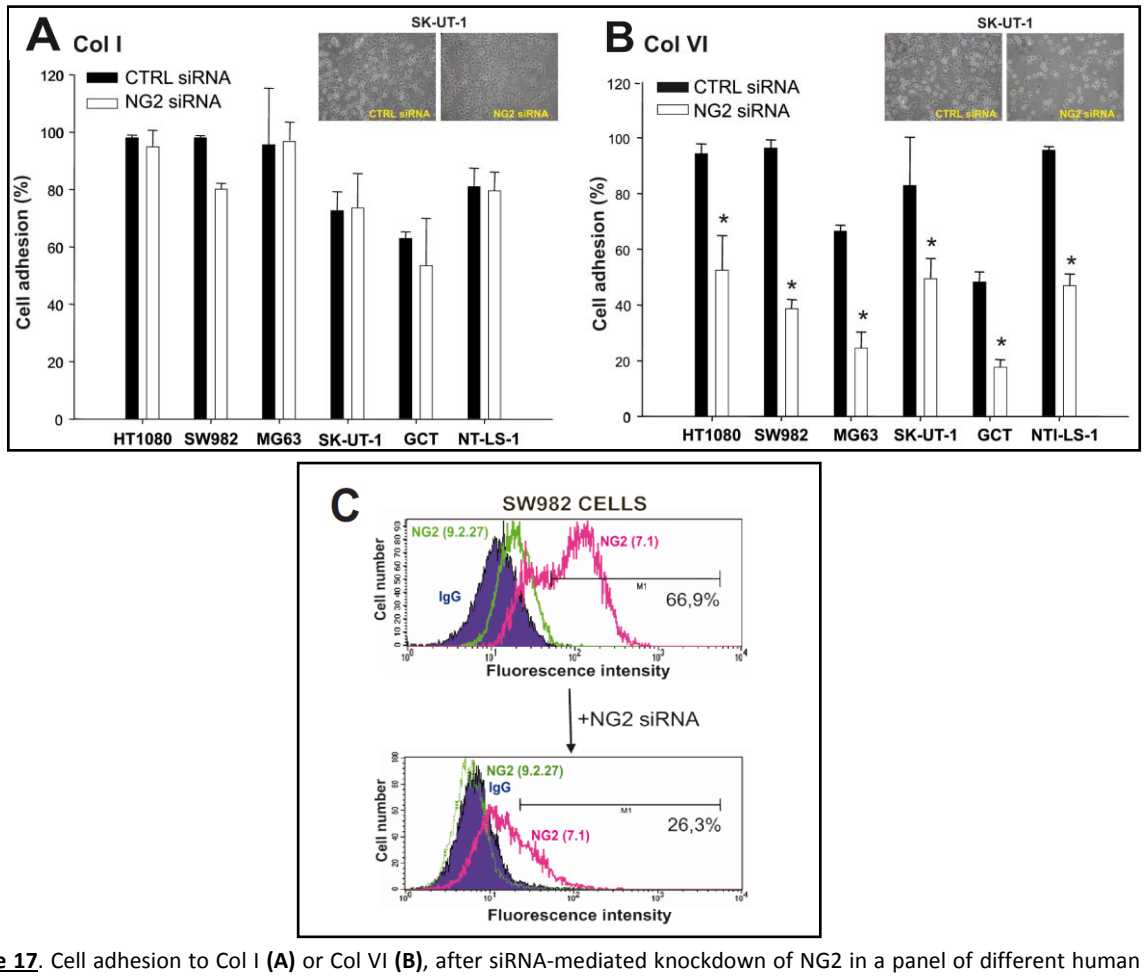

Figure 17. Cell adhesion to Col I **(A)** or Col VI **(B)**, after siRNA-mediated knockdown of NG2 in a panel of different human sarcoma cell lines with different constitutive surface levels of the PG. *Upper insets* show representative phase contrast views of SK-UT-1 cells

adhering to each of the collagens following transfection with the control or NG2-directed siRNAs. "*", $p<0.05$ by Student's *t* test. **(C)** Example of FACS analysis performed to verify the abrogation of NG2 by siRNA.

To finally gain more detailed information about the modes through which NG2 contributed to Col VI binding, as well as in the attempt to pinpoint its putative binding sites within the collagen, we assayed the NG2-dependent cell adhesion to disassembled and/or tryptic forms of the collagen (Perris et al., 1993). It was found that cells bound more tenaciously to intact Col VI tetramers encompassing the C5 segment of the α3(VI) chain, previously demonstrated to be crucial for proper macromolecular assembly of the tetrameric units into microfilaments (Lamande et al., 2006), than to any other form of collagen (**Fig. 18A,B**). This observation strongly suggests that the NG2-mediated cellular interaction with Col VI requires a native configuration of the collagen and that the NG2 binding site on the collagen has a conformational nature.

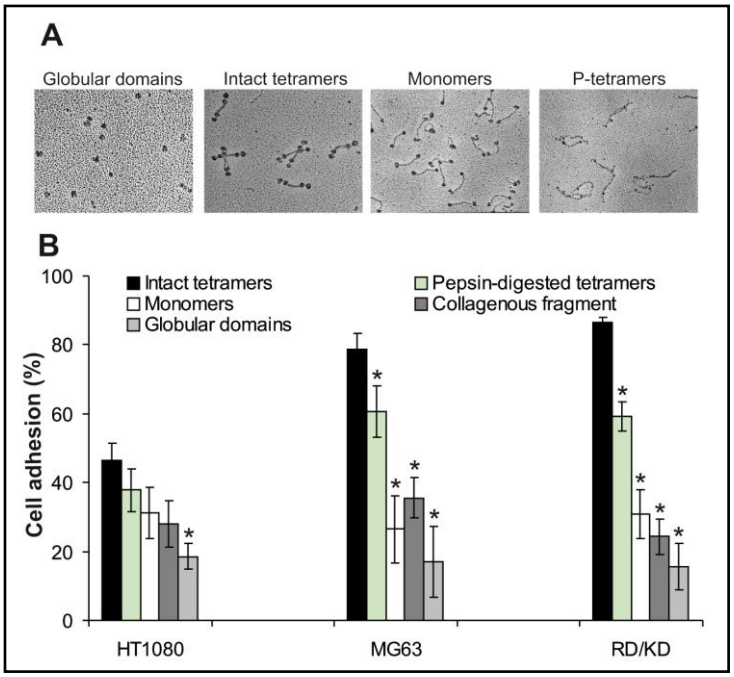

Figure 18. (A) Photographs show representative TEM/rotary shadowing images of intact tetrameric units of the collagen (*Intact tetramers*), monomeric forms of the collagen (*Monomers*), pepsin-digested tetramers (*P-tetramers*; i.e. tetrameric forms of the collagen lacking the *N*- and *C*-terminal globular domains of each of the constituent chains), a tetrameric fragment embodying only the collagenous portion of the molecule (*Collagenous fragment*) and the separated *N*- and *C*-terminal globular domains (*Globular domains*).**(B)** Adhesion patterns of three of the sarcoma cell lines used in this study when assayed on various forms of Col VI ("*"=p<0.05 by Student T-test)

Integrins of the β1 class were identified as the predominant NG2-cooperating ECM receptors. To identify which one could be involved in the interaction with Col VI we performed adhesion assays with RD/KD, HT1080 and MG63 cell lines in presence of integrins functional-blocking antibody.

The partial inhibitory effect seen with antibodies to β1-class integrins and the lack of inhibitory effects by anti-β3/β5 antibodies further suggest that NG2 may directly bind to Col VI. However the experiments performed using anti-α1/α2/α3/αv antibodies disclosed the α2β1 integrin as the one directly implicated to bind Collagen VI (**Fig. 19**).

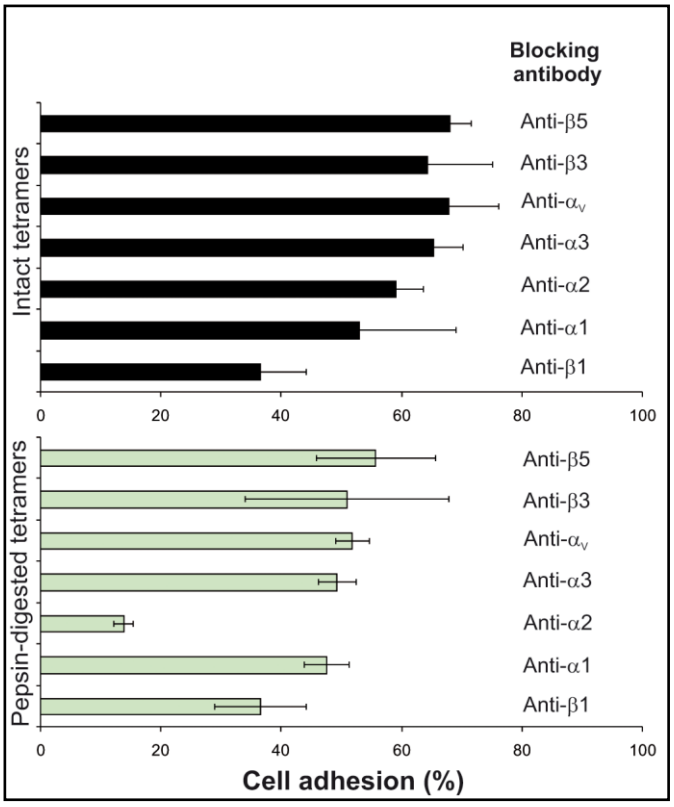

Figure 19. Integrin involvement in the attachment of the rhabdomyosarcoma cell line RD/KD to intact tetramers of Col VI (*upper graph*), or pepsin-digested tetramers (*lower graph*), as determined by the use of function-blocking antibodies against discrete integrin subunits. The RD/KD cell line was chosen as reference for these assays because of its high expression of α2β1 integrin. Similar results were, however, obtained with HT1080 and MG63 cells.

We also wondered whether the NG2-Col VI attachment could be exploited by NG2-expressing cells to form ECM-promoted cellular aggregates. Hints for this being the case were provided by culturing cells on poly-HEMA substrates (to force anchorage-dependent cells to interact with each other rather than with the culture substrate) in the presence of soluble Col VI. Same results were obtained comparing $NG2^+$ with $NG2^-$ HT1080-immunosorted subpopulation (**Fig 20A**) or SK-UT-1 cell line transfected siRNA-NG2 with control siRNA (Scramble) **(Fig. 20B)**. In both systems NG2-expressing cells formed clusters to a significantly higher extent than cells in which NG2 is absent.

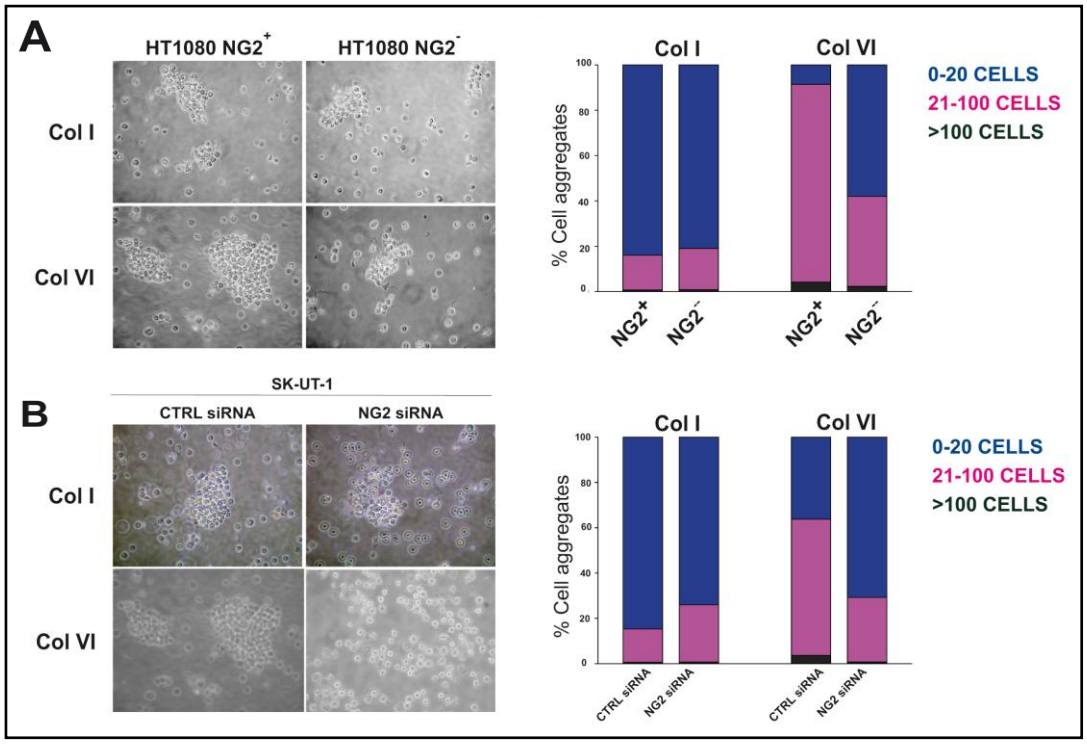

Figure 20. Representative phase-contrast images (magnification: 20X) and assessment of cell aggregation induced by either Col I or Col VI (both added in solution) in **(A)** immunosorted HT1080 $NG2^+$ and $NG2^-$ cells, or **(B)** SK-UT-1 cells treated or not with anti-NG2 siRNAs. Corresponding graphs report the relative frequency of cellular aggregates composed of the indicated amount of cells, when averaged from three independent experiments with an overall SD of <20%.

To better clarify the role of NG2-ColVI in the modulation of tumor cells to growth in anchorage-independent manner, we performed also a clonogenity assay in soft agar, highlight that the presence of Col VI in the agar increases big colonies formation of NG2 expressing cells (**Fig. 21**).

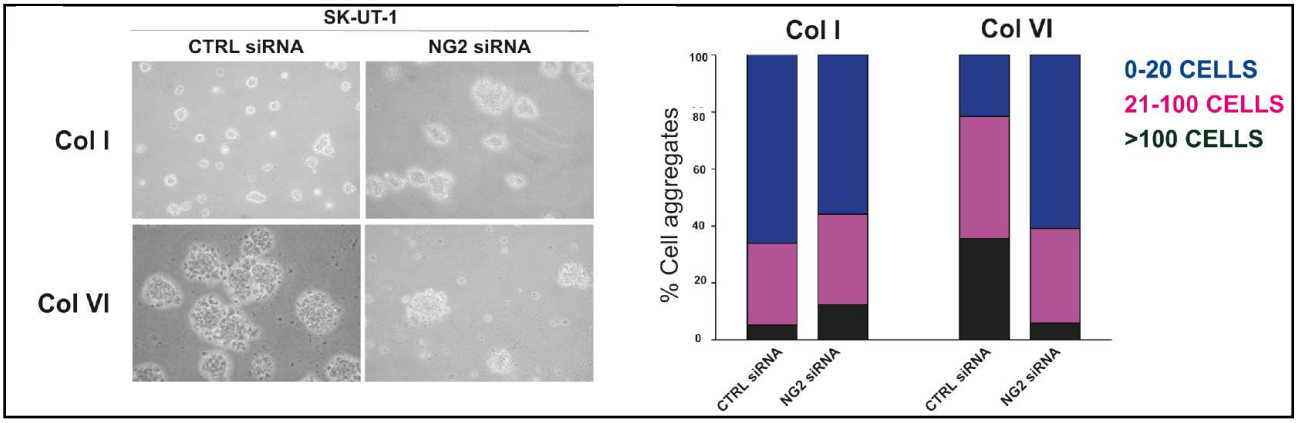

Figure 21. Representative phase-contrast images (*left panels*) of anchorage-independent colony formation in soft-agar in the presence of either Col I or Col VI and the corresponding assessment (*graphs to the right*) of the percentages of colonies with different amounts of cells.

The putative collagen-binding domain of NG2 is essential for cell anchorage to Col VI

When SK-UT-1 cells were forced to overexpress rodent NG2 constructs lacking the cytoskeleton-interacting *C*-terminal domain (a construct named NG2^{extra}), or constructs in which we had partially or entirely deleted the central "collagen-binding" segments of the ectodomain (Burg et al., 1997); i.e. constructs denoted D1D2Δ5 and D2Δ4; **Fig. 22A**), the cells bound significantly less well to Col VI (**Fig. 22B**). In contrast, cell adhesion to Col I remained largely unaffected. Identical results were obtained with immunosorted NG2-negative cells transduced with the same deletion constructs (**Fig. 22C**).

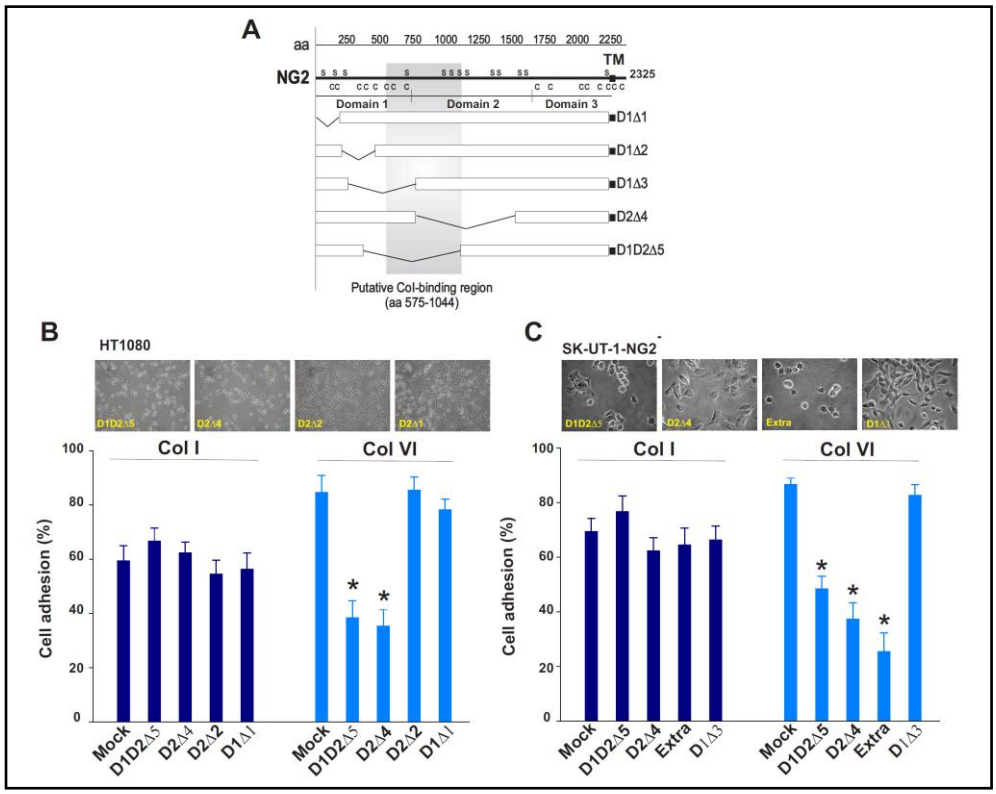

Figure 22. (A) Schematic view of the rodent NG2 deletion constructs used to engineer cells to overexpress, or express ectopically, distinct truncated forms of the PG. **(B)** Non-manipulated HT1080 cells and **(C)** immunosorted NG2$^-$ SK-UT-1 cells were transduced to express the NG2 deletion constructs described in (**A),** or NG2 molecules lacking the cytoplasmic tail (*Extra*). Cells were then assayed for their ability to adhere and spread on Col I or Col VI substrates. *Upper panels* show representative phase contrast views of the engineered cells interacting with the two substrates. ("***", $p<0.05$ by Mann-Whitney U test.)

The impaired adhesion of NG2-deficient cells to purified Col VI was indicative of an involvement of the PG in cell binding to this mono-molecular substrate, but did not fully clarify whether the same interplay was essential for cells interacting with matrix-assembled Col VI. To approach this question we isolated native cell-free ECM from murine embryonic fibroblasts derived from wild type or Col VI knockout mice. Such matrix substrates were generated using a recently re-

elaborated protocol for the isolation of native, cell-free matrices from cultured cells. Immunosorted NG2$^+$ sarcoma cells adhered more tenaciously to Col VI-containing native matrices than NG2$^-$and siRNA-treated cells, and again, higher surface levels of NG2 favoured a more pronounced binding to these ECMs (**Fig. 23A,B**). Intriguingly, native ECMs isolated from Col VI knockout fibroblasts were overall less supportive for adhesion of both NG2$^+$ and NG2$^-$ cell subsets, albeit matrices from the two genotypes exhibited apparently equivalent topographical arrangements (**Fig. 23C**).

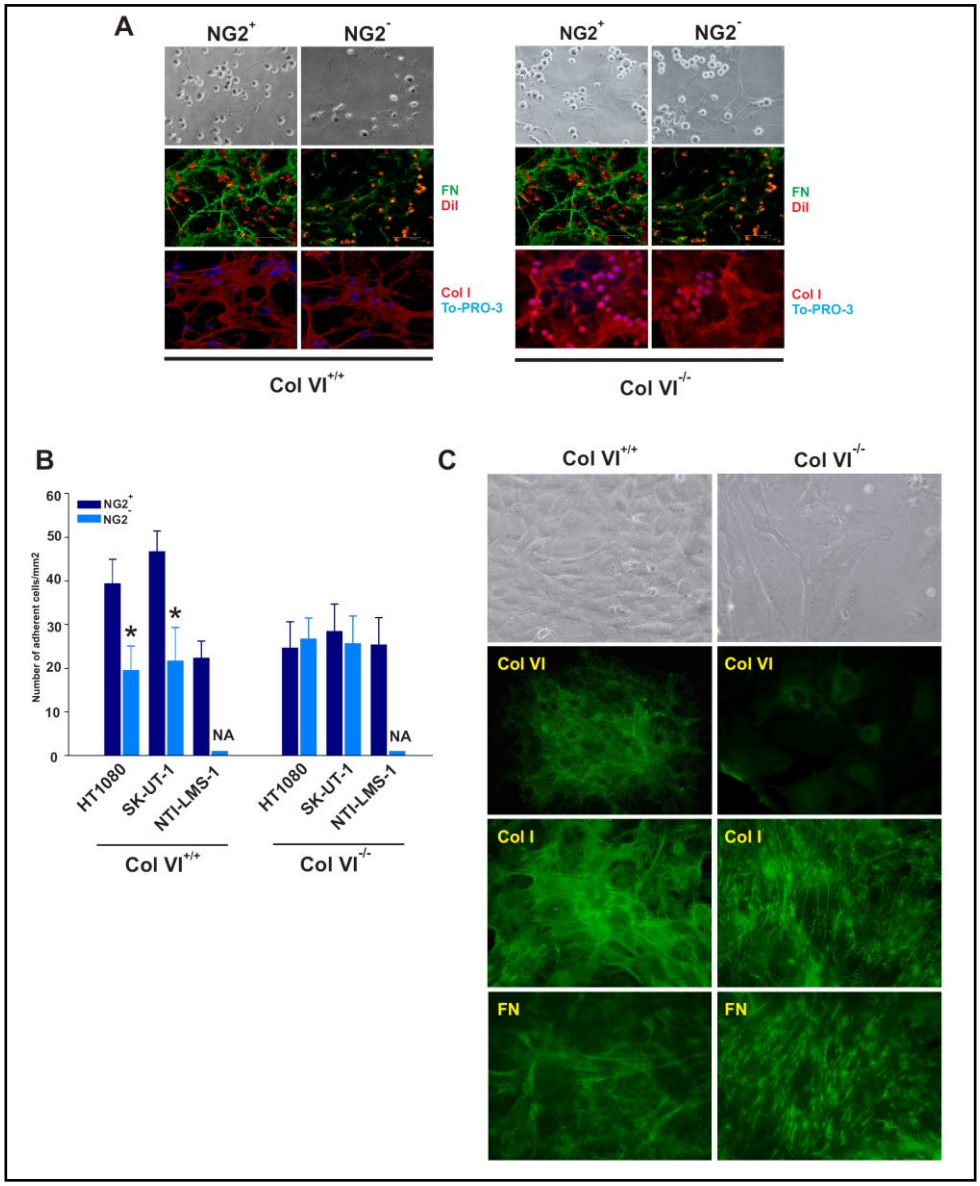

Figure 23. (A) Immunosorted NG2$^+$ and NG2$^-$ HT1080 cells binding to Col VI-containing (*left panel*) or Col VI-deficient isolated matrices (*right panel*). The ECM was stained with antibody to Fibronectin (FN) or Collagen I (Col I), and cells either tagged with DiI prior to incubation with the matrices or labelled with TO-PRO-3 after fixation of the specimens. **(B)** Assessment of cell adhesion to Col VI$^{+/+}$ and Col VI$^{-/-}$ matrices of the indicated NG2$^+$ and NG2$^-$ subsets by cell counting within randomly selected microscopic fields. "NA", not assessable (i.e. value close to "0"); "*", p<0.01 by Mann-Whittney U test. **(C)** From (Col VI$^{+/+}$) and Col VI knockout (Col VI$^{-/-}$) MEFs, visualized by contrast phase microscopy, we have isolated the matrices. Their deposition were highlighted by

immunolabelling with antibodies to murine Col VI, Col I or FN. Since Col VI null mice were created by deletion of the gene encoding the α1(VI) chain, the anti-Col VI polyclonal antiserum raised against the intact heterotrimeric collagen molecule reveals some retention of the newly synthesized α2(VI) and α3(VI) chains within the cytoplasm (presumably in part within the endoplasmatic reticulum) of the null fibroblasts generated by deletion of the COLVIA gene.

NG2 is a key surface component for cell movement

From our observations the role of NG2/CSPG4 seems to be important in the modulation of tumor cells' adhesion to ECM, but from literature the proteoglycan results also to be involved in promoting the migration and invasiveness of tumor cells. Our ECM-isolation procedure gave us the possibility to analyzed different aspect of tumor cells migration as, for instance, distance covered by tumor cells, their velocity or persistence (capability of cells to maintain the linear directionality of movement) (**Fig. 24)**

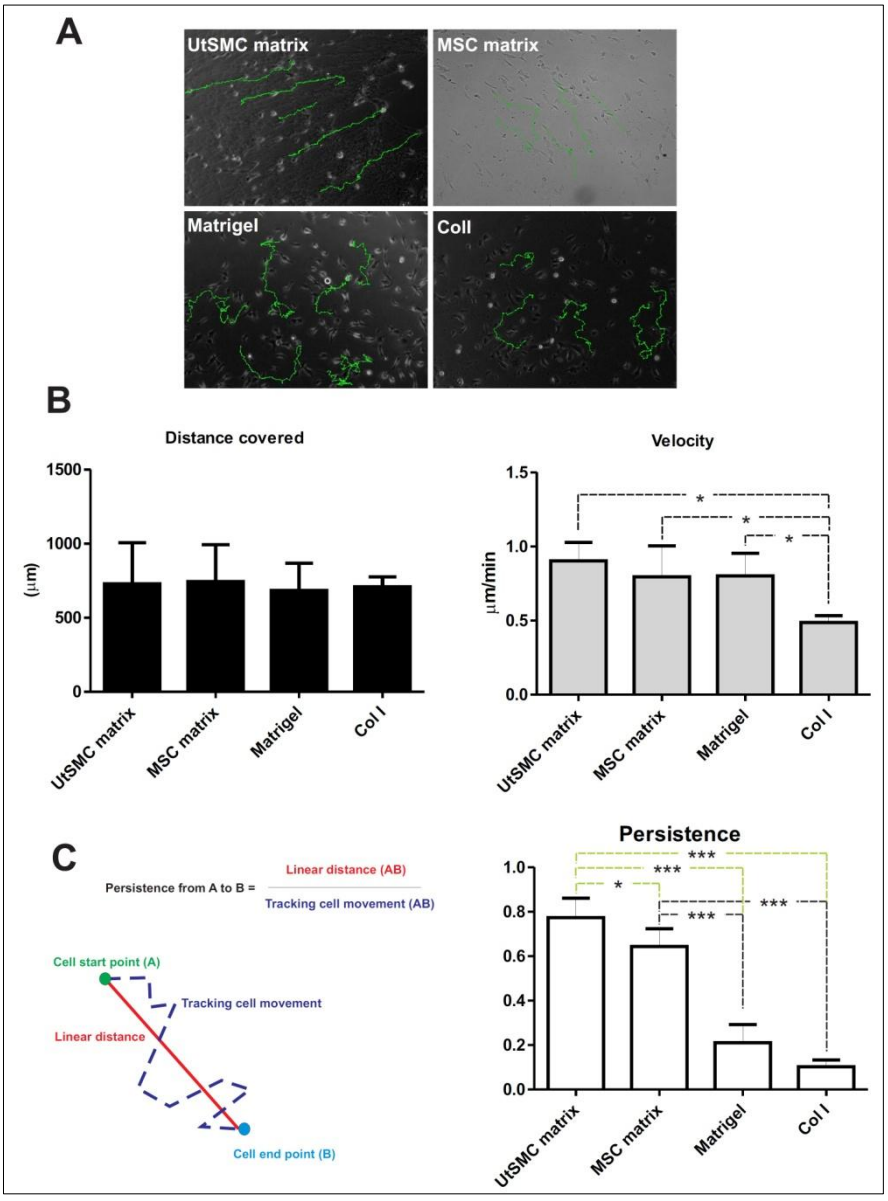

Figure 24. (A) Representative trackings of HT1080 cells migrating on native UtSMC or MSC ECM; on Matrigel or Col I. The green lines trace representative trajectories of individual cells in each condition. **(B)** Quantification of distance covered and velocity of HT1080 migrating on the different substrates. **(C)** The quantification of persistence (*right graph*), definite as the ratio between linear distance and the tracking cell movement (*left*). (*"*"=p < 0.05;"**"=p<0.001;"***"=p<0.0001;* calculated with Student's t-test)

We decided to investigate the capability of immunosorted cells to migrate on isolated UtSMC, but we did not observed any differences between the $NG2^+$ and $NG2^-$ migration velocity of tumor cells, and in both the case the linearity of migration was maintained along the fibers (**Fig. 25**).

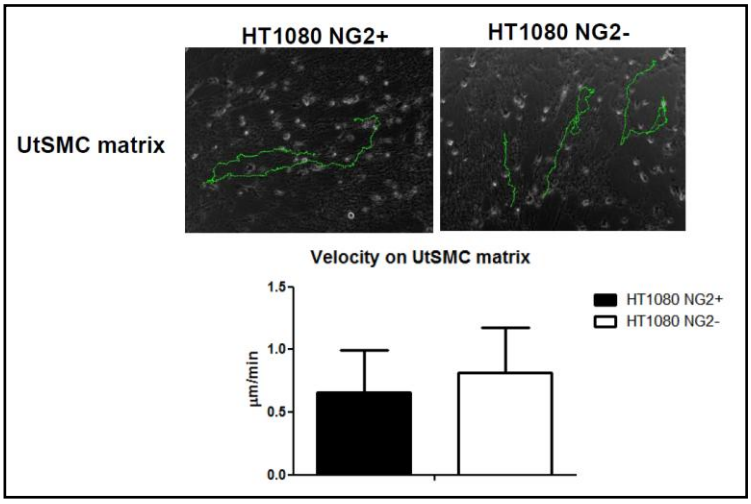

Figure 25. Representative trackings of cells migrating on native ECM. The green lines trace representative trajectories of individual cells in each condition. The graphic represents the mean velocity of 10 cells analysed in three independent experiments for each condition.

Moreover for the invasiveness analysis, we performed an haptotactic assay by Trans-wells, according with the FATIMA system (*see Material and Methods)*, plating UtSMC or MSC cells on the top side of the Trans-wells, isolating the ECM that they produced and plating on the top immunosorted tumor cells. The addiction of complete medium on the lower chamber of the well induced the migration of tumor cells through the isolated ECM (**Fig. 26**). From these experiments different results were obtained between the $NG2^+$ and $NG2^-$ HT1080 cells. Indeed if the expression of NG2 seems to facilitate the migration in presence of UtSMC ECM, an opposite behavior was observed using MSC matrix (**Fig. 26**).

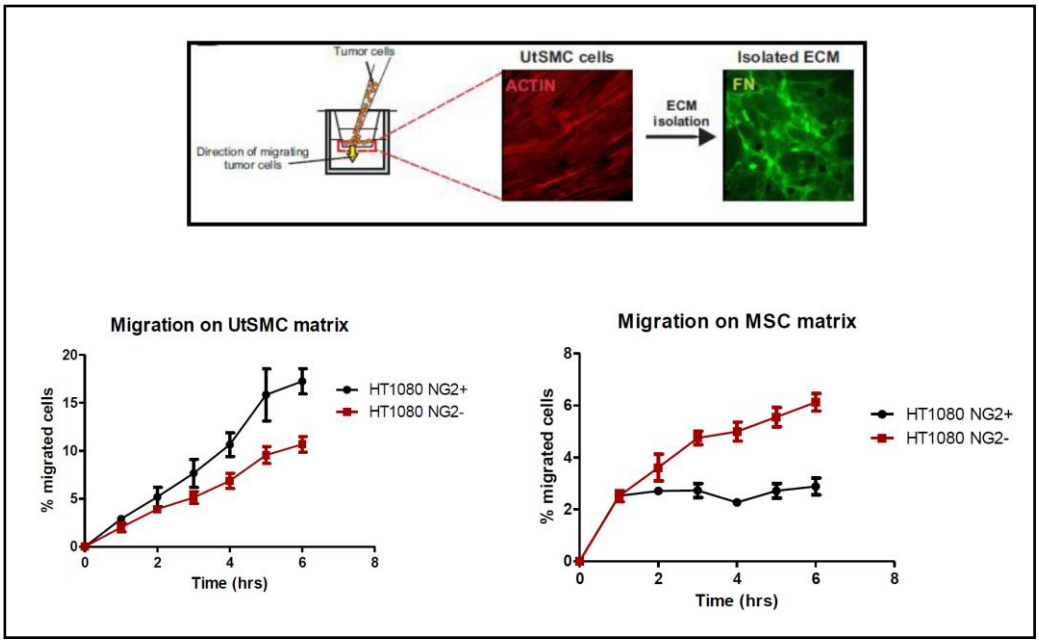

Figure 26. On the top, A schematic overview of the experimental set up for haptotactic motility (FATIMA system based on FluoBlok inserts). Fluorescently tagged HT1080 cells suspended in DMEM with 0.5% BSA were seeded on upper surface of the porous membrane covered with the native ECM isolated from UtSMC. The lower part of the well was filled with DMEM containing 10% FCS. Fluorescent panels show: actin staining of an UtSMC monolayer grown on the upper side of the membrane, and immunostaining of matrix for FN after ECM isolation. We reported in the graphs the kinetics of the migratory response of $NG2^+$ and $NG2^-$ HT1080 confronted in presence of UtSMC or MSC matrix . The mean values ± SE of three independent experiments are reported. The data obtained at 6 hrs from the beginning of experiments are significantly different ($p < 0.05$ calculated with Student's t-test)

To verify also the invasion capability of tumor cell CSPG4-dependent in a 3D contest we decided to used spheroids of $NG2^+$ or $NG2^-$, obtained plating the tumor cell on polyHEMA (*see Material and Method*), embedded in Matrigel. We observed an higher number of $NG2^+$ than $NG2^-$ tumor cell to invade the surrounding area, highlighting the capability of CSPG4 to confer an high aggressive phenotype (**Fig 27**).

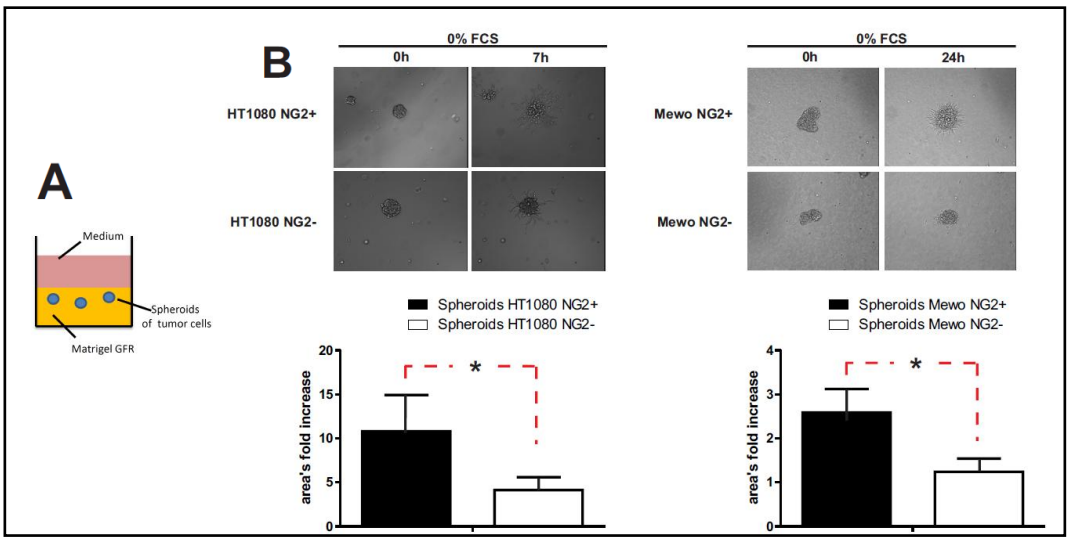

Figure 27. (A) Schematic representation of experimental setting , in which the tumor spheroid were embedded into Matrigel, and the subseguent addiction of medium on the top (in our case DMEM without serum). **(B)** Quantification of the invasion capability of HT1080 (*left*) or Mewo (*right*) immunosorted for NG2. ("*"=p<0.05 by Student T-test)

Movement on Col VI

The above findings indicate that cell-matrix interplays, promoted by the NG2-Col VI interactive pair, could be crucial for the control of cell survival, cellular aggregation and local tumour propagation. To determine whether such interactions may also be important for cell migration and invasion in response to Col VI we set up a number of dedicated in vitro assays using the cellular models and matrix substrates described above. Similarly to what observed for cell-substratum adhesion, the extent of haptotactic movement on isolated Col VI tetramers closely correlated with the different NG2 surface levels displayed by the cells (**Fig. 28A**). Loss-of-function of the PG strongly compromised this migratory behaviour, but did not perturb the lower levels of motility seen on Col I (**Fig. 28B**).

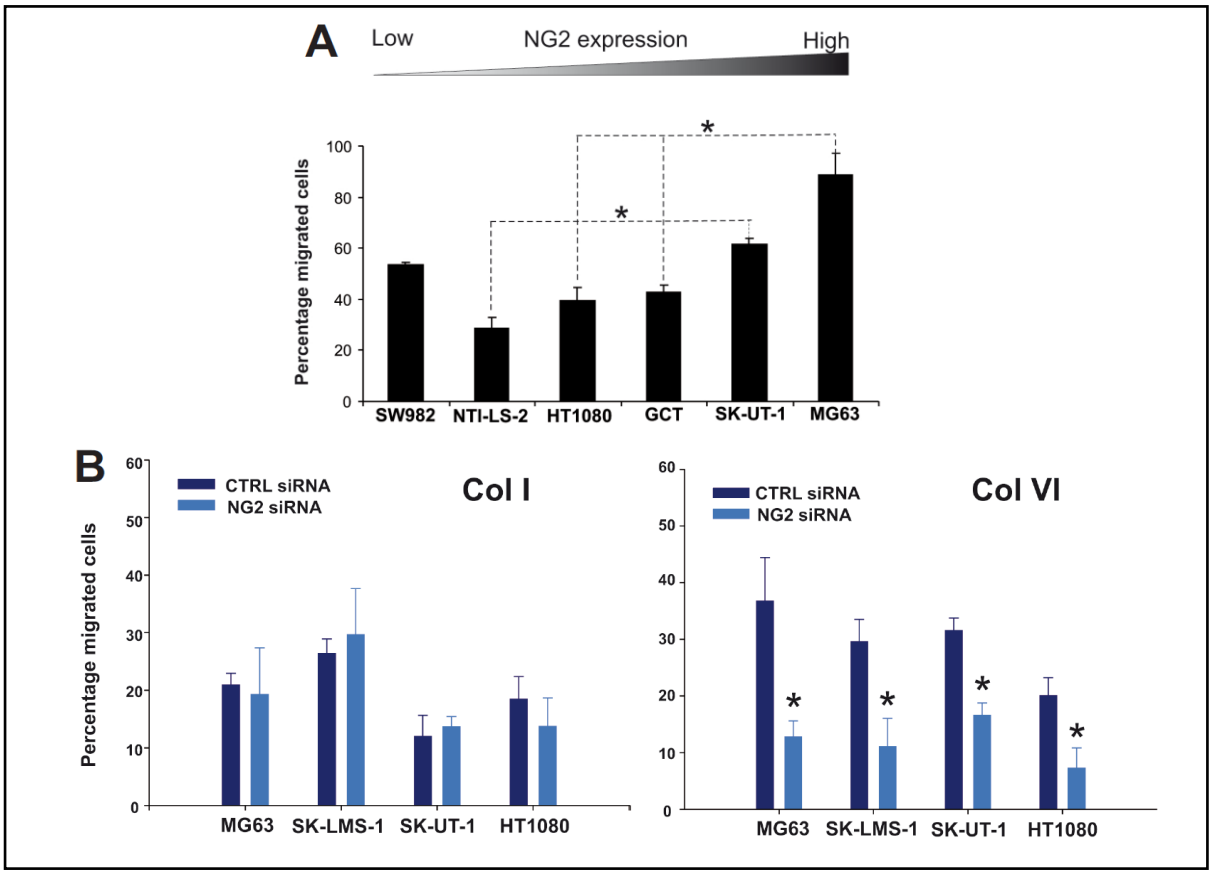

Figure 28. (A) Extents of haptotactic movement (FATIMA system) of different sarcoma cell lines on Col VI tetramers, relative to their measured NG2 surface levels. "*", *p*<0.01 by Mann-Whittney U test. **(B)** Haptotactic cell migration in response to Col I or Col

VI of different sarcoma cell lines in which NG2 was knocked down (*p<0.0054 by two-way ANOVA).

The direct role of CSPG4/NG2 in the modulation of haptotactic movement was confirmed also using immunosorted SK-UT-1-NG2$^-$ cells transduced with truncated, in presence of Col VI (**Fig. 29**)

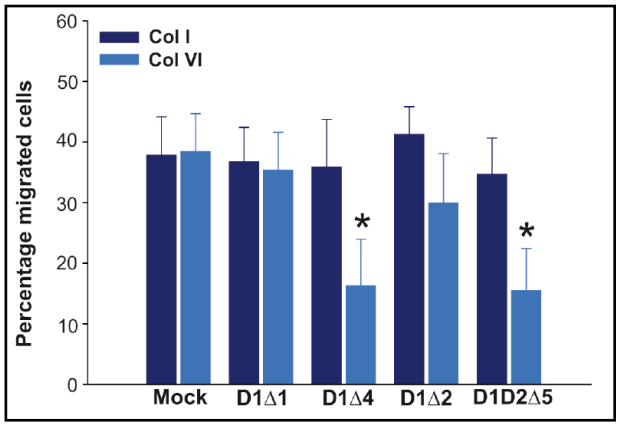

Figure 29. Extents of migration **(**FATIMA system) of immunosorted SK-UT-1-NG2$^-$ cells transduced with truncated forms of the PG and allowed to migrate on Col I or tetrameric Col VI substrates. "*", p<0.001 by two-sided ANOVA.

The higher capability of NG2$^+$ tumor cells to migrate in presence of Col VI was confirmed also in a scratch assay, resulting significantly quickly than NG2$^-$ counterpart (**Fig. 30**)

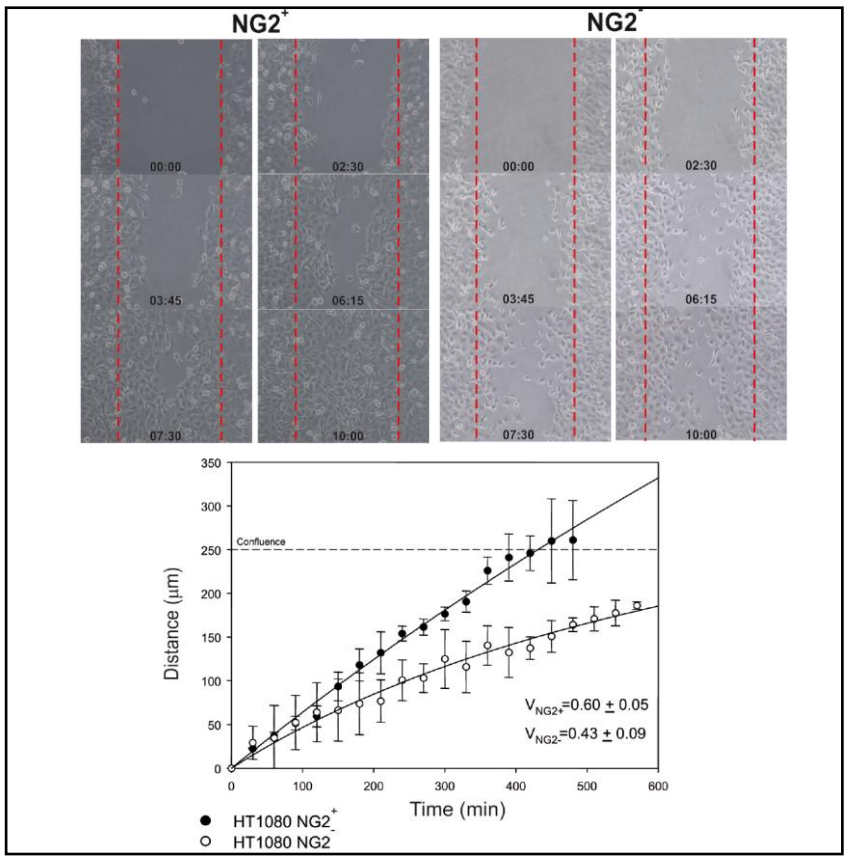

Figure 30. The upper panel is a representative migratory behaviour of HT1080 NG2$^+$ and NG2$^-$ cell subsets in response to tetrameric

Col VI (scratch assay). The graph reports the quantification, from which result that $NG2^+$ cells migrate significantly faster. "Confluence" refers to the distance within the scratch at which there was complete coverage of the scratch area and cells were progressively arrested in their movement by contact inhibition.

SiRNA-mediated abrogation of NG2 also affected the capability of the cells to penetrate complex, Col VI-containing matrices, as shown by experiments involving inclusion of cells into Matrigel droplets supplemented with Col VI. In this experimental setting, cells that had retained NG2 on their surface migrated out from the droplets more effectively than NG2 deprived cells (**Fig. 31A, B**). By exploiting our FATIMA system (Spessotto et al., 2009) and polymeric Col I or Matrigel supplemented with Col VI, it was finally possible to appreciate the higher invasive capability of NG2-expressing cells (**Fig. 31C**). Inclusion of Col VI favoured sarcoma cell movement through these 3D matrices and, consistently with the observed adhesive and motile behaviour, the invasive capabilities of the cells were intimately related to their NG2 surface levels.

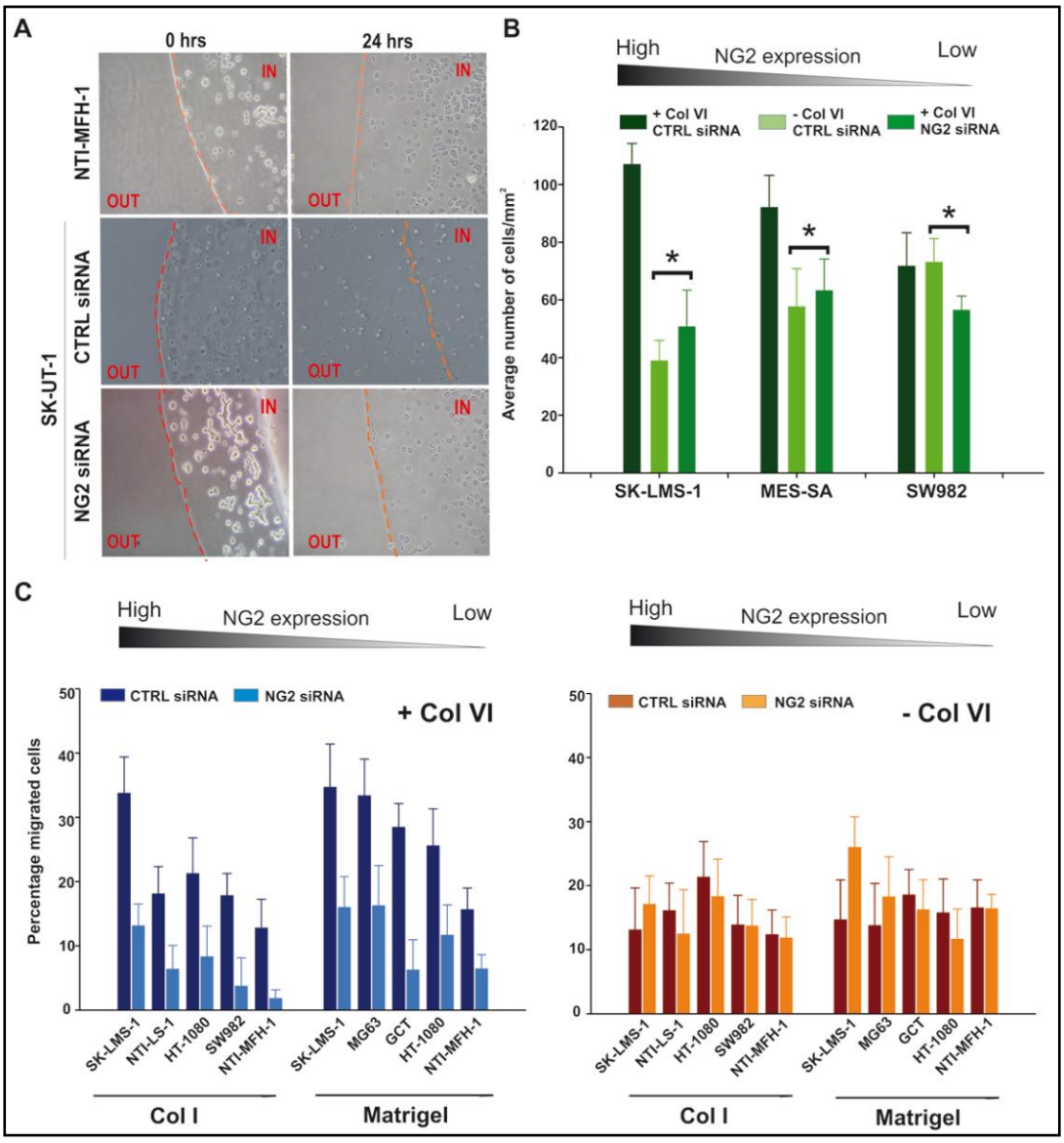

Figure 31. **(A)** Representative phase-contrast views of the capability of NTI-MFH-1 (sarcoma cells with poor surface expression of NG2), SK-LMS-1 treated with the control (CTRL siRNA), or NG2-directed siRNAs to move through Matrigel droplets supplemented with tetrameric Col VI. **(B)** Assessment (by cell counting of randomly selected microscopic fields) of the ability of cell lines displaying diverse surface levels of NG2 (SK-LMS-1,MES-SA,SW982) to evade Col VI-supplemented (+ Col VI) or non-supplemented (- Col VI) Matrigel after treatment with a control siRNA, "CTRL siRNA", or an NG2-directed siRNA, "NG2 siRNA". *p<0.01 by Student's t test. **(C)** Relative capabilities of different sarcoma cell lines to invade polymeric Col I substrates supplemented (+ Col VI) or not (- Col VI) with tetrameric Col VI, after treatment with the CTRL or NG2-directed siRNAs. In the presence of Col VI, NG2 knockdown consistently and significantly (p<0.01-0.001 by Mann-Whittney U test) reduced the invasive capabilities of the cells.

NG2-Col VI interaction triggers cell adhesive- and migration-associated PI-3K activations

To establish whether the observed NG2/Col VI-mediated promotion of cellular interactions involved the activation of defined intracellular signalling cascades, we carried out a series of antibody array- and immunoblotting-based phospho-proteomic screenings. For these we used NG2-expressing and NG2-deficient cells exposed to either purified Col VI or Col I. We adopted an experimental strategy entailing the plating of siRNA-treated cells onto poly-L-lysine-coated substrates and the addition of molar equivalents of soluble Col VI or Col I. Effectiveness of an experimental design involving soluble ECM ligands was partly supported by previous observations showing that both Col I and Col VI are capable of eliciting signal transduction events when added in solution (Ruhl et al., 1999b; Ruhl et al., 1999a). To assure the optimal neutralization of signalling phenomena evoked by $\alpha 2\beta 1$ integrin binding to the collagens, we simultaneously treated cells with anti-$\alpha 2$ integrin function-blocking antibodies and $\beta 1$ integrin-directed siRNA probes.

The appropriateness of the experimental strategy was initially verified by examining the phosphorylation patterns of the cells by semi-quantitative immunoblotting, using a platform in which about 70 phosphorylation sites in 63 selected signal transduction components were simultaneously probed. The phosphorylation screening was performed as a four-way comparative analysis of the signal transduction cascades triggered in "integrin-deprived" SK-UT-1 cells, exposed to either Col VI or Col I in the presence or absence of cell surface NG2, according to the following scheme: NG2-expressing versus NG2-deficient cells exposed to Col I; NG2-expressing versus NG2-deficient cells exposed to Col VI; NG2-expressing cells exposed to Col I versus Col VI; and NG2-deficient cells exposed to Col I versus Col VI (**Fig 32**).

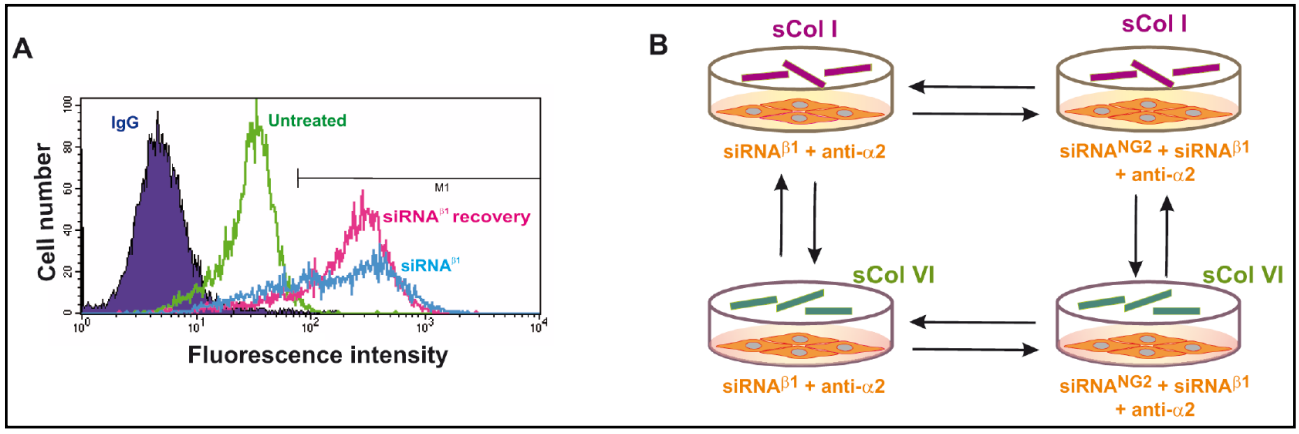

Figure 32. **(A)** Relative levels of β1 integrin subunit knock-down (as determined by flow cytometry) obtained with the employed siRNA probe in SK-UT-1 cells and the corresponding surface recovery (siRNA$^{\beta1}$ recovery) of the target to support the specificity of its induced loss-of-function. Knock-down efficacy of the siRNA probe was evaluated 3 days following transfection and surface recovery after additional 3 days (i.e. a total 6 days after transfection). A scrambled siRNA probe sequence was used as a negative control. Anti-human and anti-murine β1 integrin siRNA probes were also independently validated for their ability to inhibit cell binding to FN by at least 50% (*not shown*). **(B)** Strategy employed for the four-way comparative phospho-proteomic profiling (as depicted by the arrows) based upon semi-quantitative Western blotting with a total of 69 antibodies against phosphorylation sites within 63 signal transduction components. Starved cells were exposed for 30 min to molar equivalents of monomeric Col I and intact Col VI tetramers (i.e. 160 μg/ml of Col I monomers and 20 μg/ml of Col VI tetramers), following knock-down of the β1 integrin subunit and NG2 ("NG2-deficient"). Cells were then lysed and the solubilised material resolved by SDS-PAGE under reducing conditions and processed for immunoblotting.

The outcome of these comparisons indicated that when either NG2-positive or NG2-negative cells were compaired with Col I, 39 phosphorylation sites were either equally modulated in the two cell types, or were not identifiable in any of them (either because the molecule was not expressed or because the screened site was not phosphorylated). These sites were "filtered away" leaving 33 phosphosites as the ones specifically modulated in cells interacting with Col VI in presence or absence of NG2. The 12 sites exhibiting enhanced phosphorylation (two sites were de novo phosphorylated) in NG2 expressing cells encompassed sites of components associated with cell survival, apoptosis, stress-related responses and cytokine-typical signal transduction cascades. Conversely, 14 sites pertaining to cell-cycle regulators, growth factor/cytokine response mediators and controllers of cytoskeleton dynamics were found to be less phosphorylated in cells deficient in NG2 when compared to NG2-positive ones (**Fig. 33**).

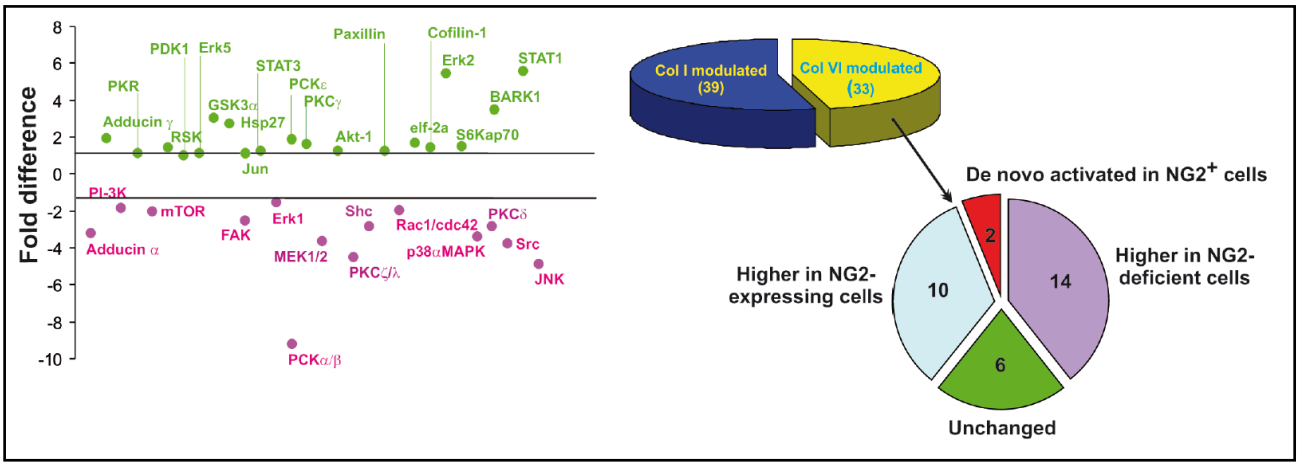

Figure 33. (A) The plot summarizes the variations in phosphorylation degree of the indicated molecules when comparing cells treated with the NG2-directed siRNA versus control siRNA probe and after normalization against the variations observed when comparing Col I- versus Col VI-exposed cells. No significant differences in phosphorylation levels were observed in cells exposed to Col I. Differences in phosphorylation degree were determined by adopting an arbitrary ±1.5 fold-difference to define significantly up- or down-regulated phosphorylation levels after normalization to the relative amount of the molecules detectable in either cell phenotype/condition. **(B)** The accompanying pie chart summarizes the total outcome of the phospho-proteomic screening using the same comparative criteria and threshold as in **(A)**.

In a parallel approach, we pursued a direct comparison of the signal transduction patterns elicited by Col I or Col VI in murine melanoma cells ectopically expressing NG2 when compared to wild type counterpart cells lacking the PG (**Fig. 34**).

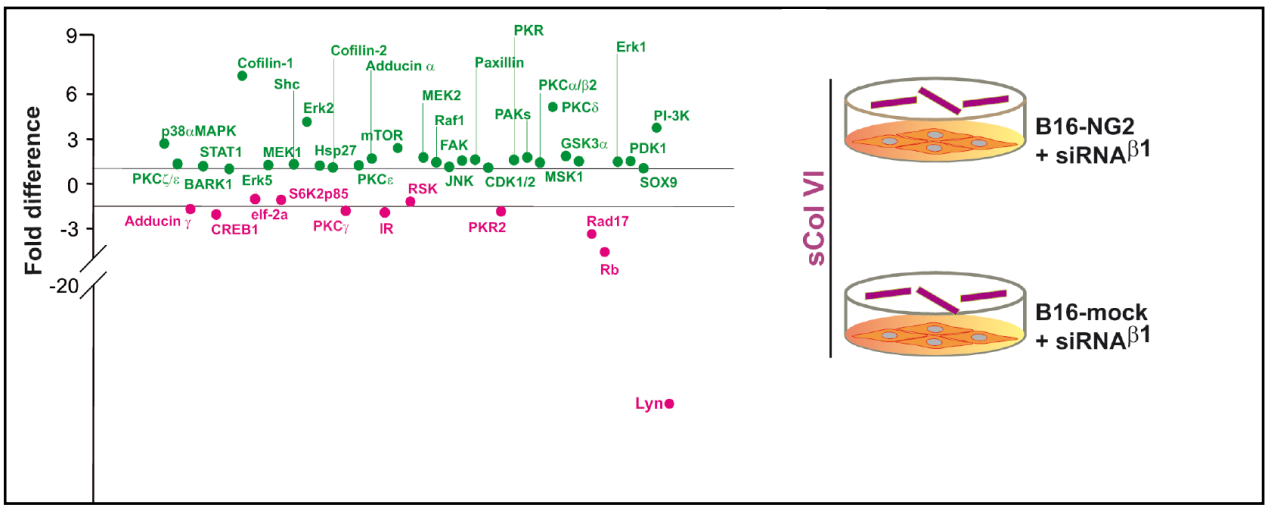

Figure 34. Summary plot of an alternative phospho-proteomic screening carried out according to the scheme depicted into the *right,* entailing murine B16 melanoma cells stably transduced to express rodent NG2 ectopically. NG2-transfected and mock-transfected cells were treated with a mouse-specific siRNA to knockdown the β1 integrin subunit and exposed for 30 min to soluble Col VI tetramers. Lysates of the cells were processed for phospho-proteomic analysis as described above.

Through this alternative approach we could corroborate the NG2/Col VI-induced up-regulation of 14 phosphosites harboured by the same classes of signalling components that were unveiled with the simpler immunoblotting-based screening approach. By contrast, 11 phosphosytes were found

to be strongly down-regulated or completely abrogated. Eighteen of the phosphosites that were not found to be modulated upon the cells' interaction with Col I remained unvaried also when cells reacted with Col VI. Comprehensively, through two independent experimental paradigms we could assert the usefulness and reproducibility of the adopted phospho-proteomic strategy and could gain important information about the signalling pathways elicited by the NG2-Col VI binding (**Fig 35**).

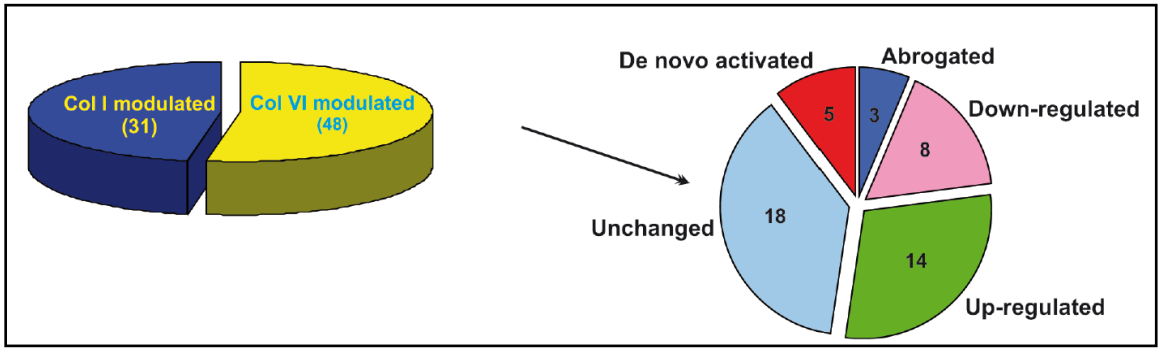

Figure 35. Global pie chart of the final of the phospho-proteomic screening using the comparative criteria explained in previous figure.

We then sought to generate a more global and definite portrait of the NG2/Col VI-induced signal transduction by relying upon a wider and more quantitative phospho-proteomic screening. For this purpose we applied the four-way comparative Col I/Col VI-based paradigm to immunosorted HT1080 $NG2^+$ and $NG2^-$ cells. The screening was performed using a 627-spot (spotted in duplicate plus control spots) fluorescent antibody-array platform, followed up by verification of the 36 primary lead phosphosites by semi-quantitative immunoblotting. In this case we adopted an arbitrary threshold setting of the system at 1.5-fold difference (95% confidence interval) for the assertion of the divergent phosphorylation status of the examined molecules. Delineation of the modulated phosphorylation pattern was based upon normalization of the actual expression levels of the molecules in the two cell types, as established by the parallel reactivity patterns of phosphorylation-independent antibodies against the individual components. Through this approach we found that phosphorylation of a total of 84 sites in 76 components was higher in $NG2^+$ versus $NG2^-$ cells interacting with Col VI (i.e. the molecules were more de-phosphorylated in NG2-deficient cells; 16-48-fold difference). *Vice versa*, 75 sites in 58 components were found to be more phosphorylated in the latter cells (**Fig. 36**).

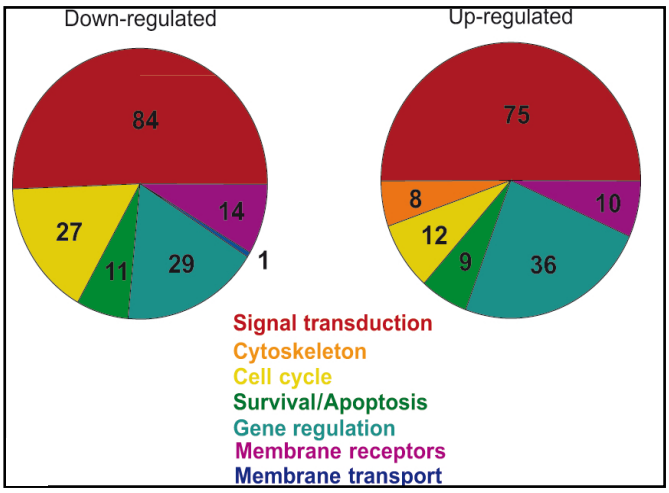

Figure 36. Summary of the ontological clustering of the molecules with modulated phosphorylation, resulted from screening performed according to the four-way comparisons (explained before) and using a fluorescent 627-spot antibody array platform.

A total of 82 phosphosites in 76 molecules, including sites within cofilin-2, PAK5, PP4C, p38aMAPK, MEK4/6, PCKβ2/PCKh, β-catenin, PDGFRα, Fos, ErbB2, PTEN, Pyk, p53, S6Kα, ZAP70, PP1/Cα, Lck, MAPKAPK2, Etk and several STATs, were found to be unchanged (i.e. <1.5-fold difference). The remaining phosphosites detected by the platform were not detectable in either cell type. In NG2-deficient cells, lower phosphorylation degree and/or complete de-phosphorylation was observed for a number of molecules controlling cell survival and promoting apoptosis, negative regulators of the cell-cycle, and components of the cytostatic IFN signalling pathway, previously documented in these cells (Gazziola et al., 2005). Conversely, molecules displaying de novo and/or enhanced phosphorylation were prevalently associated with actin microfilaments and microtubule dynamics, formation of focal adhesions, positive regulation of the cell-cycle and propagation of PCKs and MAPK/ERK pathways (**Fig. 37**).

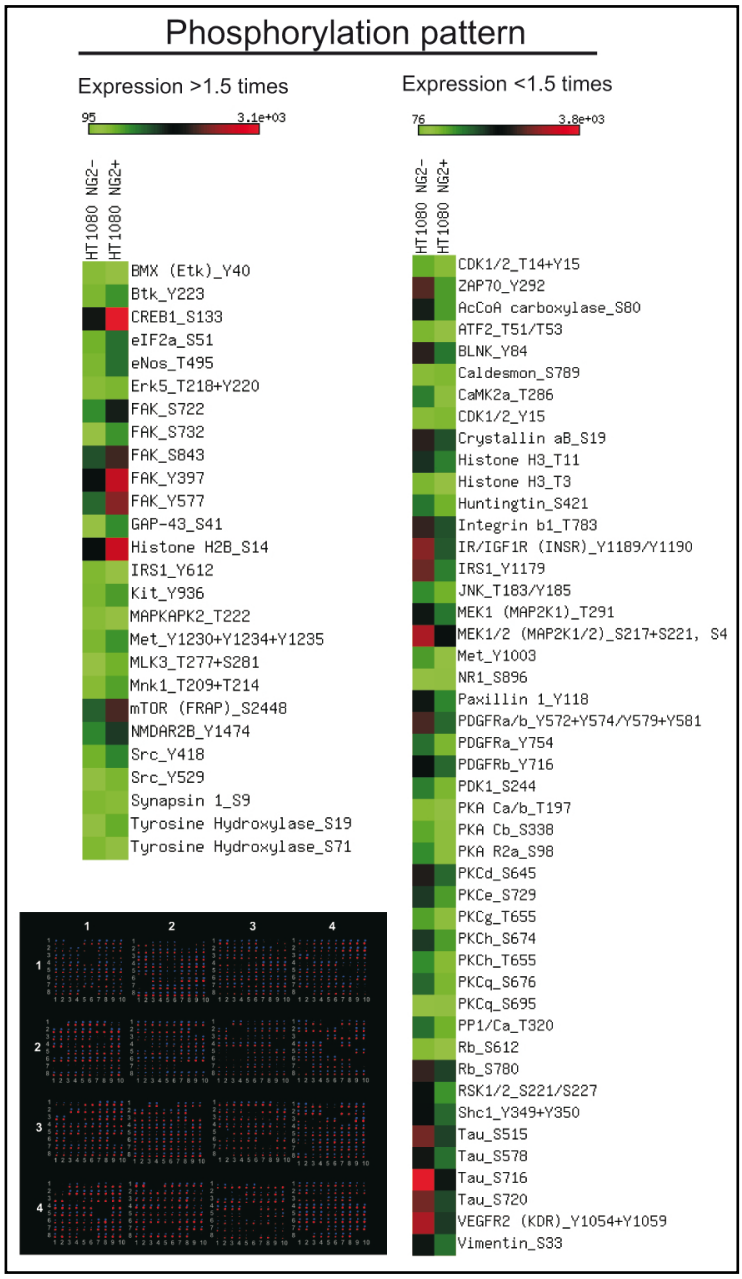

Figure 37. Heat map of the outcome of a representative phospho-proteomic comparative screening performed according to the four-way comparisons depicted before and using a fluorescent 627-spot antibody array platform (*lower image*). The map was generated by arbitrarily adopting a cut-off of 1.5-fold difference (within a 95% confidence interval) of the degree of phosphorylation of single molecules, after normalization for their relative, constitutive expression levels.

To approach the functional significance of the observed NG2/Col VI-dictated phosphorylation profiles we set up short-term cell adhesion assays with siRNA-treated and immunosorted cell subsets. Cells were allowed to adhere to Col VI or Col I substrates in the presence or absence of drugs selectively antagonizing individual signal transduction components. Addition of signalling antagonists to NG2-deficient cells did not significantly affect their poor adhesion to Col VI, whereas both the ROCK1 inhibitor Y27632 and the Src inhibitor PP2 impaired adhesion to both Col

I and Col VI in either cell phenotype (**Fig. 38**). Moreover, ATP-competitive and non-competitive antagonists of p38MAPK (PD169316 and SB203580, but not the control drug SB202474), an antagonist of MEK1/MEK2 (UO126, but not UO124), and two potent and rather selective antagonists of PI-3K (LY294002 and Wortmannin) produced selective blockades of $NG2^+$ cell binding to Col VI (**Fig. 38**).

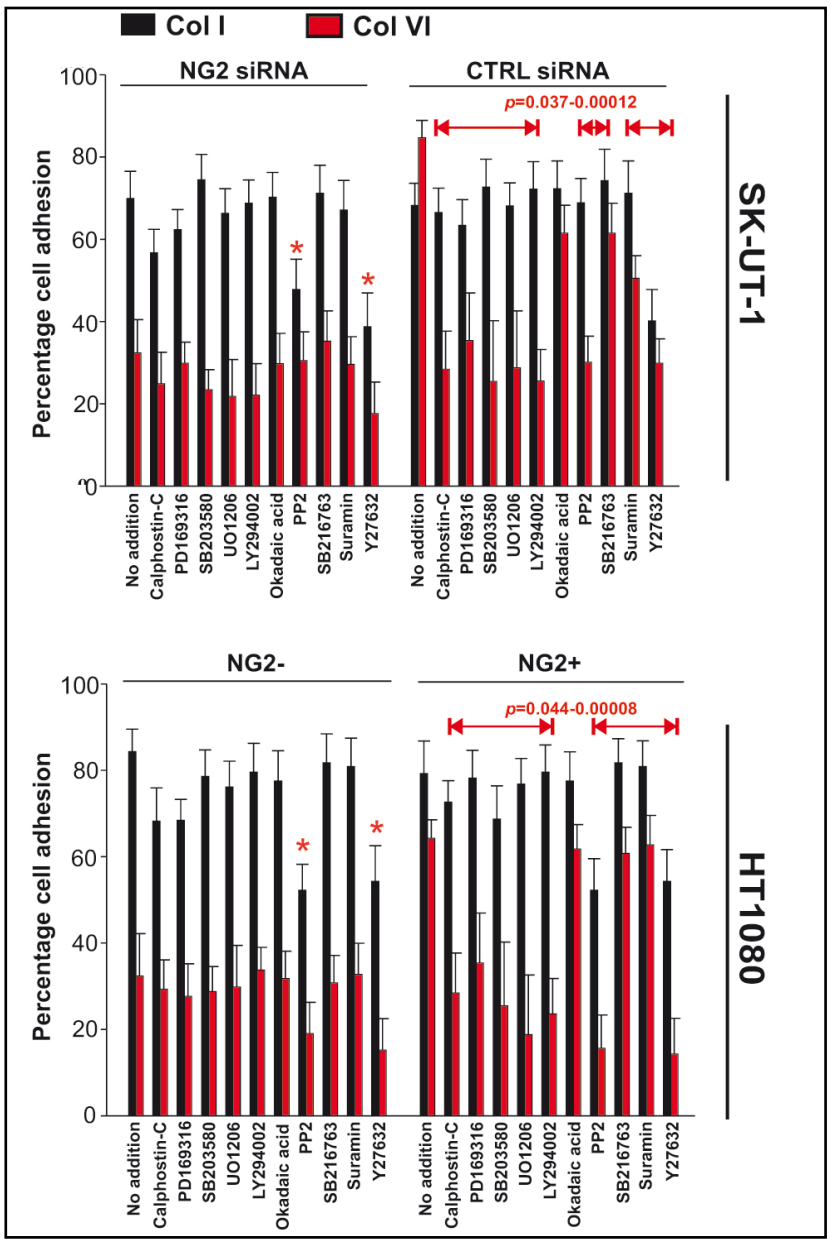

Figure 38. Effect of signalling antagonists on adhesion to Col I and Col VI of SK-UT-1 cells treated with the NG2-directed or CTRL siRNA. The *lower graph* shows the results obtained, using the same experimental paradigm, with immunosorted $NG2^-$ and $NG2^+$ HT1080 cells.

To finally investigate the potential involvement of PI-3K in cell motility regulated by NG2-Col VI interactions we performed migration assays with $NG2^+$ and $NG2^-$ cells in which, along with soluble Col VI, LY294002 or Wortmannin were added. In the presence of either inhibitor $NG2^+$ cells were

largely impeded in their movement, whereas the poorer migration rate of NG2$^-$ cells seemed to be unaffected (**Fig. 39A,B**).

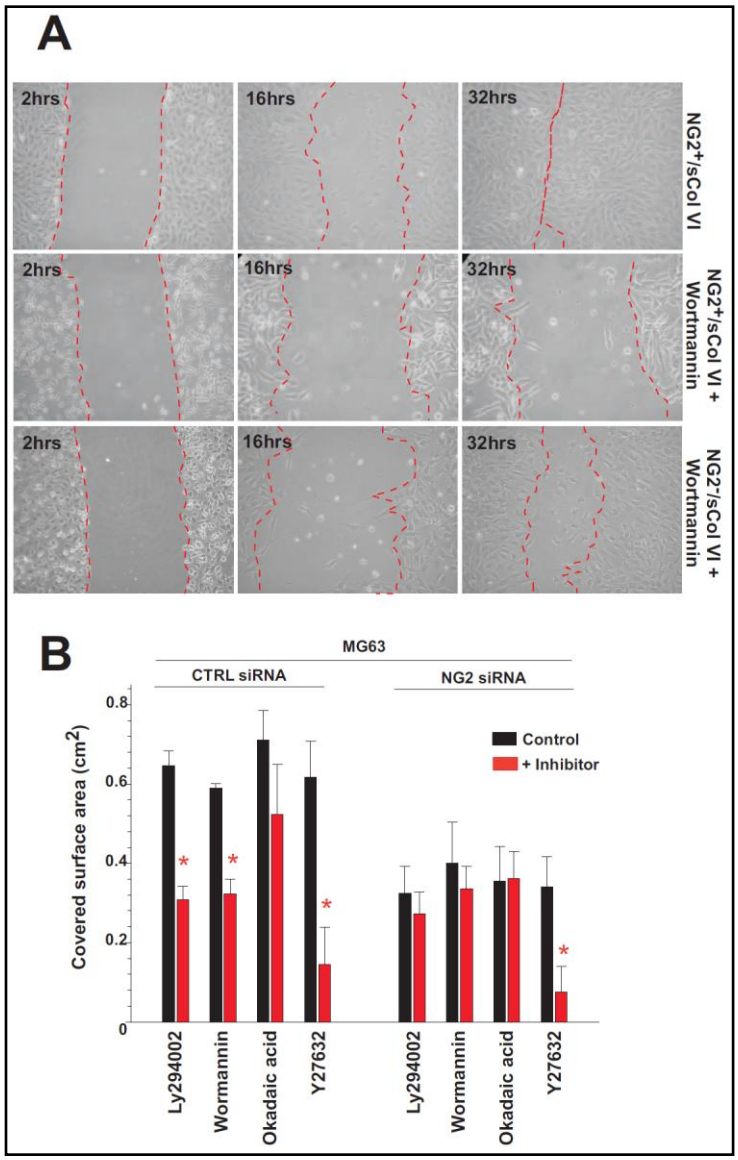

Figure 39. (A) Representative migration rates of NG2$^+$ and NG2$^-$ cells in the presence of soluble Col VI (sCol VI) and 5μM/ml of Wortmannin. **(B)** Extent of cell migration (scratch assays) of MG63 cells treated with the CTRL or NG2-directed siRNA in the simultaneous presence of Col VI and the indicated signalling inhibitors ("*"= p<0.01 by Student's t test).

On the basis of these results, the cumulative findings of our phospho-proteomic screening, and the previously published information about the NG2 connection with defined signalling cascades, we propose a scheme of how NG2 binding to Col VI microfilaments may, through a putative modulation of cytoskeletal dynamics, contribute to the convergence of integrin- and growth factor-elicited signal transduction pathways (**Fig. 40**).

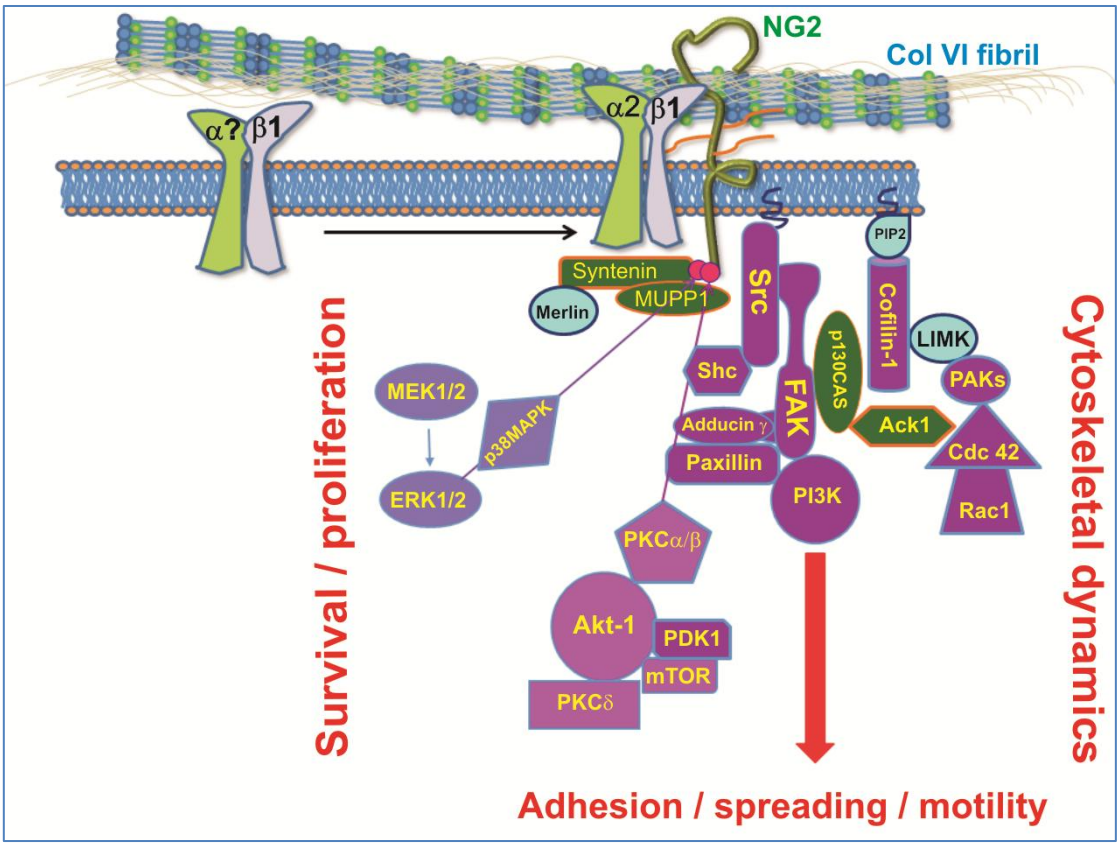

Figure 40. Proposed scheme of the signal transduction pathways activated by the NG2-Col VI interaction and believed to converge and/or agonize with the ones activated by growth factor receptors and integrins. Signal transduction components highlighted in *purple* are the ones confirmed and/or newly discovered in our study, components in *green* are molecules previously discovered to directly interact with and/or be activated by NG2 and molecules in *light blue* are inferred from previous studies.

Up-regulation of NG2 and Col VI are additively predicting metastasis formation and a dismal clinical course

In a previous study we have shown that NG2 is strongly up-regulated in primary and metastatic STS lesions and that its relative levels of expression may serve as a prognostic indicator of disease course and post-surgical metastasis formation (Benassi et al., 2009). To further substantiate this finding we have re-examined the prognostic significance of NG2 in a twice as large and more diversified cohort of patients from whom both primary and secondary STS lesions were accessible and for whom the full clinical history could be evaluated (**Table 3**).

Table 3. Demographics and baseline clinical traits of STS patients from whom surgical specimens were subjected to molecular analyses[1]

Patient	Sex	Age	Histological subtype[2]/grade[3]	Site of primary lesion	Site of metastases	Clinical course[4]
1	M	72	MFS/II	Thigh	Lymphnodes	DOD
2	M	54	MFS/II	Leg	NF	NED
3	M	63	MFS/III	Thigh	NF	NED
4	M	61	MFS/II	Shoulder	Lung	AWD
5	F	73	MFS/III	Thigh	Lung	AWD
6	F	54	MFS/III	Thigh	Lymphnodes	DOD
7	M	64	UPMS/III	Thigh	Lung	DOD
8	M	62	UPMS/III	Arm	NF	NED
9	M	38	MFS/III	Thigh	NF	NED
10	F	43	UPMS/III	Thigh	NF	NED
11	F	67	UPMS/III	Pelvic girdle	NF	DOD
12	F	72	UPMS/III	Thigh	Lung	DOD
13	F	56	UPMS/III	Thigh	Lung	DOD
14	M	38	UPMS/III	Thigh	Lung	DOD
15	M	62	UPMS/III	Pelvic girdle	Lung	NED2
16	F	66	UPMS/III	Thigh	Lung	DOD

Patient	Sex	Age	Histological subtype[2]/grade[3]	Site of primary lesion	Site of metastases	Clinical course[4]
17	M	71	LMS-c/III	Thigh	Lung	DOD
18	M	57	LMS-c/III	Forearm	Lung	AWD
19	M	63	LMS-p/III	Arm	Lung	DOD
20	F	76	LMS-p/III	Thigh	Lung	DOD
21	M	34	LMS-p/III	Thigh	Lung	DOD
22	M	62	LMS-c/III	Thigh	Lung	DOD
23	M	66	LMS-c/III	Forearm	Lung	AWD
24	M	34	LMS-p/III	Spine	Lung	DOD
25	M	55	LMS-c/III	Thigh	Lung	DOD
26	M	68	LMS-c/II	Leg	Absent	NED
27	M	38	LMS-p/II	Leg	NF	NED
28	F	61	LMS-p/III	Thigh	Lymphnodes	AWD
29	M	43	LMS-p/III	Thigh	Lung	AWD
30	M	52	LMS-p/III	Thigh	Lung	DOD
31	F	79	LMS-c/II	Thigh	NF	DOD
32	F	57	LMS-c/III	Thigh	Lung	DOD
33	M	76	LMS-p/III	Thigh	Lung	DOD
34	F	66	LMS-p/III	Leg	NF	DOD
35	F	68	LMS-p/III	Thigh	Lung	DOD
36	F	54	LMS-c/III	Thigh	Viscera	DOD
37	F	42	LMS-c/III	Thigh	Lung	DOD
38	F	71	LMS-p/III	Leg	Lung	NED2
39	F	38	LMS-c	Leg	Lung	AWD
40	F	41	LMS-c	Thigh	Bone	DOD
41	F	40	LMS-c	Thigh	NF	NED
42	M	65	LMS-p	Leg	Lymphnodes	AWD
43	M	73	LMS-p	Thigh	Lymphnodes	NED2
44	M	72	LMS-p	Thigh	NF	NED

Patient	Sex	Age	Histological subtype[2]/grade[3]	Site of primary lesion	Site of metastases	Clinical course[4]
45	M	50	LS-p/II	Thigh	Lung	AWD
46	M	42	LS-p/II	Thigh	NF	AWD
47	M	56	LS-p/III	Leg	Liver	AWD
48	M	59	LS-p/III	Thigh	Bone	DOD
49	M	47	LS-p/II	Leg	NF	NED
50	F	73	LS-p/II	Thigh	NF	NED
51	F	49	LS-p/II	Thigh	NF	NED
52	F	40	LS-p/II	Leg	NF	NED
53	M	72	LS-p/III	Thigh	NF	DOD
54	F	54	LS-dd/II	Thigh	NF	NED
55	M	63	LS-dd/III	Thigh	NF	DOD
56	F	61	FS/III	Forearm	Lung	DOD
57	M	73	FS/III	Trunk	NF	NED
58	F	54	FS/III	arm	Lung	DOD
59	M	64	FS/III	Trunk	Lung	DOD
60	M	62	FS/IIB	Forearm	NF	NED
61	F	38	FS/III	Knee	NF	NED
62	M	43	LS-rc/III	Thigh	Bone	DOD
63	M	67	LS-rc/III	Thigh	Lung	DOD
64	F	72	LS-rc/II	Leg	NF	NED
65	M	46	LS-rc/III	Thigh	Lung	NED2
66	M	38	LS-rc/III	Ischium	Lung	NED2
67	F	62	LS-rc/III	Thigh	Lung	DOD
68	M	66	LS-rc/III	Thigh	NF	NED
69	M	71	LS-rc/III	Leg	Lung	NED2
70	M	57	LS-rc/III	Thigh	NF	DOD

Patient	Sex	Age	Histological subtype[2]/grade[3]	Site of primary lesion	Site of metastases	Clinical course[4]
71	M	63	LS-rc/III	Thigh	NF	DOD
72	M	76	LS-rc/III	Leg	Lung	NED2
73	M	34	LS-rc/II	Thigh	NF	NED
74	M	62	LS-rc/III	Knee	Lymphnodes	DOD
75	F	66	LS-rc/III	Thigh	Lung	AWD
76	M	34	LS-rc/II	Thigh	NF	NED
77	M	55	LS-mx/II	Thigh	NF	NED
78	M	78	LS-mx/II	Leg	NF	NED
79	F	38	LS-mx/III	Thigh	Lymphnodes	NED2
80	M	61	LS-mx/II	Thigh	NF	NED
81	M	43	LS-mx/II	Knee	NF	NED
82	M	52	LS-mx/II	Leg	NF	NED
83	M	79	LS-mx/II	Thigh	NF	NED
84	F	57	LS-mx/III	Thigh	Lung	AWD
85	M	76	LS-mx/II	Thigh	NF	NED
86	M	66	LS-mx/II	Thigh	NF	NED
87	F	68	LS-mx/II	Thigh	NF	NED
88	M	74	LS-mx/II	Leg	NF	NED
89	M	42	LS-mx/II	Thigh	NF	NED
90	M	71	LS-mx/II	Thigh	NF	NED
91	M	38	LS.mx/II	Thigh	NF	NED
92	F	41	LS-mx/II	Thigh	NF	NED
93	M	40	LS-rc/III	Thigh	NF	DOD
94	M	65	LS-rc/III	Leg	Bone	DOD
95	F	73	LS-mx/II	Knee	Lung	NED2
96	F	72	LS-mx/II	Knee	Lung	NED2
97	M	50	LS-rc/III	Knee	Lung	DOD

Patient	Sex	Age	Histological subtype[2]/grade[3]	Site of primary lesion	Site of metastases	Clinical course[4]
98	M	42	SS	Knee	Lung	NED2
99	F	56	SS	Elbow	NF	NED
100	M	59	SS	Thigh	Lung	AWD
101	M	47	SS	Forearm	Lung	AWD
102	M	73	SS	Elbow	Bone	DOD
103	F	49	SS	Shoulder	Lymphnodes	DOD
104	F	40	SS	Forearm	Lung	NED2
105	M	42	SS	Thigh	NF	NED
106	M	55	SS	Thigh	Lung	NED2
107	F	63	SS	Forearm	NF	NED
108	M	75	SS	Thigh	Lung	NED2

[1]All specimens were collected under informed consent from STS patients who underwent surgical and post-surgical treatments at the Rizzoli Orthopaedic Institute;
[2]Histological subtypes and their variants were as follows: MFS, mixofibrosarcoma; UPMS, undifferentiated pleomorphic sarcoma of the storiform type; LMS-c, conventional leiomyosarcoma, of cutaneous or somatic soft-tissue type (depending upon the anatomical location); LMS-p, pleomorphic leiomyosarcoma; LS-pm, pleomorphic liposarcoma; LS-dd, dedifferentiated liposarcoma; LS-mx, myxoid liposarcoma; LS-rc, round-cell liposarcoma; FS, fibrosarcoma. SS monophasic synovial sarcoma.
[3]Tumor grading was according to that established by the American Joint Committee for Cancer and the French Fédération Nationale des Centres de Lutte contre le Cancer;
[4]As established at a 5 years follow-up: DOD, patients dead because of the disease; AWD, patients alive but with detectable disease; NED, patients with no evidence of disease; NED2, patients who relapsed but had a subsequent disease regression.
NF= no found

To this end, we selected homogeneously treated patients, considering both pre- and post-surgical treatments, who remained free from other "non sarcoma" tumours (see *Materials and Methods*). Analysis of mRNA expression in this cohort of patients confirmed the enhancement of NG2 (up to 100-fold) in metastatic lesions (primarily pulmonary ones) and additionally demonstrated consistently higher levels of Collagen VI (Col VI) , by analysis of the α3(VI) chain mRNA, in metastases, when compared to primary lesions and the adjacent healthy tissue of the surgical resection margins (**Fig. 41A,B**). A direct comparison of the metastasis-associated expression patterns with those of the healthy lung tissue, surrounding the metastatic formations, was not technically possible because of the lack of accessibility to such healthy material from these patients.

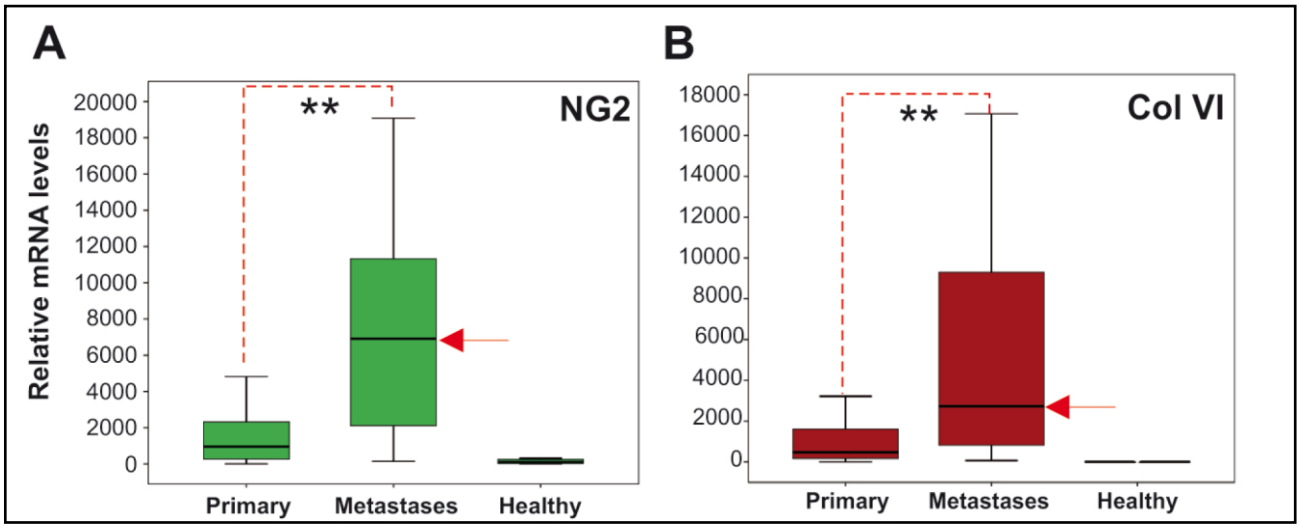

Figure 41. **(A)** Levels of NG2 and **(B)** α3(VI) chain mRNAs in primary lesions (*Primary*), pulmonary metastases (*Metastases*) and surgical resection margins (*Healthy*) of the primary lesions removed from patients affected by various STS histological subtypes (*red arrows* point to median values); "**"= p<0.01 by Mann Whitney test.

Interestingly, when we considered the individual STS histotypes, the maximal detectable levels of NG2 and Col VI mRNAs showed a substantial diversity and did not perfectly coincide; synovial sarcomas showed the highest overall NG2 expression, whereas fibrosarcomas and leiomyosarcomas showed an equal or superior levels of Col VI (**Fig. 42A,B**).

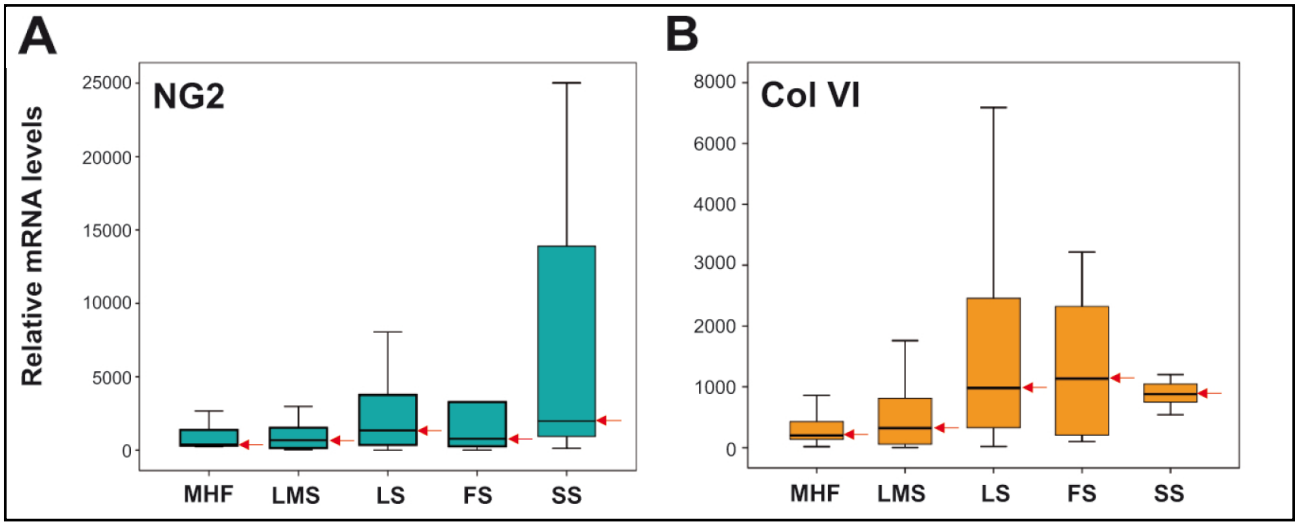

Figure 42. Pattern of expression of NG2 **(A)** and Col VI **(B)** mRNAs in the different histotypes represented by the examined patient cohort: MHF, malignant fibroshistocytoma-like pleomorphic sarcoma; LMS, leiomyosarcomas; LS, various variants of liposarcoma; FS, fibrosarcoma; and SS, synovial sarcoma.

The enrichment of NG2 on the surface of neoplastic cells and neovascular structures of primary and secondary tumour masses were independently confirmed by immunolabelling with the anti-

NG2 polyclonal antiserum D2 (Virgintino et al., 2009). More than 60% of the cells in primary lesions and >90% in metastatic lesions stained positively for NG2, detecting the PG either within the cytoplasm, on the cell surface and occasionally as a secreted (i.e. as cell surface shedded) molecule in the interstitial space (**Fig. 43A-F**). In contrast to NG2, Col VI was prevalently found to be associated with the intra-lesional stroma and to a lesser degree with the neoplastic cells themselves (**Fig. 43G-L**).

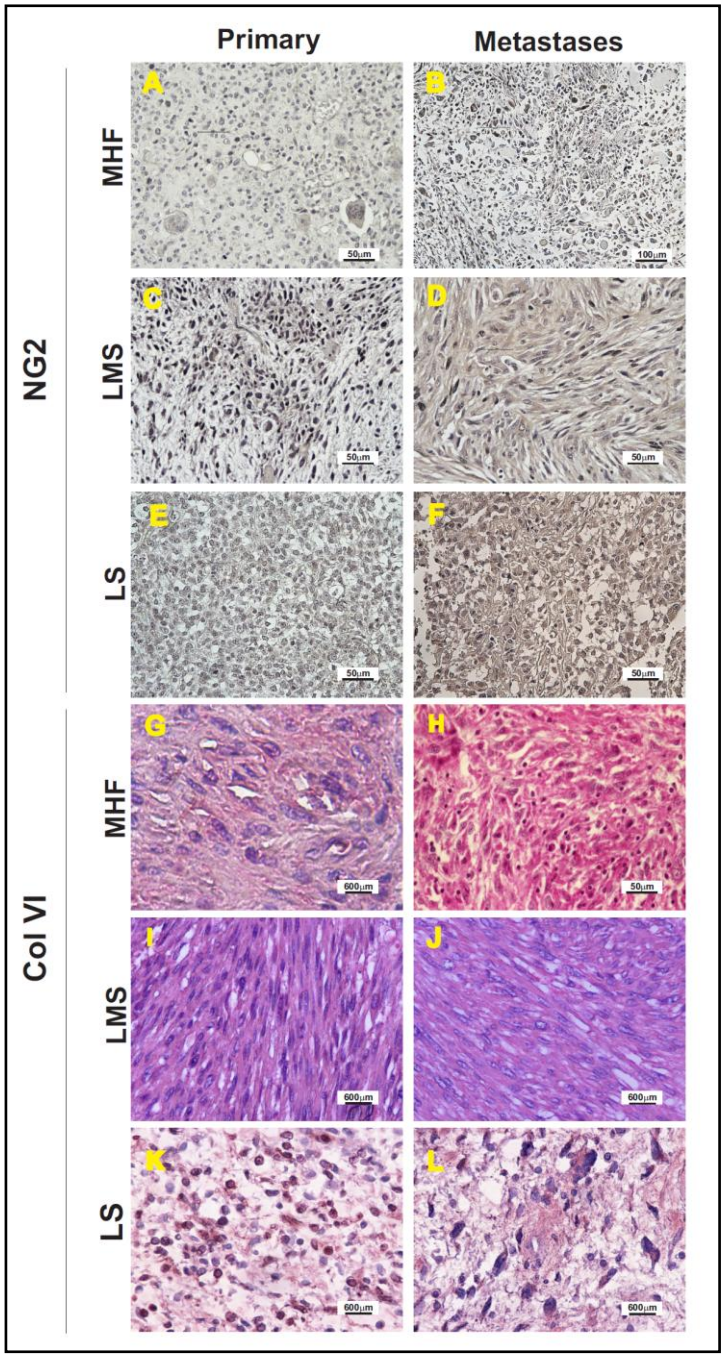

Figure 43. Representative immunohistochemical staining for NG2 **(A-F)** and Col VI [α3(VI) chain; **G-L**] proteins in primary and metastatic lesions derived from patients with the indicated histotypes .

Collectively, these findings indicate a precise spatial relationship in the distribution of the two molecules: NG2 was predominantly associated with the tumour cells (as well as decorated pericytes of the neovasculature), whereas Col VI was tied to the tumour stroma.

Comparing the disease course of patients with NG2 levels that were above average in their metastatic lesions with that of patients whose NG2 levels were below average disclosed a group of individuals with a significantly more unfavourable clinical course (**Fig. 44**). Enhanced expression of Col VI also had a negative impact on disease course, which was significantly worsened in patients who presented both higher levels of NG2 and Col VI.

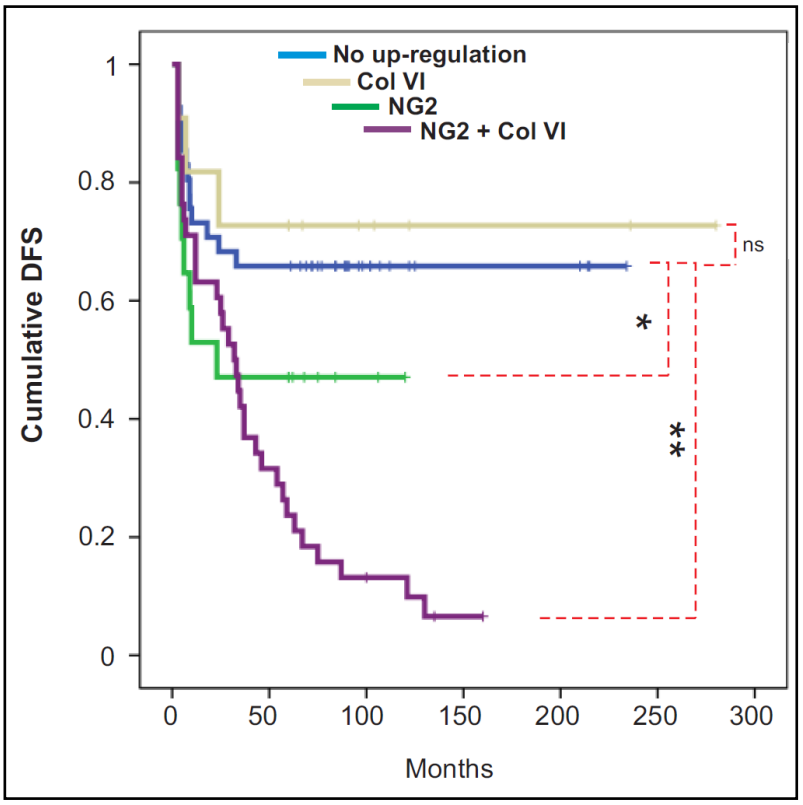

Figure 44. Probability rates of disease-free survival (DFS) in patients presenting NG2 and Col VI mRNAs levels above and below the *median values* in their metastatic lesions ("*"= $p<0.05$; "**"= $p<0.01$ by Breslow's test).

Accordingly, a multivariate Cox regression analysis, which took into account the prognostic factors recognized to date to be of clinical relevance in STS, substantiated that the high expression of NG2 (i.e. above median values) was an independent prognostic parameter (**Table 4**).

Table 4. Summary of a Cox regression, multivariate analysis confirming the independence scoring of NG2 overexpression in metastatic lesions as a prognostic factor. "*Therapy*" refers to the type of post-surgery therapeutical intervention; "*Size >10*" refers to primary masses with a size larger than 10 mm.

Variables	*Exp (B) (odds ratio)*	*95% CI*		*p*
		Inferior	*Superior*	
NG2 > 1000	1.41	1.03	1.94	0.03
Therapy	0.79	0.53	1.18	0.25
Site	0.95	0.65	1.37	0.77
Size>10	1.04	0.74	1.46	0.82
Age	0.98	0.96	1.03	0.09
Gender	1.27	0.88	1.81	0.18

We next re-evaluated whether relative expression levels of NG2 and Col VI mRNAs in primary lesions could provide information on the possible occurrence of future metastasis in patients free of metastatic disease at the time of diagnosis. To this end, we assessed the relative levels of the two transcripts in primary lesions of patients who developed distant metastases and compared these values with those found in analogous lesions of patients who remained free of metastases during a seven year follow-up period . We noted that both NG2 and Col VI were more abundant in primary lesions of patients who manifested post-surgical metastatic disease (**Fig. 45A,B**), thus implying a tight correlation between augmented NG2 mRNA levels in primary tumors and the development of post-surgery metastases.

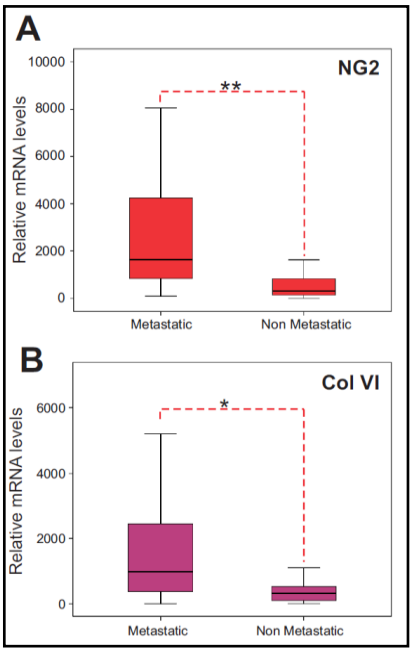

Figure 45. Relative levels of NG2 **(A)** and α3(VI) **(B)** chain mRNA expression in primary lesions of STS patients who developed metastases (*Metastatic*), when compared to individuals who did not develop such secondary lesions (*Non-metastatic*), and as

evaluated during a (post-surgical) follow-up period of up to 9 years. ("**", p<0.01; by Mann Whitney test)

Comparison of the clinical course of the patient subgroup with high levels of NG2 in primary lesions and affected by metastatic disease revealed a further distinction. Individuals with lower levels of NG2 developed metastases preferentially after five or more years after removal of their primary tumour masses. By contrast, patients with the highest NG2 levels were more likely to develop metastases within 12 months after surgical intervention. Thus, expression levels of NG2 in primary pre-surgical lesions also determined a temporal parameter of metastases formation and discriminated patient subsets with longer and shorter metastasis-free lag periods **(Fig. 46)**.

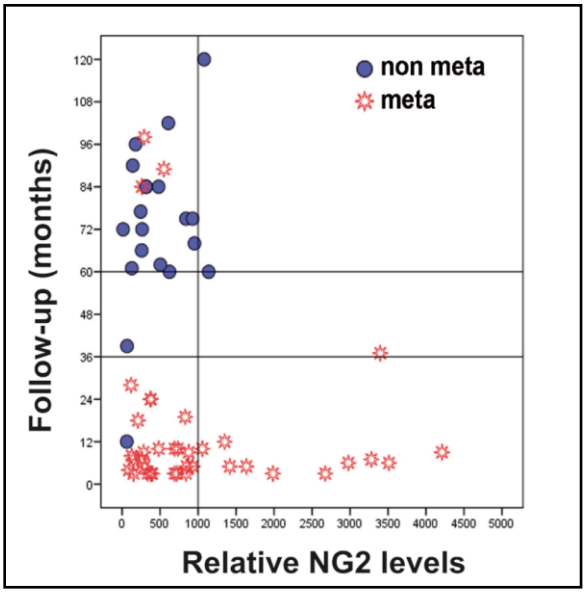

Figure 46. Timing of detection of metastatic disease ("meta") in post-surgery STS patients as a function of the NG2 transcriptional levels in their primary lesions ("non meta" refers to metastasis-free patients).

At this stage, we cannot establish to what extent the NG2 up-regulation seen in cells building up metastatic lesions is a primary event (i.e. occurring prior to or concurrently with the tissue dissemination of the pro-metastatic cells and defining a pre-committed metastatic phenotype), or whether NG2 was up-regulated in metastatic lesions after their formation (i.e. a secondary event).

DISCUSSION

Comparative assaying of the tumorigenic potential of NG2-expressing cells by xenografting in athymic mice highlighted a marked correlation between surface abundance of the PG and malignancy, and this observation was sustained also by another experimental finding. When we separated by immunosorting $NG2^+$ and $NG2^-$ cell subsets, and comparatively assayed their tumorigenic behaviour in nude mice, we found that the former subset gave rise to local tumour masses more rapidly and more extensively than the latter one.

This observation was consistent with corollary in vitro findings showing sustained anchorage-independent growth of NG2-expressing (but not NG2-deficient) cells and called upon the potential, more direct implication of the PG in the control of tumour cell engraftment and survival. However, since the ability of $NG2^+$ cells to engraft and form tumours in nude mice did not seem to correlate with their intrinsic proliferation index, the pro-tumorigenic role of NG2 was unlikely to be restricted to a mere control of cell division. Indeed, the absence of NG2 is associated with a higher percentage of apoptosis/necrosis cell in tumors masses, and a difference degree in the tumor vessels maturation.

Moreover, we hypothesized that high surface levels of NG2 may have conferred a more malignant behaviour to sarcoma cells by controlling multiple facets of their host microenvironmental interaction, essential for bringing about loco-regional growth and tissue infiltration. These aspect were confirmed in adhesion or migration experiments , using isolated cell-free matrix from some stroma cells (i.e. MSC) or from SMC , usually found within the walls of blood vessels. The presence of NG2 on the tumor cells surface induce a change in their adhesion capability with ECM not only in static condition, but also in perfusion experiments. Moreover, the expression of NG2 could modulate the tumor cells' behavior in haptotatic movement as well as in scratch assay or in 3D movement.

Having as reference previous observations reported in the literature, we verified the involvement of the interaction NG2-Col VI in the modulation of the cancer cells' behavior. NG2 effectively mediated the interaction of cells with both naturally assembled forms (i.e. microfilaments) of Col VI and with its isolated tetrameric units. By contrast, it was ineffective when cells were confronted with fragmented forms of the collagen. While the *N*-terminal portion of the PG core protein appeared to bind the trimeric globular domains of the collagen, other parts of NG2 synergized with integrin $\alpha2\beta1$ (which in turn recognizes the triple-helical region of the collagen) to stabilize the PG-collagen interaction. Cooperation of NG2 with integrins has previously been documented for both $\alpha3\beta1$ (Fukushi et al., 2004) and $\alpha4\beta1$(Iida et al., 1992; Iida et al., 1995),

but the precise modes of these interplays have remained veiled. Our findings are also at variance with a previous publication suggesting a role for NG2 in mediating β1 integrin-independent binding to Col VI (Tillet et al., 2002). We also noted that the NG2-Col VI interaction induced cell-cell cohesion and enhanced anchorage-independent growth. These observations suggested that NG2-driven retention of the collagen on the cell surface could be exploited by mesenchymal tumor cells to form ECM-mediated homotypic cell aggregates.

Cells lacking NG2 showed a strongly attenuated ability to adhere and migrate on both purified Col VI and native Col VI-containing matrices, as well as markedly failed to invade reconstituted basement membrane matrices supplemented with Col VI. Similar observations were done with cells engineered to overproduce, or express ectopically, NG2 molecules deprived of their *N*-terminal collagen-binding region or cytoplasmic domain. These cells were found to be defective in their interaction with Col VI, but were not impaired in their binding and migration on other ECM components. Collectively, these findings sustain a cardinal role of the cytoplasmic tail of NG2 in promoting cell-substrate interactions and cell motility (Fang et al., 1999; Makagiansar et al., 2004) and provide novel insights into the importance of the NG2-Col VI interaction in governing ECM-promoted cellular phenomena. To what extent the PG mediates these phenomena by acting beyond a direct binding to Col VI remains to be further asserted.

By cooperating with integrins, or by direct binding to extracellular ligands, NG2 is believed to affect filopodia extension and stabilization and activate lamellopodial signalling cascades propagated via p130CAS, Rac/cdc42 and FAK-ERK phosphorylations (Eisenmann et al., 1999; Majumdar et al., 2003; Yang et al., 2004). The NG2-induced rearrangement of the actin cytoskeleton may occur through ancillary actin-binding intermediates and more recently syntenin-1 has been added to the list of putative NG2-cytoskeletal linker/adaptor molecules in migrating oligodendrocytes (Chatterjee et al., 2008). In accordance with some of those previous findings, NG2-expressing sarcoma cells showed a defined spreading behaviour on Col VI substrates that involved a canonical reorganization of the cytoskeleton and an accompanying paxillin phosphorylation. The augmented adhesive, motile and invasive properties of NG2-expressing cells in response to Col VI substrates prompted us to investigate the signal transduction cascades triggered through NG2 in cells confronted with the collagen. To this end, we carried out comparative profilings of the intracellular phosphorylation patterns triggered by alternative exposure to Col I or Col VI in three distinct, β1/α2 integrin subunit-depleted cellular models, which were matched by their counterpart non-manipulated cells. These included siRNA-treated cells,

cells ectopically expressing NG2 and cells enriched for their constitutive NG2 surface levels by immunosorting. Experiments with these cellular models consistently delineated the differential activation of multiple signal transduction pathways in NG2-expressing versus NG2-deficient cells upon selective confrontation with Col VI.

We identified diverse phosphorylation patterns in both components linked to cell survival pathways of the PCK-PI-3K-Akt-1-mTOR-type and molecules associated with growth-promoting pathways of the ERK-MAPK-type; the latter already known to be associated with the phosphorylation of the cytoplasmic NG2 threonine residues (Makagiansar et al., 2004; Makagiansar et al., 2007). Modulation of the phosphorylation state of molecules affecting the actomyosin-regulated cell contractility and focal adhesion formation was in partial agreement with previous Col VI-unrelated findings and provided additional evidence for a tight NG2 exerted control of the actin microfilament dynamics in critical cytoplasmic domains of motile cells. The NG2-induced cofilin-1 and PCK-dependent adducin γ phosphorylations were particularly intriguing in light of our preliminary evidence of a physical NG2-cofilin-1 intracellular linkage and the previously documented bilateral NG2-PCKα inter-relationship. Furthermore, engagement of NG2 in Col VI binding induced enhanced phosphorylation of the FAK-controlled tyrosine residue Y118 of paxillin, but not residue Y31, suggesting that upon specific interactions with certain ECM components NG2 may also influence focal adhesion disassembly and the dynamics of the retracting end apparatus of locomotory cells.

The putative significance of the signalling pathways triggered by the NG2-Col VI interplay was therefore further addressed in the context of cell adhesion and movement through the use of drug antagonists. These experiments unravelled an NG2-Col VI induction of PI-3K isoform-specific phosphorylation and functionally confirmed the activation of pathways dependent upon and/or involving p38MAPK and MEK1/2/ERK1/2 enzymatic activities. Conversely, NG2 binding to Col VI did not specifically influence the Rho-ROCK-1, Crk or Csk participation in cell-substrate interactions. Since PI-3K has recently been implicated in the control of cell spreading and random cell movement, through a bypass of the canonical integrin-elicited signal transduction machinery (Weiger et al., 2009), we specifically assayed whether a Col VI-NG2-PI-3K axis was established during sarcoma cell adhesion and motility. Such connection was suggested by the adhesion/migration-inhibitory effects exerted by antagonists of this kinase in NG2-expressing cells, but not NG2-deficient ones, or in cells overexpressing cytoplasmic deletion constructs of the PG.

Conclusively, the present findings consolidate the unprecedented role of NG2 as a metastasis-

predicting biomarker in STS and as a malignancy-accentuating factor in discrete cell subsets of these tumours. The PG appears to control tumour progression by mediating the interaction of neoplastic cells with the host ECM, in particular with the Col VI that accumulates in the peri- and intra-lesional stroma. The importance of this interaction in cancer is thus underscored and proposed to be central for the governing of the aggressiveness of sarcomas. It is proposed that sustained NG2-Col VI interplays, alongside with other molecular interactions that "sarcoma NG2" may mediate with discrete cues in the tumour microenvironment, may be pivotal in predisposing for enhanced local growth and tissue infiltration. Hence, these interactions are believed to impact on the STS cells' dissemination to distant sites.

To relate the above in vivo-in vitro experimental findings with clinical situations, we performed molecular analyses on a cohort of more than 100 STS patients confirming that NG2 is associated with neoplastic transformation, being de novo expressed in primary lesions and being strongly up-regulated in metastases developing in these individuals. A first unsupervised clustering of the patients according to their metastatic NG2 expression profile unveiled a subgroup with a more dismal clinical course. A second clustering exercise taking into consideration both up-regulation of NG2 and its putative ligand Col VI identified a subgroup exhibiting a dramatically unfavourable prognosis, suggesting that co-enhancement of the two molecules drives tumorigenesis. The application of multivariate regression analyses established that up-regulation of NG2, but not Col VI, was an *independent* prognostic factor, thus paralleling the previously proposed clinical importance of NG2 in glioblastoma multiforme, neuroblastoma, breast carcinoma, melanoma and mesothelioma (Kageshita et al., 1992; Goto et al., 2008; Morandi et al., 2011; Al-Mayhani et al., 2011; Svendsen et al., 2011; Rivera et al., 2012). The putative clinical impact of NG2 in soft-tissue sarcomas adds to the previously discovered value of the PG in the prognostication of rare infant and adult leukemia (Smith et al., 1996; Petrovici et al., 2010).

Rather than simply adding another post to the infinite "list" of tumour biomarkers correlating with overall patient survival, the present findings on STS suggest that evaluation of NG2 expression may have a more direct utility in the daily clinical management of cancer patients. In fact, relative abundance of the PG in primary lesions of metastasis-free individuals affords a unique potential in the prediction with ≥60% probability the future occurrence of post-surgical metastases. Relative levels of NG2 expression in primary tumours also defined the tentative timing of appearance of such secondary lesions. Therefore, assessment of the transcriptional rates of NG2 in surgically removed (or sampled through biopsy) primary tumour masses may represent an

unprecedented molecular tool for the disclosure of occult metastatic lesions emerging after removal of loco-regional ones; this parameter being independent of the type of adjuvant or neoadjuvant treatment, tumour histotype, or clinical history of the patient. To our knowledge altered expression of NG2 in primary lesions is the first tangible metastasis-predicting factor ever to be identified in STSs and, as such, it may be a more potent biomarker than what previously proposed in other solid tumours. Larger case studies than the present one should be able to decipher the clinical significance of this finding and more precisely define its probability scoring.

REFERENCES

Airola, K., T. Karonen, M. Vaalamo, K. Lehti, J. Lohi, A.L. Kariniemi, J. Keski-Oja, and U.K. Saarialho-Kere. 1999. Expression of collagenases-1 and -3 and their inhibitors TIMP-1 and -3 correlates with the level of invasion in malignant melanomas. *Br.J.Cancer.* 80:733-743. doi: 10.1038/sj.bjc.6690417.

Al-Mayhani, M.T., R. Grenfell, M. Narita, S. Piccirillo, E. Kenney-Herbert, J.W. Fawcett, V.P. Collins, K. Ichimura, and C. Watts. 2011. NG2 expression in glioblastoma identifies an actively proliferating population with an aggressive molecular signature. *Neuro Oncol.* 13:830-845. doi: 10.1093/neuonc/nor088.

Baeuerle, P.A., P. Kufer, and R. Bargou. 2009. BiTE: Teaching antibodies to engage T-cells for cancer therapy. *Curr.Opin.Mol.Ther.* 11:22-30.

Barrett, J.C., D.G. Clayton, P. Concannon, B. Akolkar, J.D. Cooper, H.A. Erlich, C. Julier, G. Morahan, J. Nerup, C. Nierras, V. Plagnol, F. Pociot, H. Schuilenburg, D.J. Smyth, H. Stevens, J.A. Todd, N.M. Walker, S.S. Rich, and Type 1 Diabetes Genetics Consortium. 2009. Genome-wide association study and meta-analysis find that over 40 loci affect risk of type 1 diabetes. *Nat.Genet.* 41:703-707. doi: 10.1038/ng.381; 10.1038/ng.381.

Behm, F.G., F.O. Smith, S.C. Raimondi, C.H. Pui, and I.D. Bernstein. 1996. Human homologue of the rat chondroitin sulfate proteoglycan, NG2, detected by monoclonal antibody 7.1, identifies childhood acute lymphoblastic leukemias with t(4;11)(q21;q23) or t(11;19)(q23;p13) and MLL gene rearrangements. *Blood.* 87:1134-1139.

Benassi, M.S., L. Pazzaglia, A. Chiechi, M. Alberghini, A. Conti, S. Cattaruzza, B. Wassermann, P. Picci, and R. Perris. 2009. NG2 expression predicts the metastasis formation in soft-tissue sarcoma patients. *J.Orthop.Res.* 27:135-140. doi: 10.1002/jor.20694.

Bluemel, C., S. Hausmann, P. Fluhr, M. Sriskandarajah, W.B. Stallcup, P.A. Baeuerle, and P. Kufer. 2010. Epitope distance to the target cell membrane and antigen size determine the potency of T cell-mediated lysis by BiTE antibodies specific for a large melanoma surface antigen. *Cancer Immunol.Immunother.* 59:1197-1209. doi: 10.1007/s00262-010-0844-y; 10.1007/s00262-010-0844-y.

Bomanji, J., A. Garner, J. Prasad, D.M. Albert, J.L. Hungerford, M. Granowska, and K.E. Britton. 1987. Characterisation of ocular melanoma with cutaneous melanoma antibodies. *Br.J.Ophthalmol.* 71:647-650.

Bumol, T.F., L.E. Walker, and R.A. Reisfeld. 1984. Biosynthetic studies of proteoglycans in human melanoma cells with a monoclonal antibody to a core glycoprotein of chondroitin sulfate proteoglycans. *J Biol Chem.* 259(20):12733-12741.

Burg, M.A., A. Nishiyama, and W.B. Stallcup. 1997. A central segment of the NG2 proteoglycan is critical for the ability of glioma cells to bind and migrate toward type VI collagen. *Exp.Cell Res.* 235:254-264. doi: 10.1006/excr.1997.3674.

Burns, W.R., Y. Zhao, T.L. Frankel, C.S. Hinrichs, Z. Zheng, H. Xu, S.A. Feldman, S. Ferrone, S.A. Rosenberg, and R.A. Morgan. 2010. A high molecular weight melanoma-associated antigen-

specific chimeric antigen receptor redirects lymphocytes to target human melanomas. *Cancer Res.* 70:3027-3033. doi: 10.1158/0008-5472.CAN-09-2824.

Campoli, M., S. Ferrone, and X. Wang. 2010. Functional and clinical relevance of chondroitin sulfate proteoglycan 4. *Adv.Cancer Res.* 109:73-121. doi: 10.1016/B978-0-12-380890-5.00003-X.

Cattaruzza, S., U. Ozerdem, M. Denzel, B. Ranscht, P. Bulian, U. Cavallaro, D. Zanocco, A. Colombatti, W.B. Stallcup, and R. Perris. 2012. Multivalent proteoglycan modulation of FGF mitogenic responses in perivascular cells. *Angiogenesis.* doi: 10.1007/s10456-012-9316-7.

Chang, A., A. Nishiyama, J. Peterson, J. Prineas, and B.D. Trapp. 2000. NG2-positive oligodendrocyte progenitor cells in adult human brain and multiple sclerosis lesions. *J.Neurosci.* 20:6404-6412.

Chatterjee, N., J. Stegmuller, P. Schatzle, K. Karram, M. Koroll, H.B. Werner, K.A. Nave, and J. Trotter. 2008. Interaction of syntenin-1 and the NG2 proteoglycan in migratory oligodendrocyte precursor cells. *J.Biol.Chem.* 283:8310-8317. doi: 10.1074/jbc.M706074200.

Chekenya, M., M. Hjelstuen, P.O. Enger, F. Thorsen, A.L. Jacob, B. Probst, O. Haraldseth, G. Pilkington, A. Butt, J.M. Levine, and R. Bjerkvig. 2002. NG2 proteoglycan promotes angiogenesis-dependent tumor growth in CNS by sequestering angiostatin. *FASEB J.* 16:586-588.

Chekenya, M., C. Krakstad, A. Svendsen, I.A. Netland, V. Staalesen, B.B. Tysnes, F. Selheim, J. Wang, P.O. Sakariassen, T. Sandal, P.E. Lonning, T. Flatmark, P.O. Enger, R. Bjerkvig, M. Sioud, and W.B. Stallcup. 2008. The progenitor cell marker NG2/MPG promotes chemoresistance by activation of integrin-dependent PI3K/Akt signaling. *Oncogene.* 27:5182-5194. doi: 10.1038/onc.2008.157.

Cohen, S.J., C.J. Punt, N. Iannotti, B.H. Saidman, K.D. Sabbath, N.Y. Gabrail, J. Picus, M. Morse, E. Mitchell, M.C. Miller, G.V. Doyle, H. Tissing, L.W. Terstappen, and N.J. Meropol. 2008. Relationship of circulating tumor cells to tumor response, progression-free survival, and overall survival in patients with metastatic colorectal cancer. *J.Clin.Oncol.* 26:3213-3221. doi: 10.1200/JCO.2007.15.8923; 10.1200/JCO.2007.15.8923.

Cristofanilli, M. 2006. Circulating tumor cells, disease progression, and survival in metastatic breast cancer. *Semin.Oncol.* 33:S9-14. doi: 10.1053/j.seminoncol.2006.03.016.

Daniels, K.J., H.C. Boldt, J.A. Martin, L.M. Gardner, M. Meyer, and R. Folberg. 1996. Expression of type VI collagen in uveal melanoma: its role in pattern formation and tumor progression. *Lab.Invest.* 75:55-66.

de Bono, J.S., H.I. Scher, R.B. Montgomery, C. Parker, M.C. Miller, H. Tissing, G.V. Doyle, L.W. Terstappen, K.J. Pienta, and D. Raghavan. 2008. Circulating tumor cells predict survival benefit from treatment in metastatic castration-resistant prostate cancer. *Clin.Cancer Res.* 14:6302-6309. doi: 10.1158/1078-0432.CCR-08-0872; 10.1158/1078-0432.CCR-08-0872.

De Giorgi, V., P. Pinzani, F. Salvianti, M. Grazzini, C. Orlando, M. Santucci, T. Lotti, M. Pazzagli, and D. Massi. 2011. Circulating Tumor Cells in Cutaneous Melanoma. *Journal of Investigative Dermatology.* 131:1776-1777.

Drake, A.S., M.T. Brady, X.H. Wang, S.J. Sait, J.C. Earp, S. Ghoshal Gupta, S. Ferrone, E.S. Wang, and M. Wetzler. 2009. Targeting 11q23 positive acute leukemia cells with high molecular weight-melanoma associated antigen-specific monoclonal antibodies. *Cancer Immunol.Immunother.* 58:415-427. doi: 10.1007/s00262-008-0567-5.

Eisenmann, K.M., J.B. McCarthy, M.A. Simpson, P.J. Keely, J.L. Guan, K. Tachibana, L. Lim, E. Manser, L.T. Furcht, and J. Iida. 1999. Melanoma chondroitin sulphate proteoglycan regulates cell spreading through Cdc42, Ack-1 and p130cas. *Nat.Cell Biol.* 1:507-513. doi: 10.1038/70302.

Erfurt, C., Z. Sun, I. Haendle, B. Schuler-Thurner, C. Heirman, K. Thielemans, P. van der Bruggen, G. Schuler, and E.S. Schultz. 2007. Tumor-reactive CD4+ T cell responses to the melanoma-associated chondroitin sulphate proteoglycan in melanoma patients and healthy individuals in the absence of autoimmunity. *J.Immunol.* 178:7703-7709.

Fang, X., M.A. Burg, D. Barritt, K. Dahlin-Huppe, A. Nishiyama, and W.B. Stallcup. 1999. Cytoskeletal reorganization induced by engagement of the NG2 proteoglycan leads to cell spreading and migration. *Mol.Biol.Cell.* 10:3373-3387.

Freeman, J.B., E.S. Gray, M. Millward, R. Pearce, and M. Ziman. 2012. Evaluation of a multi-marker immunomagnetic enrichment assay for the quantification of circulating melanoma cells. *Journal of Translational Medicine.* 10:192.

Fukushi, J., I.T. Makagiansar, and W.B. Stallcup. 2004. NG2 proteoglycan promotes endothelial cell motility and angiogenesis via engagement of galectin-3 and alpha3beta1 integrin. *Mol.Biol.Cell.* 15:3580-3590. doi: 10.1091/mbc.E04-03-0236.

Fusi, A., Z. Liu, V. Kummerlen, A. Nonnemacher, J. Jeske, and U. Keilholz. 2012. Expression of chemokine receptors on circulating tumor cells in patients with solid tumors. *J.Transl.Med.* 10:52-5876-10-52. doi: 10.1186/1479-5876-10-52; 10.1186/1479-5876-10-52.

Gautier, L., M. Moller, L. Friis-Hansen, and S. Knudsen. 2004. Alternative mapping of probes to genes for Affymetrix chips. *BMC Bioinformatics.* 5:111. doi: 10.1186/1471-2105-5-111.

Gazziola, C., N. Cordani, S. Carta, E. De Lorenzo, A. Colombatti, and R. Perris. 2005. The relative endogenous expression levels of the IFNAR2 isoforms influence the cytostatic and pro-apoptotic effect of IFNalpha on pleomorphic sarcoma cells. *Int.J.Oncol.* 26:129-140.

Ghali, L., S.T. Wong, N. Tidman, A. Quinn, M.P. Philpott, and I.M. Leigh. 2004. Epidermal and hair follicle progenitor cells express melanoma-associated chondroitin sulfate proteoglycan core protein. *J.Invest.Dermatol.* 122:433-442. doi: 10.1046/j.0022-202X.2004.22207.x.

Ghose, T., S. Ferrone, A.H. Blair, Y. Kralovec, M. Temponi, M. Singh, and M. Mammen. 1991. Regression of human melanoma xenografts in nude mice injected with methotrexate linked to

monoclonal antibody 225.28 to human high molecular weight-melanoma associated antigen. *Cancer Immunol.Immunother.* 34:90-96.

Gibby, K., W.K. You, K. Kadoya, H. Helgadottir, L.J. Young, L.G. Ellies, Y. Chang, R.D. Cardiff, and W.B. Stallcup. 2012. Early vascular deficits are correlated with delayed mammary tumorigenesis in the MMTV-PyMT transgenic mouse following genetic ablation of the NG2 proteoglycan. *Breast Cancer Res.* 14:R67. doi: 10.1186/bcr3174.

Goretzki, L., M.A. Burg, K.A. Grako, and W.B. Stallcup. 1999. High-affinity binding of basic fibroblast growth factor and platelet-derived growth factor-AA to the core protein of the NG2 proteoglycan. *J.Biol.Chem.* 274:16831-16837.

Goretzki, L., C.R. Lombardo, and W.B. Stallcup. 2000. Binding of the NG2 proteoglycan to kringle domains modulates the functional properties of angiostatin and plasmin(ogen). *J.Biol.Chem.* 275:28625-28633. doi: 10.1074/jbc.M002290200.

Goto, Y., T. Arigami, R. Murali, R.A. Scolyer, A. Tanemura, M. Takata, R.R. Turner, L. Nguyen, T. Nguyen, D.L. Morton, S. Ferone, and D.S. Hoon. 2010. High molecular weight-melanoma-associated antigen as a biomarker of desmoplastic melanoma. *Pigment Cell.Melanoma Res.* 23:137-140. doi: 10.1111/j.1755-148X.2009.00660.x; 10.1111/j.1755-148X.2009.00660.x.

Goto, Y., S. Ferrone, T. Arigami, M. Kitago, A. Tanemura, E. Sunami, S.L. Nguyen, R.R. Turner, D.L. Morton, and D.S. Hoon. 2008. Human high molecular weight-melanoma-associated antigen: utility for detection of metastatic melanoma in sentinel lymph nodes. *Clin.Cancer Res.* 14:3401-3407. doi: 10.1158/1078-0432.CCR-07-1842.

Hafner, C., S. Wagner, D. Allwardt, A.B. Riemer, O. Scheiner, H. Pehamberger, and H. Breiteneder. 2005. Cross-reactivity of mimotopes with a monoclonal antibody against the high molecular weight melanoma-associated antigen (HMW-MAA) does not predict cross-reactive immunogenicity. *Melanoma Res.* 15:111-117.

Hedman, K., M. Kurkinen, K. Alitalo, A. Vaheri, S. Johansson, and M. Hook. 1979. Isolation of the pericellular matrix of human fibroblast cultures. *J.Cell Biol.* 81:83-91.

Iida, J., A.M. Meijne, R.C. Spiro, E. Roos, L.T. Furcht, and J.B. McCarthy. 1995. Spreading and focal contact formation of human melanoma cells in response to the stimulation of both melanoma-associated proteoglycan (NG2) and alpha 4 beta 1 integrin. *Cancer Res.* 55:2177-2185.

Iida, J., D. Pei, T. Kang, M.A. Simpson, M. Herlyn, L.T. Furcht, and J.B. McCarthy. 2001. Melanoma chondroitin sulfate proteoglycan regulates matrix metalloproteinase-dependent human melanoma invasion into type I collagen. *J.Biol.Chem.* 276:18786-18794. doi: 10.1074/jbc.M010053200.

Iida, J., A.P. Skubitz, L.T. Furcht, E.A. Wayner, and J.B. McCarthy. 1992. Coordinate role for cell surface chondroitin sulfate proteoglycan and alpha 4 beta 1 integrin in mediating melanoma cell adhesion to fibronectin. *J.Cell Biol.* 118:431-444.

Iyengar, P., V. Espina, T.W. Williams, Y. Lin, D. Berry, L.A. Jelicks, H. Lee, K. Temple, R. Graves, J. Pollard, N. Chopra, R.G. Russell, R. Sasisekharan, B.J. Trock, M. Lippman, V.S. Calvert, E.F. Petricoin 3rd, L. Liotta, E. Dadachova, R.G. Pestell, M.P. Lisanti, P. Bonaldo, and P.E. Scherer. 2005. Adipocyte-derived collagen VI affects early mammary tumor progression in vivo, demonstrating a critical interaction in the tumor/stroma microenvironment. *J.Clin.Invest.* 115:1163-1176. doi: 10.1172/JCI23424.

Jensen, K.B., J. Jones, and F.M. Watt. 2008. A stem cell gene expression profile of human squamous cell carcinomas. *Cancer Lett.* 272:23-31. doi: 10.1016/j.canlet.2008.06.014; 10.1016/j.canlet.2008.06.014.

Kageshita, T., T. Kimura, A. Yoshi, S. Hirai, T. Ono, and S. Ferrone. 1994. Antigenic profile of mucosal melanoma lesions. *Int.J.Cancer.* 56:370-374.

Kageshita, T., N. Kuriya, T. Ono, T. Horikoshi, M. Takahashi, G.Y. Wong, and S. Ferrone. 1993. Association of high molecular weight melanoma-associated antigen expression in primary acral lentiginous melanoma lesions with poor prognosis. *Cancer Res.* 53:2830-2833.

Kageshita, T., T. Nakamura, M. Yamada, N. Kuriya, T. Arao, and S. Ferrone. 1991. Differential expression of melanoma associated antigens in acral lentiginous melanoma and in nodular melanoma lesions. *Cancer Res.* 51:1726-1732.

Kageshita, T., M. Yamada, T. Arao, and S. Ferrone. 1992. Expression of high molecular weight-melanoma associated antigen (HMW-MAA) in primary ALM lesions is associated with a poor prognosis. *Pigment Cell Res.* Suppl 2:132-135.

Kitago, M., K. Koyanagi, T. Nakamura, Y. Goto, M. Faries, S.J. O'Day, D.L. Morton, S. Ferrone, and D.S. Hoon. 2009. mRNA expression and BRAF mutation in circulating melanoma cells isolated from peripheral blood with high molecular weight melanoma-associated antigen-specific monoclonal antibody beads. *Clin.Chem.* 55:757-764. doi: 10.1373/clinchem.2008.116467; 10.1373/clinchem.2008.116467.

Kozanoglu, I., C. Boga, H. Ozdogu, O. Sozer, E. Maytalman, A.C. Yazici, and F.I. Sahin. 2009. Human bone marrow mesenchymal cells express NG2: possible increase in discriminative ability of flow cytometry during mesenchymal stromal cell identification. *Cytotherapy.* 11:527-533. doi: 10.1080/14653240902923153; 10.1080/14653240902923153.

Kuo, H.J., C.L. Maslen, D.R. Keene, and R.W. Glanville. 1997. Type VI collagen anchors endothelial basement membranes by interacting with type IV collagen. *J.Biol.Chem.* 272:26522-26529.

Lamande, S.R., M. Morgelin, N.E. Adams, C. Selan, and J.M. Allen. 2006. The C5 domain of the collagen VI alpha3(VI) chain is critical for extracellular microfibril formation and is present in the extracellular matrix of cultured cells. *J.Biol.Chem.* 281:16607-16614. doi: 10.1074/jbc.M510192200.

Latzka, J., S. Gaier, G. Hofstetter, N. Balazs, U. Smole, S. Ferrone, O. Scheiner, H. Breiteneder, H. Pehamberger, and S. Wagner. 2011. Specificity of mimotope-induced anti-high molecular weight-

melanoma associated antigen (HMW-MAA) antibodies does not ensure biological activity. *PLoS One.* 6:e19383. doi: 10.1371/journal.pone.0019383; 10.1371/journal.pone.0019383.

Li, Y., M.C. Madigan, K. Lai, R.M. Conway, F.A. Billson, R. Crouch, and B.J. Allen. 2003. Human uveal melanoma expresses NG2 immunoreactivity. *Br.J.Ophthalmol.* 87:629-632.

Lucci, A., C.S. Hall, A.K. Lodhi, A. Bhattacharyya, A.E. Anderson, L. Xiao, I. Bedrosian, H.M. Kuerer, and S. Krishnamurthy. 2012. Circulating tumour cells in non-metastatic breast cancer: a prospective study. *Lancet Oncol.* 13:688-695. doi: 10.1016/S1470-2045(12)70209-7; 10.1016/S1470-2045(12)70209-7.

Luo, W., X. Wang, T. Kageshita, S. Wakasugi, A.R. Karpf, and S. Ferrone. 2006. Regulation of high molecular weight-melanoma associated antigen (HMW-MAA) gene expression by promoter DNA methylation in human melanoma cells. *Oncogene.* 25:2873-2884. doi: 10.1038/sj.onc.1209319.

Majumdar, M., K. Vuori, and W.B. Stallcup. 2003. Engagement of the NG2 proteoglycan triggers cell spreading via rac and p130cas. *Cell.Signal.* 15:79-84.

Makagiansar, I.T., S. Williams, K. Dahlin-Huppe, J. Fukushi, T. Mustelin, and W.B. Stallcup. 2004. Phosphorylation of NG2 proteoglycan by protein kinase C-alpha regulates polarized membrane distribution and cell motility. *J.Biol.Chem.* 279:55262-55270. doi: 10.1074/jbc.M411045200.

Makagiansar, I.T., S. Williams, T. Mustelin, and W.B. Stallcup. 2007. Differential phosphorylation of NG2 proteoglycan by ERK and PKCalpha helps balance cell proliferation and migration. *J.Cell Biol.* 178:155-165. doi: 10.1083/jcb.200612084.

Mangahas, C.R., G.V. dela Cruz, R.J. Schneider, and S. Jamal. 2004. Endothelin-1 upregulates MCAM in melanocytes. *J.Invest.Dermatol.* 123:1135-1139. doi: 10.1111/j.0022-202X.2004.23480.x.

Mauvieux, L., E. Delabesse, P. Bourquelot, I. Radford-Weiss, A. Bennaceur, G. Flandrin, F. Valensi, and E.A. MacIntyre. 1999. NG2 expression in MLL rearranged acute myeloid leukaemia is restricted to monoblastic cases. *Br.J.Haematol.* 107:674-676.

Mazzucato, M., M.R. Cozzi, M. Battiston, M. Jandrot-Perrus, M. Mongiat, P. Marchese, T.J. Kunicki, Z.M. Ruggeri, and L. De Marco. 2009. Distinct spatio-temporal Ca2+ signaling elicited by integrin alpha2beta1 and glycoprotein VI under flow. *Blood.* 114:2793-2801. doi: 10.1182/blood-2008-12-193490; 10.1182/blood-2008-12-193490.

Medic, S., and M. Ziman. 2010. PAX3 expression in normal skin melanocytes and melanocytic lesions (naevi and melanomas). *PLoS One.* 5:e9977. doi: 10.1371/journal.pone.0009977; 10.1371/journal.pone.0009977.

Midwood, K.S., and D.M. Salter. 2001. NG2/HMPG modulation of human articular chondrocyte adhesion to type VI collagen is lost in osteoarthritis. *J.Pathol.* 195:631-635. doi: 10.1002/path.985.

Midwood, K.S., and D.M. Salter. 1998. Expression of NG2/human melanoma proteoglycan in human adult articular chondrocytes. *Osteoarthritis Cartilage.* 6:297-305. doi: 10.1053/joca.1998.0128.

Mittelman, A., G.Z. Chen, G.Y. Wong, C. Liu, S. Hirai, and S. Ferrone. 1995. Human high molecular weight-melanoma associated antigen mimicry by mouse anti-idiotypic monoclonal antibody MK2-23: modulation of the immunogenicity in patients with malignant melanoma. *Clin.Cancer Res.* 1:705-713.

Mittelman, A., Z.J. Chen, T. Kageshita, H. Yang, M. Yamada, P. Baskind, N. Goldberg, C. Puccio, T. Ahmed, and Z. Arlin. 1990. Active specific immunotherapy in patients with melanoma. A clinical trial with mouse antiidiotypic monoclonal antibodies elicited with syngeneic anti-high-molecular-weight-melanoma-associated antigen monoclonal antibodies. *J.Clin.Invest.* 86:2136-2144. doi: 10.1172/JCI114952.

Mittelman, A., Z.J. Chen, C.C. Liu, S. Hirai, and S. Ferrone. 1994. Kinetics of the immune response and regression of metastatic lesions following development of humoral anti-high molecular weight-melanoma associated antigen immunity in three patients with advanced malignant melanoma immunized with mouse antiidiotypic monoclonal antibody MK2-23. *Cancer Res.* 54:415-421.

Mittelman, A., Z.J. Chen, H. Yang, G.Y. Wong, and S. Ferrone. 1992. Human high molecular weight melanoma-associated antigen (HMW-MAA) mimicry by mouse anti-idiotypic monoclonal antibody MK2-23: induction of humoral anti-HMW-MAA immunity and prolongation of survival in patients with stage IV melanoma. *Proc.Natl.Acad.Sci.U.S.A.* 89:466-470.

Morandi, F., M.V. Corrias, I. Levreri, P. Scaruffi, L. Raffaghello, B. Carlini, P. Bocca, I. Prigione, S. Stigliani, L. Amoroso, S. Ferrone, and V. Pistoia. 2011. Serum levels of cytoplasmic melanoma-associated antigen at diagnosis may predict clinical relapse in neuroblastoma patients. *Cancer Immunol.Immunother.* 60:1485-1495. doi: 10.1007/s00262-011-1052-0.

Morris, J.A., K. Oates, and W.G. Staff. 1986. Scanning electron microscopy of adenomatoid tumours. *Br.J.Urol.* 58:183-187.

Munn, L.L., R.J. Melder, and R.K. Jain. 1994. Analysis of cell flux in the parallel plate flow chamber: implications for cell capture studies. *Biophys.J.* 67:889-895. doi: 10.1016/S0006-3495(94)80550-8.

Murray, J.L., M. Gillogly, K. Kawano, C.L. Efferson, J.E. Lee, M. Ross, X. Wang, S. Ferrone, and C.G. Ioannides. 2004. Fine specificity of high molecular weight-melanoma-associated antigen-specific cytotoxic T lymphocytes elicited by anti-idiotypic monoclonal antibodies in patients with melanoma. *Cancer Res.* 64:5481-5488. doi: 10.1158/0008-5472.CAN-04-0517.

Namba, H., M. Nakashima, T. Hayashi, N. Hayashida, S. Maeda, T.I. Rogounovitch, A. Ohtsuru, V.A. Saenko, T. Kanematsu, and S. Yamashita. 2003. Clinical implication of hot spot BRAF mutation, V599E, in papillary thyroid cancers. *J.Clin.Endocrinol.Metab.* 88:4393-4397.

Natali, P.G., P. Giacomini, C. Russo, G. Steinbach, C. Fenoglio, and S. Ferrone. 1983. Antigenic profile of human melanoma cells. Analysis with monoclonal antibodies to histocompatibility antigens and to melanoma-associated antigens. *J.Cutan.Pathol.* 10:225-237.

Natali, P.G., K. Imai, B.S. Wilson, A. Bigotti, R. Cavaliere, M.A. Pellegrino, and S. Ferrone. 1981. Structural properties and tissue distribution of the antigen recognized by the monoclonal antibody 653.40S to human melanoma cells. *J.Natl.Cancer Inst.* 67:591-601.

Nishi, H., Y. Inoue, T. Kageshita, M. Takata, and H. Ihn. 2010. The expression of human high molecular weight melanoma-associated antigen in acral lentiginous melanoma. *Biosci.Trends.* 4:86-89.

Nishiyama, A., and W.B. Stallcup. 1993. Expression of NG2 proteoglycan causes retention of type VI collagen on the cell surface. *Mol.Biol.Cell.* 4:1097-1108.

Pankova, D., N. Jobe, M. Kratochvilova, R. Buccione, J. Brabek, and D. Rosel. 2012. NG2-mediated Rho activation promotes amoeboid invasiveness of cancer cells. *Eur.J.Cell Biol.* 91:969-977. doi: 10.1016/j.ejcb.2012.05.001; 10.1016/j.ejcb.2012.05.001.

Parkinson, H., U. Sarkans, N. Kolesnikov, N. Abeygunawardena, T. Burdett, M. Dylag, I. Emam, A. Farne, E. Hastings, E. Holloway, N. Kurbatova, M. Lukk, J. Malone, R. Mani, E. Pilicheva, G. Rustici, A. Sharma, E. Williams, T. Adamusiak, M. Brandizi, N. Sklyar, and A. Brazma. 2011. ArrayExpress update--an archive of microarray and high-throughput sequencing-based functional genomics experiments. *Nucleic Acids Res.* 39:D1002-4. doi: 10.1093/nar/gkq1040; 10.1093/nar/gkq1040.

Perris, R., H.J. Kuo, R.W. Glanville, S. Leibold, and M. Bronner-Fraser. 1993. Neural crest cell interaction with type VI collagen is mediated by multiple cooperative binding sites within triple-helix and globular domains. *Exp.Cell Res.* 209:103-117. doi: 10.1006/excr.1993.1290.

Petrini, S., A. Tessa, R. Carrozzo, M. Verardo, R. Pierini, T. Rizza, and E. Bertini. 2003. Human melanoma/NG2 chondroitin sulfate proteoglycan is expressed in the sarcolemma of postnatal human skeletal myofibers. Abnormal expression in merosin-negative and Duchenne muscular dystrophies. *Mol.Cell.Neurosci.* 23:219-231.

Petrovici, K., M. Graf, K. Hecht, S. Reif, K. Pfister, and H. Schmetzer. 2010. Use of NG2 (7.1) in AML as a tumor marker and its association with a poor prognosis. *Cancer.Genomics Proteomics.* 7:173-180.

Pfosser, A., M. Brandl, H. Salih, L. Grosse-Hovest, and G. Jung. 1999. Role of target antigen in bispecific-antibody-mediated killing of human glioblastoma cells: a pre-clinical study. *Int.J.Cancer.* 80:612-616.

Pluschke, G., M. Vanek, A. Evans, T. Dittmar, P. Schmid, P. Itin, E.J. Filardo, and R.A. Reisfeld. 1996. Molecular cloning of a human melanoma-associated chondroitin sulfate proteoglycan. *Proc.Natl.Acad.Sci.U.S.A.* 93:9710-9715.

Polito, A., and R. Reynolds. 2005. NG2-expressing cells as oligodendrocyte progenitors in the normal and demyelinated adult central nervous system. *J.Anat.* 207:707-716. doi: 10.1111/j.1469-7580.2005.00454.x.

Pouly, S., B. Becher, M. Blain, and J.P. Antel. 1999. Expression of a homologue of rat NG2 on human microglia. *Glia.* 27:259-268.

Price, M.A., L.E. Colvin Wanshura, J. Yang, J. Carlson, B. Xiang, G. Li, S. Ferrone, A.Z. Dudek, E.A. Turley, and J.B. McCarthy. 2011. CSPG4, a potential therapeutic target, facilitates malignant progression of melanoma. *Pigment Cell.Melanoma Res.* 24:1148-1157. doi: 10.1111/j.1755-148X.2011.00929.x; 10.1111/j.1755-148X.2011.00929.x.

Pride, M.W., S. Shuey, A. Grillo-Lopez, G. Braslawsky, M. Ross, S.S. Legha, O. Eton, A. Buzaid, C. Ioannides, and J.L. Murray. 1998. Enhancement of cell-mediated immunity in melanoma patients immunized with murine anti-idiotypic monoclonal antibodies (MELIMMUNE) that mimic the high molecular weight proteoglycan antigen. *Clin.Cancer Res.* 4:2363-2370.

Quan, W.D.,Jr, G.E. Dean, L. Spears, C.P. Spears, S. Groshen, J.A. Merritt, and M.S. Mitchell. 1997. Active specific immunotherapy of metastatic melanoma with an antiidiotype vaccine: a phase I/II trial of I-Mel-2 plus SAF-m. *J.Clin.Oncol.* 15:2103-2110.

Rae, J.M., C.J. Creighton, J.M. Meck, B.R. Haddad, and M.D. Johnson. 2007. MDA-MB-435 cells are derived from M14 melanoma cells--a loss for breast cancer, but a boon for melanoma research. *Breast Cancer Res.Treat.* 104:13-19. doi: 10.1007/s10549-006-9392-8.

Rivera, Z., S. Ferrone, X. Wang, S. Jube, H. Yang, H.I. Pass, S. Kanodia, G. Gaudino, and M. Carbone. 2012. CSPG4 As a Target of Antibody-Based Immunotherapy For Malignant Mesothelioma. *Clin.Cancer Res.* doi: 10.1158/1078-0432.CCR-12-0628.

Ross, D.T., U. Scherf, M.B. Eisen, C.M. Perou, C. Rees, P. Spellman, V. Iyer, S.S. Jeffrey, M. Van de Rijn, M. Waltham, A. Pergamenschikov, J.C. Lee, D. Lashkari, D. Shalon, T.G. Myers, J.N. Weinstein, D. Botstein, and P.O. Brown. 2000. Systematic variation in gene expression patterns in human cancer cell lines. *Nat.Genet.* 24:227-235. doi: 10.1038/73432.

Rousselle, P., G.P. Lunstrum, D.R. Keene, and R.E. Burgeson. 1991. Kalinin: an epithelium-specific basement membrane adhesion molecule that is a component of anchoring filaments. *J.Cell Biol.* 114:567-576.

Ruf, P., M. Jager, J. Ellwart, S. Wosch, E. Kusterer, and H. Lindhofer. 2004. Two new trifunctional antibodies for the therapy of human malignant melanoma. *Int.J.Cancer.* 108:725-732. doi: 10.1002/ijc.11630.

Ruhl, M., M. Johannsen, J. Atkinson, D. Manski, E. Sahin, R. Somasundaram, E.O. Riecken, and D. Schuppan. 1999a. Soluble collagen VI induces tyrosine phosphorylation of paxillin and focal adhesion kinase and activates the MAP kinase erk2 in fibroblasts. *Exp.Cell Res.* 250:548-557. doi: 10.1006/excr.1999.4540.

Ruhl, M., E. Sahin, M. Johannsen, R. Somasundaram, D. Manski, E.O. Riecken, and D. Schuppan. 1999b. Soluble collagen VI drives serum-starved fibroblasts through S phase and prevents apoptosis via down-regulation of Bax. *J.Biol.Chem.* 274:34361-34368.

Sakaizawa, K., Y. Goto, Y. Kiniwa, A. Uchiyama, K. Harada, S. Shimada, T. Saida, S. Ferrone, M. Takata, H. Uhara, and R. Okuyama. 2012. Mutation analysis of BRAF and KIT in circulating melanoma cells at the single cell level. *Br.J.Cancer.* 106:939-946. doi: 10.1038/bjc.2012.12; 10.1038/bjc.2012.12.

Satyamoorthy, K., G. Li, M.R. Gerrero, M.S. Brose, P. Volpe, B.L. Weber, P. Van Belle, D.E. Elder, and M. Herlyn. 2003. Constitutive mitogen-activated protein kinase activation in melanoma is mediated by both BRAF mutations and autocrine growth factor stimulation. *Cancer Res.* 63:756-759.

Schlingemann, R.O., F.J. Rietveld, R.M. de Waal, S. Ferrone, and D.J. Ruiter. 1990. Expression of the high molecular weight melanoma-associated antigen by pericytes during angiogenesis in tumors and in healing wounds. *Am.J.Pathol.* 136:1393-1405.

Schlingemann, R.O., F.J. Rietveld, F. Kwaspen, P.C. van de Kerkhof, R.M. de Waal, and D.J. Ruiter. 1991. Differential expression of markers for endothelial cells, pericytes, and basal lamina in the microvasculature of tumors and granulation tissue. *Am.J.Pathol.* 138:1335-1347.

Schmidt, P., C. Kopecky, A. Hombach, P. Zigrino, C. Mauch, and H. Abken. 2011. Eradication of melanomas by targeted elimination of a minor subset of tumor cells *PNAS.* 108 (6):2474-2479.

Schrappe, M., F.G. Klier, R.C. Spiro, T.A. Waltz, R.A. Reisfeld, and C.L. Gladson. 1991. Correlation of chondroitin sulfate proteoglycan expression on proliferating brain capillary endothelial cells with the malignant phenotype of astroglial cells. *Cancer Res.* 51:4986-4993.

Sherman-Baust, C.A., A.T. Weeraratna, L.B. Rangel, E.S. Pizer, K.R. Cho, D.R. Schwartz, T. Shock, and P.J. Morin. 2003. Remodeling of the extracellular matrix through overexpression of collagen VI contributes to cisplatin resistance in ovarian cancer cells. *Cancer.Cell.* 3:377-386.

Shih, I.M., D.E. Elder, M.Y. Hsu, and M. Herlyn. 1994. Regulation of Mel-CAM/MUC18 expression on melanocytes of different stages of tumor progression by normal keratinocytes. *Am.J.Pathol.* 145:837-845.

Shin, G., T.W. Kang, S. Yang, S.J. Baek, Y.S. Jeong, and S.Y. Kim. 2011. GENT: gene expression database of normal and tumor tissues. *Cancer.Inform.* 10:149-157. doi: 10.4137/CIN.S7226; 10.4137/CIN.S7226.

Shoshan, Y., A. Nishiyama, A. Chang, S. Mork, G.H. Barnett, J.K. Cowell, B.D. Trapp, and S.M. Staugaitis. 1999. Expression of oligodendrocyte progenitor cell antigens by gliomas: implications for the histogenesis of brain tumors. *Proc.Natl.Acad.Sci.U.S.A.* 96:10361-10366.

Smalley, K.S. 2003. A pivotal role for ERK in the oncogenic behaviour of malignant melanoma? *Int.J.Cancer.* 104:527-532. doi: 10.1002/ijc.10978.

Smith, F.O., C. Rauch, D.E. Williams, C.J. March, D. Arthur, J. Hilden, B.C. Lampkin, J.D. Buckley, C.V. Buckley, W.G. Woods, P.A. Dinndorf, P. Sorensen, J. Kersey, D. Hammond, and I.D. Bernstein. 1996. The human homologue of rat NG2, a chondroitin sulfate proteoglycan, is not expressed on the cell surface of normal hematopoietic cells but is expressed by acute myeloid leukemia blasts from poor-prognosis patients with abnormalities of chromosome band 11q23. *Blood.* 87:1123-1133.

Spessotto, P., K. Lacrima, P.A. Nicolosi, E. Pivetta, M. Scapolan, and R. Perris. 2009. Fluorescence-based assays for in vitro analysis of cell adhesion and migration. *Methods Mol.Biol.* 522:221-250. doi: 10.1007/978-1-59745-413-1_16.

Spitler, L.E., M. del Rio, A. Khentigan, N.I. Wedel, N.A. Brophy, L.L. Miller, W.S. Harkonen, L.L. Rosendorf, H.M. Lee, and R.P. Mischak. 1987. Therapy of patients with malignant melanoma using a monoclonal antimelanoma antibody-ricin A chain immunotoxin. *Cancer Res.* 47:1717-1723.

Stallcup, W.B., K. Dahlin, and P. Healy. 1990. Interaction of the NG2 chondroitin sulfate proteoglycan with type VI collagen. *J.Cell Biol.* 111:3177-3188.

Stallcup, W.B., and F.J. Huang. 2008. A role for the NG2 proteoglycan in glioma progression. *Cell.Adh Migr.* 2:192-201.

Svendsen, A., J.J. Verhoeff, H. Immervoll, J.C. Brogger, J. Kmiecik, A. Poli, I.A. Netland, L. Prestegarden, J. Planaguma, A. Torsvik, A.B. Kjersem, P.O. Sakariassen, J.I. Heggdal, W.R. Van Furth, R. Bjerkvig, M. Lund-Johansen, P.O. Enger, J. Felsberg, N.H. Brons, K.J. Tronstad, A. Waha, and M. Chekenya. 2011. Expression of the progenitor marker NG2/CSPG4 predicts poor survival and resistance to ionising radiation in glioblastoma. *Acta Neuropathol.* 122:495-510. doi: 10.1007/s00401-011-0867-2; 10.1007/s00401-011-0867-2.

Tillet, E., B. Gential, R. Garrone, and W.B. Stallcup. 2002. NG2 proteoglycan mediates beta1 integrin-independent cell adhesion and spreading on collagen VI. *J.Cell.Biochem.* 86:726-736. doi: 10.1002/jcb.10268.

Tillet, E., F. Ruggiero, A. Nishiyama, and W.B. Stallcup. 1997. The membrane-spanning proteoglycan NG2 binds to collagens V and VI through the central nonglobular domain of its core protein. *J.Biol.Chem.* 272:10769-10776.

Tordsson, J.M., L.G. Ohlsson, L.B. Abrahmsen, P.J. Karlstrom, P.A. Lando, and T.N. Brodin. 2000. Phage-selected primate antibodies fused to superantigens for immunotherapy of malignant melanoma. *Cancer Immunol.Immunother.* 48:691-702.

Ulmer, A., J. Beutel, D. Susskind, R.D. Hilgers, F. Ziemssen, M. Luke, M. Rocken, M. Rohrbach, G. Fierlbeck, K.U. Bartz-Schmidt, and S. Grisanti. 2008. Visualization of circulating melanoma cells in peripheral blood of patients with primary uveal melanoma. *Clin.Cancer Res.* 14:4469-4474. doi: 10.1158/1078-0432.CCR-08-0012; 10.1158/1078-0432.CCR-08-0012.

van der Pol, J.P., M.J. Jager, D. de Wolff-Rouendaal, P.J. Ringens, C. Vennegoor, and D.J. Ruiter. 1987. Heterogeneous expression of melanoma-associated antigens in uveal melanomas. *Curr.Eye Res.* 6:757-765.

Virgintino, D., D. Perissinotto, F. Girolamo, M.T. Mucignat, L. Montanini, M. Errede, T. Kaneiwa, S. Yamada, K. Sugahara, L. Roncali, and R. Perris. 2009. Differential distribution of aggrecan isoforms in perineuronal nets of the human cerebral cortex. *J Cell Mol Med.* 13:3151-3173. doi: 10.1111/j.1582-4934.2009.00694.x.

Virgintino, D., F. Girolamo, M. Errede, C. Capobianco, D. Robertson, W.B. Stallcup, R. Perris, and L. Roncali. 2007. An intimate interplay between precocious, migrating pericytes and endothelial cells governs human fetal brain angiogenesis. *Angiogenesis.* 10:35-45. doi: 10.1007/s10456-006-9061-x.

Virgintino, D., U. Ozerdem, F. Girolamo, L. Roncali, W.B. Stallcup, and R. Perris. 2008. Reversal of cellular roles in angiogenesis: implications for anti-angiogenic therapy. *J.Vasc.Res.* 45:129-131. doi: 10.1159/000109965.

Wagner, S., C. Krepler, D. Allwardt, J. Latzka, S. Strommer, O. Scheiner, H. Pehamberger, U. Wiedermann, C. Hafner, and H. Breiteneder. 2008. Reduction of human melanoma tumor growth in severe combined immunodeficient mice by passive transfer of antibodies induced by a high molecular weight melanoma-associated antigen mimotope vaccine. *Clin.Cancer Res.* 14:8178-8183. doi: 10.1158/1078-0432.CCR-08-0371.

Wang, J., A. Svendsen, J. Kmiecik, H. Immervoll, K.O. Skaftnesmo, J. Planaguma, R.K. Reed, R. Bjerkvig, H. Miletic, P.O. Enger, C.B. Rygh, and M. Chekenya. 2011a. Targeting the NG2/CSPG4 proteoglycan retards tumour growth and angiogenesis in preclinical models of GBM and melanoma. *PLoS One.* 6:e23062. doi: 10.1371/journal.pone.0023062.

Wang, X., A. Katayama, Y. Wang, L. Yu, E. Favoino, K. Sakakura, A. Favole, T. Tsuchikawa, S. Silver, S.C. Watkins, T. Kageshita, and S. Ferrone. 2011b. Functional characterization of an scFv-Fc antibody that immunotherapeutically targets the common cancer cell surface proteoglycan CSPG4. *Cancer Res.* 71:7410-7422. doi: 10.1158/0008-5472.CAN-10-1134.

Wang, X., T. Osada, Y. Wang, L. Yu, K. Sakakura, A. Katayama, J.B. McCarthy, A. Brufsky, M. Chivukula, T. Khoury, D.S. Hsu, W.T. Barry, H.K. Lyerly, T.M. Clay, and S. Ferrone. 2010a. CSPG4 protein as a new target for the antibody-based immunotherapy of triple-negative breast cancer. *J.Natl.Cancer Inst.* 102:1496-1512. doi: 10.1093/jnci/djq343.

Wang, X., Y. Wang, L. Yu, K. Sakakura, C. Visus, J.H. Schwab, C.R. Ferrone, E. Favoino, Y. Koya, M.R. Campoli, J.B. McCarthy, A.B. DeLeo, and S. Ferrone. 2010b. CSPG4 in cancer: multiple roles. *Curr.Mol.Med.* 10:419-429.

Weiger, M.C., C.C. Wang, M. Krajcovic, A.T. Melvin, J.J. Rhoden, and J.M. Haugh. 2009. Spontaneous phosphoinositide 3-kinase signaling dynamics drive spreading and random migration of fibroblasts. *J.Cell.Sci.* 122:313-323. doi: 10.1242/jcs.037564.

Wesseling, P., R.O. Schlingemann, F.J. Rietveld, M. Link, P.C. Burger, and D.J. Ruiter. 1995. Early and extensive contribution of pericytes/vascular smooth muscle cells to microvascular proliferation in glioblastoma multiforme: an immuno-light and immuno-electron microscopic study. *J.Neuropathol.Exp.Neurol.* 54:304-310.

Westekemper, H., S. Karimi, D. Susskind, G. Anastassiou, M. Freistuhler, D. Meller, M. Zeschnigk, K.P. Steuhl, N. Bornfeld, K.W. Schmid, and F. Grabellus. 2010. Expression of MCSP and PRAME in conjunctival melanoma. *Br.J.Ophthalmol.* 94:1322-1327. doi: 10.1136/bjo.2009.167445; 10.1136/bjo.2009.167445.

Wilson, B.S., K. Imai, P.G. Natali, and S. Ferrone. 1981. Distribution and molecular characterization of a cell-surface and a cytoplasmic antigen detectable in human melanoma cells with monoclonal antibodies. *Int.J.Cancer.* 28:293-300.

Wu, J.J., D.R. Eyre, and H.S. Slayter. 1987. Type VI collagen of the intervertebral disc. Biochemical and electron-microscopic characterization of the native protein. *Biochem.J.* 248:373-381.

Yang, J., M.A. Price, G.Y. Li, M. Bar-Eli, R. Salgia, R. Jagedeeswaran, J.H. Carlson, S. Ferrone, E.A. Turley, and J.B. McCarthy. 2009. Melanoma proteoglycan modifies gene expression to stimulate tumor cell motility, growth, and epithelial-to-mesenchymal transition. *Cancer Res.* 69:7538-7547. doi: 10.1158/0008-5472.CAN-08-4626.

Yang, J., M.A. Price, C.L. Neudauer, C. Wilson, S. Ferrone, H. Xia, J. Iida, M.A. Simpson, and J.B. McCarthy. 2004. Melanoma chondroitin sulfate proteoglycan enhances FAK and ERK activation by distinct mechanisms. *J.Cell Biol.* 165:881-891. doi: 10.1083/jcb.200403174.

Yang, X., and X. Yu. 2009. An introduction to epitope prediction methods and software. *Rev.Med.Virol.* 19:77-96. doi: 10.1002/rmv.602; 10.1002/rmv.602.

You, W.K., P. Bonaldo, and W.B. Stallcup. 2012. Collagen VI ablation retards brain tumor progression due to deficits in assembly of the vascular basal lamina. *Am.J.Pathol.* 180:1145-1158. doi: 10.1016/j.ajpath.2011.11.006.

Yu, L., E. Favoino, Y. Wang, Y. Ma, X. Deng, and X. Wang. 2011. The CSPG4-specific monoclonal antibody enhances and prolongs the effects of the BRAF inhibitor in melanoma cells. *Immunol.Res.* 50:294-302. doi: 10.1007/s12026-011-8232-z; 10.1007/s12026-011-8232-z.

ACKNOWLEDGMENTS

I am grateful to a number of colleagues in particular to: Dr. Sabrina Cattaruzza, Dr. Daniela Zanocco, Dr. Elisabetta Lombardi, Dr. Alice Dallatomasina. I want thank also Dr. Stefano Marastoni, Dr. Alessandra Silvestri, Dr. Roberta Colladel and all the "Studio Borsisti". I am also appreciative of Dr. Paola Spessotto and Dr. Maurizio Mongiat for their assistance and support in the Confocal Microscopy acquisitions. Dr. Douglas Keene is thanked for providing the TEM rotary shadowing images of various forms of Col VI.

I wish to tank prof. Roberto Perris and prof. Alfonso Colombatti for critical comments and valuable discussions about the work and all the people working at the National Cancer Insitute, Experimental Division for Oncology 2, Aviano.

A special thank to Daniela.

The work was supported by grants from Associazione Italiana per la Ricerca sul Cancro (AIRC to Roberto Perris), the Italian Ministry of Health (grants "Rare Diseases" and "Alleanza Contro il Cancro to Roberto Perris and Maria Serena Benassi) and intramural research funds from the University of Parma, the National Cancer Institute of Aviano and Rizzoli Orthopeadic Research Institutes. During the course of the study I was supported by fellowships from the Associazione "Via di Natale", Pordenone, Italy.